DISS. ETH NO. 29382

Development of Physically-actuated Bioelectronic Implants Controlling Designer Therapeutic Cells

A thesis submitted to attain the degree of

DOCTOR OF SCIENCES

(Dr. sc. ETH Zurich)

presented by

Haijie Zhao

M.Sc., Jinan University (China)

born on *25.12.1991*

accepted on the recommendation of

Prof. Dr. Martin Fussenegger
Prof. Dr. Michael Nash
Prof. Dr. Nicola Aceto

2023

TABLE OF CONTENTS

SUMMARY

Diabetes is a chronic condition characterized by high levels of glucose in the blood. While there are treatments available for diabetes, including insulin injections and lifestyle modifications, there is still a need for more effective therapies to manage this condition and its associated complications. With the rapid development of biotechnology, therapeutic strategies for diabetes have explored from stem cell-derived β-cell transplantation to synthetic biology-inspired cell-based therapy. These innovative approaches aim to overcome the shortcomings of conventional insulin injections and achieve a cure for the disease.

Taking advantage of physical cues, electrical stimuli offer traceless, non-invasive, and accessible control for in-situ production and real-time dosing of therapeutic proteins in engineered cell-based therapies. The first work presents a self-sufficient subcutaneous push-button-controlled cellular implant that bypasses the requirement for sophisticated electronics and external energy supplies for power and control. The piezoelectric membrane-embedded implant can power and activate the release of insulin by exerting repeated gentle finger pressure on the overlying skin.

In the second work, to further enrich the synthetic biology toolbox, we established a direct molecular link between music and cellular behavior by constructing a **mus**ic-**i**nducible cellular **c**ontrol device (MUSIC) consisting of human cells ectopically expressing the bacterial large-conductance mechanosensitive channel (MscL). The engineered cells could be activated by music exposure, which generate cell membrane deformation, opening MscL channels, thereby allowing calcium influx. Endogenous calcium signalling triggers rapid vesicular insulin release for type-1 diabetes therapy.

We demonstrate a proof-of-concept for the subcutaneous implant by showing that its activation through finger pressure can restore normoglycemia in a mouse model of type-1 diabetes. Such self-sufficient push-button devices could offer greater convenience for patients in controlling their cell-based therapies. Additionally, we investigate an innovative approach to diabetes therapy by establishing a direct link between cell behavior and music, which may be a promising strategy to improve compliance with cell-based therapies.

ZUSAMMENFASSUNG

Diabetes ist eine chronische Erkrankung, die durch hohe Glukosewerte im Blut gekennzeichnet ist. Obwohl es Behandlungsmöglichkeiten für Diabetes gibt, einschließlich Insulininjektionen und Lebensstilanpassungen, besteht dennoch Bedarf an wirksameren Therapien zur Behandlung dieser Erkrankung und ihrer damit verbundenen Komplikationen. Mit der schnellen Entwicklung der Biotechnologie wurden therapeutische Strategien für Diabetes von der Transplantation von β-Zellen aus Stammzellen bis hin zur zellbasierten Therapie auf Basis der synthetischen Biologie erforscht. Diese innovativen Ansätze zielen darauf ab, die Nachteile konventioneller Insulininjektionen zu überwinden und eine Heilung für die Krankheit zu erreichen.

Unter Ausnutzung physikalischer Signale bieten elektrische Reize eine spurlose, nicht-invasive und zugängliche Kontrolle für die In-situ-Produktion und die Echtzeit-Dosierung therapeutischer Proteine in zellbasierten Therapien. Die erste Arbeit präsentiert ein eigenständiges subkutan implantiertes zellbasiertes Gerät mit Druckknopfsteuerung, das keine anspruchsvolle Elektronik oder externe Energiequellen für Stromversorgung und Steuerung erfordert. Das in eine piezoelektrische Membran eingebettete Implantat kann durch wiederholten sanften Fingerdruck auf die darüber liegende Haut Insulin freisetzen und aktivieren.

In der zweiten Arbeit haben wir zur weiteren Bereicherung des Werkzeugkastens der synthetischen Biologie eine direkte molekulare Verbindung zwischen Musik und zellulärem Verhalten hergestellt, indem wir eine musikinduzierbare zelluläre Steuervorrichtung (MUSIC) konstruiert haben, die aus menschlichen Zellen besteht, die den bakteriellen mechanosensitiven Kanal mit großer Leitfähigkeit (MscL) ektopisch exprimieren. Die manipulierten Zellen können durch Musikexposition aktiviert werden, was zu einer Deformation der Zellmembran führt, die die MscL-Kanäle öffnet und dadurch den Calciumeinstrom ermöglicht. Das endogene Calcium-Signal löst eine schnelle vesikuläre Insulinfreisetzung für die Therapie von Typ-1-Diabetes aus.

Wir demonstrieren den Proof-of-Concept für das subkutane Implantat, indem wir zeigen, dass seine Aktivierung durch Fingerdruck eine normoglykämische Situation in einem Mausmodell für Typ-1-Diabetes wiederherstellen kann. Solche eigenständigen Druckknopfgeräte könnten den Patienten eine größere Bequemlichkeit bei der Kontrolle ihrer zellbasierten Therapien bieten. Darüber hinaus untersuchen wir einen innovativen Ansatz zur Diabetes-Therapie, indem wir eine direkte Verbindung zwischen dem Verhalten von Zellen

und Musik herstellen, was eine vielversprechende Strategie sein könnte, um die Einhaltung von zellbasierten Therapien zu verbessern.

CHAPTER 1: Introduction

Synthetic biology has presented immense potential in the last 20 years. With the increasing abundance of tools inspired by synthetic biology, which regulate transcription, post-transcription, and post-translation to control cellular behavior, it has played an increasingly important role in curing diseases that small molecule drugs have not been successful in treating. This work aims to expand the tools of synthetic biology to control cellular behavior for the treatment of type 1 diabetes. This introduction provides an overview of the current therapeutic strategies for diabetic treatment and the design principles of synthetic biology that use physical cues in emerging cell therapy.

Current status of diabetes and treatment strategies

Diabetes is a chronic disease characterized by high levels of glucose in the blood. There are two main types of diabetes: type 1, which is an autoimmune disorder that occurs when the body's immune system attacks and destroys the insulin-producing beta cells in the pancreas; and type 2, which is a metabolic disorder that occurs when the body cannot properly use insulin or produce enough of it. The number of diabetic patients increased from 108 million in 1980 to 422 million in 2014, and directly causing 1.5 million deaths in 2019. Diabetes-related complications include both micro- and macro-vascular diseases, for instance retinal neurodegeneration, tubulointerstitial disease, metabolic damage (e.g., in the heart and liver), and nonclassical conditions such as cognitive decline, impaired pulmonary function, or increased risk of cancer [1].

In the past 100 years, exogenous insulin therapy has become a life-saving, gold-standard therapy for patients with insulin-dependent diabetes mellitus (T1D and late-stage T2D). However, there is a potential risk of severe hypoglycemia resulting from insufficient mimicking of the endogenous insulin secretion pattern. To overcome this risk, pancreas transplantation as a definitive treatment was developed in 1960s, and currently the graft survival rate at 1 year after transplantation is 85.5%. But the invasive pancreas transplantation surgery with vascular anastomosis and enteric or bladder drainage potentially leads to cardiovascular or cerebrovascular events and infection[2].

Pancreatic islets are the mini-organs of the pancreas containing its endocrine cells for the regulation of glucose metabolism. Islet transplantation was explored and optimized to minimize the complications of pancreas transplantation. The 1 year islet allograft survival rate was 41% which is insufficient for recognizing generalized treatment before 2000[3]. In 2000, the “Edmonton protocol” was reported by James Shapiro et al. as a key advance in islet

transplantation with 100% allograft survival rate and maintained insulin independence by using a glucocorticoid-free immunosuppressive regimen[4]. Even though the allograft survival rate has been improved, in the real scenario, islet allografts from 2 to 4 donors can only be enough for one type 1 diabetic patient. In 2005, Hering et al. reported a refinement of immunosuppressive therapy using T cell-depleting antibody (thymoglobulin) peritransplant management that greatly increased the proportion of subjects maintaining insulin independence with a single-donor islet infusion[5].

Although the safety of surgery and the transplantation efficacy have greatly improved, the availability of donor is limited for the demand of diabetes patients[6]. Furthermore, patients receiving transplantation surgery require lifelong immnunosuppression in order to avoid graft rejection. Therefore, self-renewable human embryonic stem cells (hESCs) and human induced pluripotent stem cells (iPSCs) have been researched as a virtually unlimited source to generate human endocrine cells to fulfill the needs for diabetes therapy. The protocols for hESCs-derived definitive endoderm have been developed[7,8], and the well-functioning glucose-responsive beta-like cells tested in T1D diabetes mice[9,10]. However, even though the differentiation efficiency of hESCs is relatively high (30%-40%)[11], those non-differentiated cells may produce teratomas upon transplantation[9]. Taking the advantages of synthetic biology, hESCs engineered with two suicide gene circuits had been developed in order to avoid the potential risk[12]. The initial switch is derived from the herpes simplex virus thymidine kinase (HSV-TK), and it activates in cells that resume or continue tumorigenic proliferation. On the other hand, the second switch carries nitroreductase (NTR) and only triggers when insulin is expressed. The NTR module, flanked by loxP regions, is excised by the human insulin promoter-induced expression of Cre.[13]. HSV-TK is driven by the telomerase promoter, which is active only in undifferentiated cell types[14]. Compared with hESCs, iPSCs include fewer ethical concerns, the potential for autologous transplantation and the potential to model disease in a patient-specific manner[15]. Many iPSCs-based differentiation studies for the in vitro generation of insulin-secreting β-like cells have been reported[16-21]. Even the most effective protocol for generating suitable β-like cells for transplantation relies on the complex growth factor and small-molecule compound cocktail[11,22]. The differentiation of pancreatic progenitor cells into β -like cells are widely regarded as the most challenging aspect of stem cell research for diabetes, as current protocols have shown limited success and inconsistent results in effectively programming pancreatic progenitor cells to become glucose-sensitive and insulin-secreting β-like cells[23-25]. Saxena et al. reported a synthetic lineage-control network enables

differentiation of iPSCs-derived pancreatic progenitor cells by programming the dynamic expression of the transcription facotrs[26].

While stem cell therapy holds great promise in treating a wide range of diseases, including diabetes, researchers are also exploring the potential of mammalian synthetic biology for cell therapy. The field of synthetic biology involves the design and construction of new biological systems or the modification of existing ones for specific applications. In the context of cell therapy, synthetic biology offers exciting possibilities for creating genetically engineered cells that can better target and treat diseases. In the following section, we will delve into this emerging field and explore its potential for revolutionizing cell therapy.

Physical cues-driven synthetic biology in mammalian cells

Synthetic biology brings engineering principles into biology to design and build novel biomolecular components, networks and pathways, and to use these tools to rewire and reprogram organisms to function in a desirable way[27-34]. A completely engineered gene circuit is comprised of an input signal, a responding process and an output module for various applications[35]. As the ever-growing synthetic biology toolbox, the input signal can be small-molecules[30,32-34,36], biological components (e.g., antibodies[37,38], hormone[39] and small peptides[40]). However, there are several disadvantages such as limited bioavailability, inappropriate pharmacodynamics and a broad biodistribution that may lead to evitable side effects. Physical cues such as light[41-46], physical force[47,48], heat[49], electrical field[50], magnetic field[51] provides a precise, effective, safe and non-invasive traceless approach that enables remotely controlling the induction of therapeutic engineered cells with flexible spatiotemporal administation[52]. Based on different applications, the cellular outputs include therapeutic protein production, controlling cell behavior and diagnostic marker expression.

Optogenetics

Light-dependent processes occur in widely diverse organisms from bacteria, plants to animals, regulating the processes of orientation and development. Optogenetic technology combines light and genetic sciences, which enrich the toolbox of synthetic biology for different applications. Optogenetics harbors unprecedented features:1). very high resolution; 2). spatiotemporally precise activation of target cells; 3). enabling fine-tune gene expression levels by adjusting light intensity or exposure time; 4). non-invasive and easy accessibility for the treatment; 5). reversible gene expression. In 2005, light-controllable mammalian cells were first established in neurons to activate membrane potential[53]. In 2006, an optogenetic gene was applied to inner retinal neurons to photosensitive cells to restore visual response[54]. Five years

later, there was a breakthrough in to use of optogenetic gene circuits in mammalian cells enabling inducible insulin secretion for metabolic disease therapy[41].

With the rapid development of optogenetics, the light-responsive receptors or photoswitchable proteins are explored to sense different wavelength regions, ranging from ultraviolet (UV)[55,56] to near-infrared (NIR)[57,58]. The wide range of light-sensitive tools provides great flexibility and the possibility for efficient and sophisticated gene circuits to meet different applications. The mechanism of the photoactivatable protein activation is diverse. By exposure to appropriate excitation, they will undergo conformational changes with inter-protein or intra-protein interactions, resulting in protein allostersim, heterodimerization, and oligomerization. After understanding the mechanism of the photoactivatable protein, many reasonably designed gene circuits have been developed for different usages.

Photoreceptors are natural receptors, chimeric receptors, or ion channels that are located in the plasma membrane and trigger endogenous signaling pathways upon activation. The activated photoreceptors induce intracellular calcium release from the endoplasmic reticulum (ER), triggering the calcium response signaling pathway. For example, Ye et al. reported that the activated melanopsin was activated by blue light stimulation, which sequentially triggers the phosphokinase C (PKC), transient receptor potential channels (TRPCs), and intracellular Ca^{2+} surge. This initiates the activation of NFAT signaling pathway, resulting in GLP1 expression for type 2 diabetic mice therapy[41] (**Fig. 1A**). In 2021, Mansouri et al. reported a rapid insulin secretion strategy by a designed blue-light controlled calcium response secretion pathway, which achieved rapidly reversed hyperglycemia in a mouse model of type-1 diabetes with an easily accessible smartphone flashlight[45].

By using the mechanism of photoswitchable proteins (e.g., dimerization, oligomerization, monoerization and conformational change), the orthogonal systems were developed for cross-talking with endogenous signaling pathways. To achieve precise control over biological activities, light-sensitive domains can be fused to DNA-binding domains such as dCas9[55], zinc finger nucleases[59], transcriptional activators[57] (**Fig. 1B**), or protein-binding domains such as nanobodies[29,60]. To further increase the flexibility and accessibility of optogenetic technology, Maysam et al. developed a green-light controlled gene circuit controlled by a green LED light of Apple-watch. The gene circuit is composed of an engineered membrane-tethered green-light-sensitive cobalamin-binding domain of Thermus thermophilus (TtCBD) CarH protein in combination with a synthetic cytosolic TtCBD-transactivator fusion protein, which manages the translocation of TtCBD-transactivator into the nucleus to trigger expression of transgenes upon illumination[46]. This approach allows light to be used to induce

or reverse the assembly or dissociation of complexes, activating or sequestering the desired protein and thereby modulating the biological function.

Overall, the development of photosensory modules has opened up exciting new possibilities for non-neural optogenetics, enabling precise control over biological activities through the use of light-induced signaling pathways. These technologies have the potential to revolutionize fields such as synthetic biology, drug discovery, and regenerative medicine, providing new tools for understanding and manipulating biological systems. However, there are still challenges that need to be addressed, such as the need for improved delivery methods and a better understanding of the long-term effects of these systems on cellular function and viability.

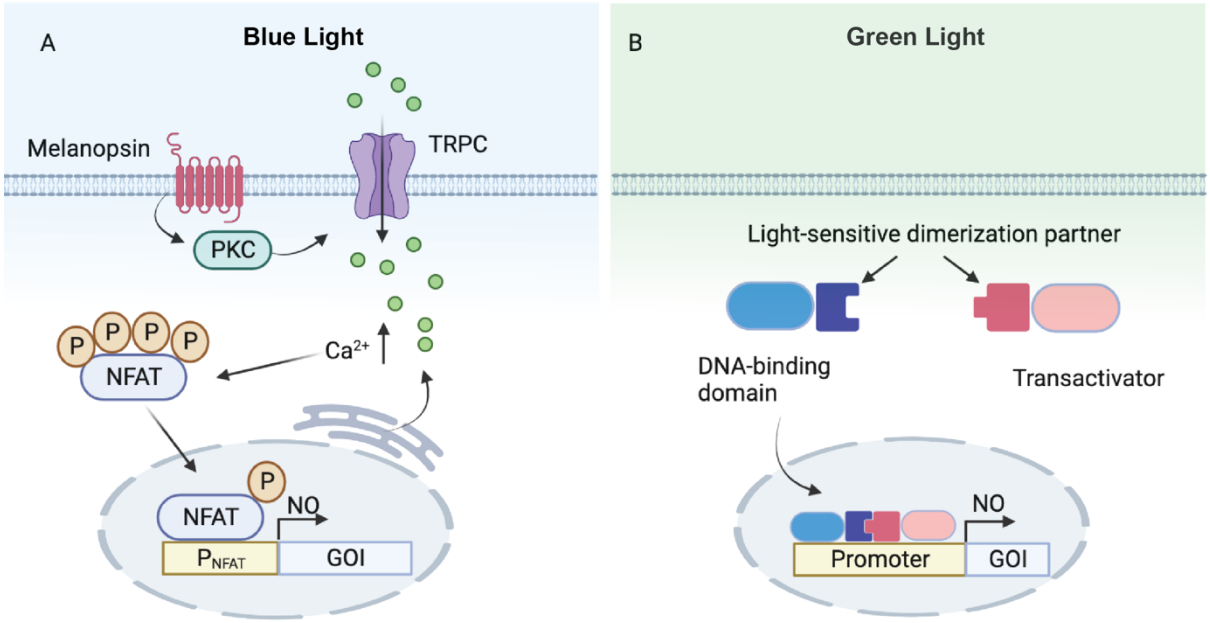

Figure 1. The principle of light-inducible synthetic pathway. (**A**) Melanopsin-based blue light-activated system links to the activation of phosphate kinase C (PKC), leading to the increase of intracellular calcium concentration by opening transient receptor potential ion channels (TRPCs) and releasing Ca^{2+} from ER. NFAT is then phosphorylated and transported into the nucleus, and the promoter responding to NFAT (P_{NFAT}) is activated to express the gene of interest (GOI). (**B**) The light-sensitive photoswitch system functions by inducing the reconstruction of a fusion protein consisting of a DNA-binding domain and a transactivator fusion protein upon exposure of engineered cells to specific wavelengths of light, such as green light. This is achieved through the dimerization of photoswitch proteins. Once reconstructed,

the fusion protein translocates to the nucleus and binds to the synthesis promoter, resulting in the expression of the gene of interest. The figure created with BioRender.

Mechanogenetics

Mechanical response is an intricate and fundamental process by which cells can sense mechanical stimuli such as pressure, stretch, tension, and compression from their environment and convert them into chemical[61] and biochemical signals[62] that trigger a wide range of cellular responses. This process is vital for living organisms to adapt and respond to various environmental cues and physical forces, such as gravity, touch, sound, and fluid flow[63,64]. Mechanosensation is present in all domains of life, from bacteria to humans, and it plays a crucial role in many physiological and pathological conditions, including tissue development and repair, sensory perception, immune responses, and cancer metastasis[65].

Mechanogenetics is composed of mechanical signals and responsive gene circuits for manipulating gene expression or protein activity. One of the approach used in mechanogenetics is the use of mechanosensitive ion channels such as PIEZO1/2[66,67], transient receptor potential channels (TRPs)[68].. By using ultrasonic stimulation to activate or deactivate these ion channels, which enables to control of neuronal activity with high spatiotemporal precision[69]. Alternatively, mechanosensitive channels from bacteria, such as small and large conductance mechanosensitive channels (respectively, MscS[70,71] and MscL[72,73]), were utilized in a mammalian cell gene circuit controlled by shear force. The activated mechanosensitive channel (MS) initiates intracellular calcium influx and sequentially triggers NFAT signaling pathway for expressing gene of interest[47] (**Fig. 2A**). MS ion channels are expressed in neurons, and they can be used to control the activity of neurons in a specific manner[69] (**Fig. 2B**).

Another strategy used in mechanogenetics is the mechanosensitive transcriptional regulator. These regulators respond to changes in mechanical force by either activating or repressing gene expression[62,74]. They are typically engineered to be activated or repressed at specific force ranges, allowing for precise control of gene expression. Wnt signaling is a highly conserved pathway for regulating stem cell renewal, proliferation, and differentiation[75] (**Fig. 2C**). This pathway responds to external mechanical force, lateral cell–cell interactions, and mechanical properties (stiffness and composition) of the extracellular matrix. The iPSCs exposed to shear force, activating the TCF-3-responsive promoter of Wnt pathway and promote differentiation of hiPSCs in a commercially available medium[48]. Recently, acoustic mechanogenetics employed ultrasound waves to precisely control chimeric antigen receptor T cells (CART cells) activation in the tumor area. Focused ultrasound (FUS) delivers energy in

a safe and non-invasive way into tissues to a depth of centimeters. The FUS stimulation allows the CAR expression by heat shock promoter, which mitigates on-target, off-tumor activity and enhances the suppression of tumor growth, compared with the performance of non-inducible CAR-T cells[76].

The use of mechanogenetics has provided a powerful tool for controlling biological activities with high spatiotemporal precision. However, there are still challenges to be addressed, such as the need for a better understanding of the long-term effects of mechanogenetics manipulations on cellular function and viability. Nonetheless, the field of mechanogenetics continues to hold great promise for a range of applications in biological research and therapeutic development.

In conclusion, mechanogenetics provides a novel approach for controlling biological activities using mechanical forces. By combining principles of mechanical engineering and genetics, researchers have developed a range of tools for manipulating gene expression, neuronal activity, and protein activity with high spatiotemporal precision. While challenges still exist, the potential applications of mechanogenetics are vast and continue to be explored by researchers around the world.

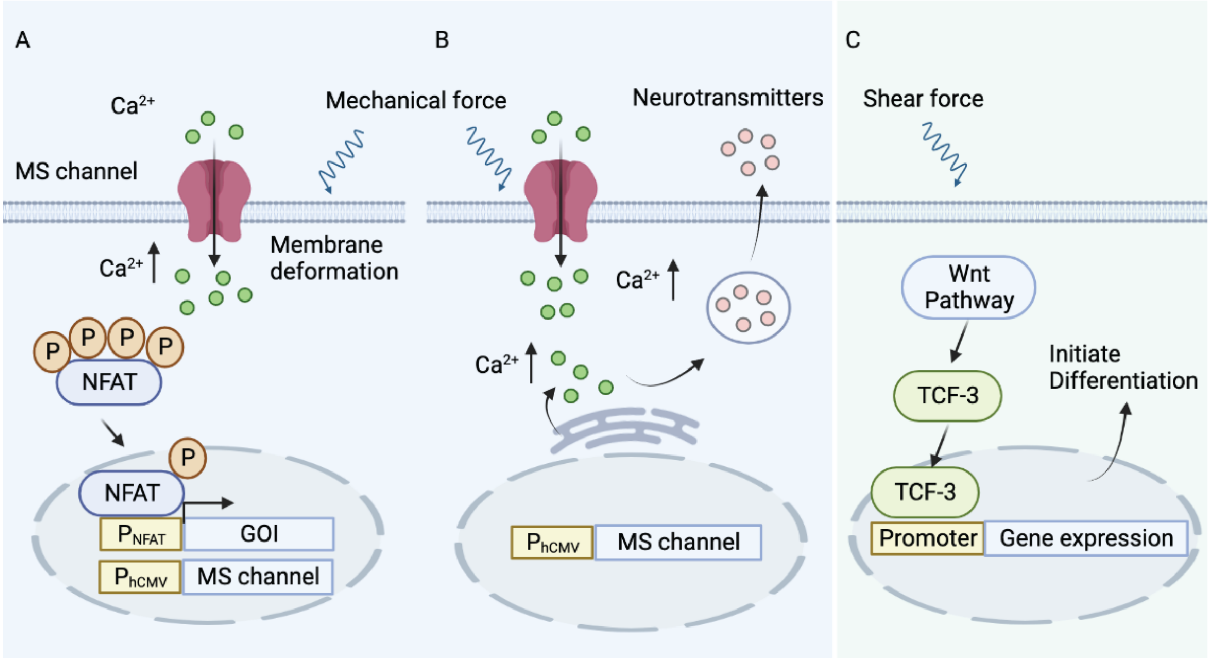

Figure 2. The design of mechanical force controlled cell behaviors. (**A and B**) Mechano-sensitive (MS) channel engineered cells were activated by applying external mechanical force, which generates membrane deformation and opens the MS channel for extracellular calcium influx. The result leads to (**A**) the activation of NFAT promoter or (**B**) the regulation of neurotransmitter secretion pathway. (**C**) The differentiation of stem cells was initiated by

external shear force, which activated the TCF-3 response promoter of the Wnt pathway. The figure created with BioRender.

Thermogenetics

Thermogenetics is an emerging field of synthetic biology that allows for the remote control of cellular behavior using temperature as the input signal by employing genetic engineering techniques. In the natural system, there are two major types of biomolecules involved in thermal sensing, including proteins and RNA thermometers (RNATs)[77]. Firstly, the wide range of thermosensitive proteins undergoes conformational changes in response to the changes of temperature, which triggers the transcription and transduction. Human transient receptor potential melastatin 8 (hTRPM8) ion channel, a TRP channel family member, is employed in designer HEK cells in response to low temperature stimulation by applying menthol. The activated hTRPM8 induced extracellular calcium influx, and consequently enabled NFAT transcription factor to bind P_{NFAT} promoter for therapeutic protein expression[78]. Alternatively, in order to control the calcium-response fast secretion pathway, the transient receptor potential cation channel subfamily V member 1 (hTRPV1) ion channel expressed in β-cells rewires the insulin secretion pathway by sunlight exposure[44]. To meet the specific needs of medical application in human, a precise, robust and reversible temperature-adjustable gene expression within the pathophysiological range (37-40 °C) has been developed. The cytoplasmic protein of Salmonella typhimurium TipA C-terminally fused with transcription activator (PhCMV-TlpA39-VP16-pA) and N-terminally fused with DNA binding domain of tetracycline-dependent transactivator (PhCMV-TlpA39-VP16-pA). The dimerization of TipA39 coiled-coil domains at 37 °C led to the reconstruction of tetracycline-dependent transactivator (tTA) variant (TetR-TlpA39-TlpA39-VP16) for standard tTA-dependent tetracycline-responsive promoters activation. At 40 °C, the unfolded coiled-coil domains of tTA variant were split, thereby shutting off the target gene expression[49]. Heat-shock promoters were widely used to control transcription activation. The heat shock protein (HSPA6) promoter was utilized to trigger localized T cell activation, reaching 200 fold difference after the heat stimulation.

Another strategy consists of a wide range of RNATs that serve as temperature-sensitive regulatory elements located near the 5′ untranslated region (UTR) of various bacterial genes responsible for intrinsic virulence, as well as responses to heat shock and cold shock[79,80]. Enabling the reliable designs of synthetic RNATs for tuning thermal-responses temparature[81], the computational software such as NUPACK[82] and DINAMelt[82] were developed. For example,

a synthetic RNAT was produced to improve the maximal expression and reduce the inherent leakiness. At low temperatures (27 °C), the RNase E cleavage site is sequestered in a stem-loop which allows gene expression. At high temperature (37 °C), the stem-loop unfolds, leading to the mRNA degradation and turning off gene expression[83].

Overall, while thermogenetics is a powerful tool for controlling cellular behavior, it is important to consider its limitations and potential drawbacks when designing experimental or therapeutic applications. Ongoing research efforts are focused on addressing limitations of long-term effect, and improving the precision and specificity of thermogenetic systems, with the goal of expanding their utility in diverse applications.

Electrogenetics

Electrical stimulation as a physical stimulus plays an important role in cell processes, such as proliferation and differentiation[84,85] via modulations in ion channel distribution[86]. It shows great potential in disease treatment[87,88], tissue regeneration[89], wound healing[90], and mechanism studies[91]. Electrogenetics use an electrical field to control the native or designed signaling pathway for regulating cell behaviors. Electrical stimulation provides a simple, efficient, safe and non-invasive traceless approach that enables wireless induction of therapeutic engineered cells with high spatiotemporal precision.

There are direct or indirect strategies for the engineering of electro-sensitive mammalian designer cells. In the direct approach, engineered cells respond to the electrical field itself. Voltage-gated ion channels regulate the polarization of the plasma membrane in excitable cells such as neurons or β cells, allowing selected inorganic ions to pass across the cell membrane and activate downstream signaling pathways. In order to control the therapeutic protein expression in HEK cells ($_{Electro}$HEK cells), a voltage-gated circuit including a voltage-gated calcium channel ($Ca_V1.2$) and inwardly rectifying potassium channel ($K_{ir}2.1$) (**Fig. 3A**). The electric field stimulation initiates cell membrane depolarization, intracellular potassium efflux and extracellular calcium influx. The change of intracellular calcium concentration activates the NFAT promoter for insulin expression. Furthermore, the electrogenetic circuit was applied to β cells ($_{Electro}$β cells) to rewire the calcium response insulin secretion pathway, which provides a rapid kinetic of insulin secretion in response to electrical stimulation for type-1 diabetes therapy[50] (**Fig. 3B**).

In the indirect approach, engineered cells were designed to sense the biological or chemical product of electrical stimulation, such as nitric oxide (NO) or reactive oxygen species (ROS). It has been proven that these redox reagents can activate the downstream native or

artificial pathway[92,93]. The induction of gene expression in mammalian cells through indirectly electrogenetic means was successfully demonstrated through the implementation of an electronic transcription control circuit. This circuit linked the production of acetaldehyde, resulting from the electrochemical oxidation of ethanol, to the expression of a transgene that is inducible by acetaldehyde. The acetaldehyde-dependent transactivator AlcR was applied to designer cells for controlling acetaldehyde-inducible promoter P_{AIR}, which induces the gene of interest expression[94] (**Fig. 3C**).

In conclusion, electrogenetics has emerged as a promising tool in mammalian synthetic biology for cell-based therapy. The ability to control gene expression through electrical signals has the potential to revolutionize the field of regenerative medicine. The use of electronic transcription control circuits to induce gene expression in response to specific electrochemical signals has shown great potential in improving the efficiency and specificity of gene therapy. While further research is needed to fully realize the potential of electrogenetics in cell-based therapy, the current progress suggests that this approach could offer a powerful means to engineer cells for therapeutic applications[95].

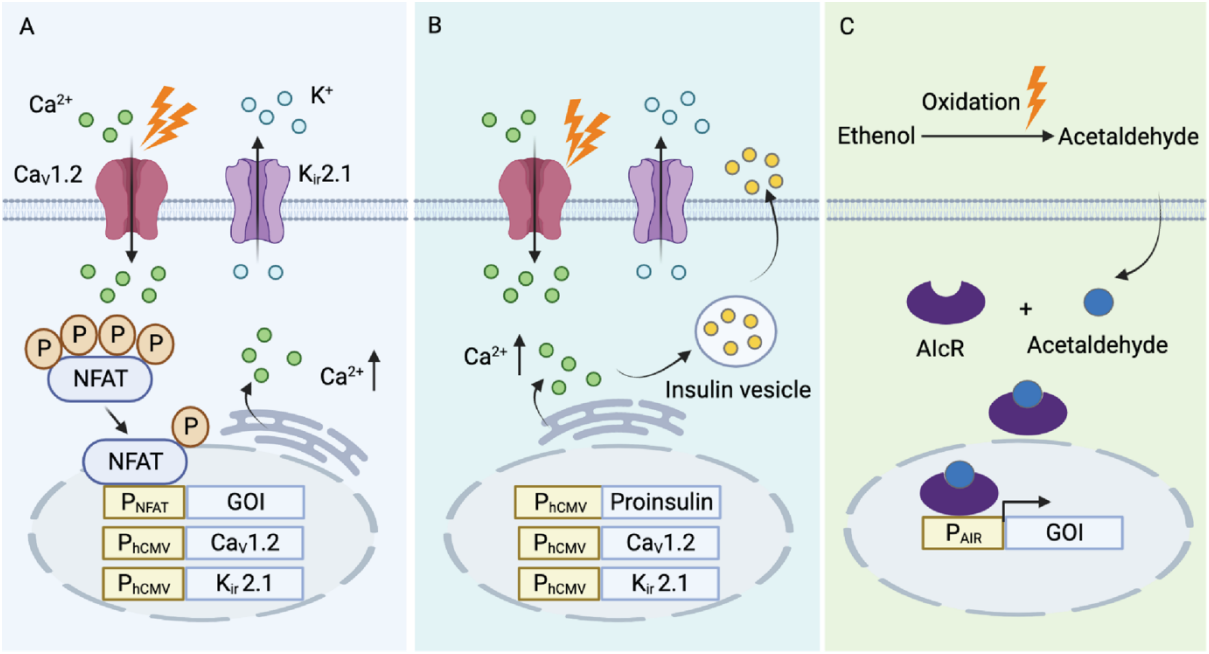

Figure 3. Designer electro-sensitive cells in mammalian systems. (**A**) $_{Electro}$HEK cells are engineered to express a $Ca_V1.2/K_{ir}2.1$ ion channel circuit that responds to electrostimulation. The calcium influx triggers dephosphorylation of the NFAT transcription factor, leading to its translocation to the nucleus and transcriptional activation of the target gene through synthetic

expression units containing NFAT-responsive elements. (**B**) $_{Electro}$β cells express both the $Ca_V1.2/K_{ir}2.1$ channel and a proinsulin construct. Upon plasma membrane depolarization induced by electrostimulation, insulin is rapidly released from the secretory vesicles within 10 minutes. (**C**) CHO cells express an acetaldehyde-inducible gene expression system activated by acetaldehyde produced via electrodes. Acetaldehyde diffuses into the designer cells and binds to its receptor (AlcR), resulting in transcriptional activation of the gene of interest from an acetaldehyde-responsive promoter. The figure created with BioRender.

Magnetogenetics

Magnetogenetics is an emerging field of research that combines genetic engineering and magnetic fields to control the activity of cells. This technique involves introducing magnetic nanoparticles into cells by externally injected inorganic magnetic nanoparticles[96,97] or by genetically encoded nanoparticles. It offers a wireless and non-invasive remote control of cell therapy. The energy of magnetic field is sensed by those nanoparticles, converting signals to heat or strong mechanical force[98,99]. An example of magntogenetics tool based on an inorganic nanoparticle (Manganese ferrite, $MnFe_2O_4$) injection that receives and converts the magnetic stimuli to heat, transmitting to nearby cell membrane thermosensitive ion channels (TRPV1), which responds by opening to allow calcium influx[96]. This results in the opening of these channels and the subsequent influx of calcium ions, enabling the activation of intracellular calcium-dependent signaling pathways. By leveraging this ability of magnetic fields, it is possible to regulate the NFAT-dependent transcriptional activity of a therapeutic gene. As a result, externally applied magnetic fields can be utilized to activate implanted therapeutic cells, allowing for precise control over the timing and dosage of the therapy. Here is an example of genenetically encoded biological nanoparticle that expresses TRPV1 N-terminally fused a magnetosensing nanoparticle (ferritin) for sensing and converting magnetic field to heat for calcium induced NFAT pathway activation[51].

Furthermore, magnetic fields guide in vivo genome editing by CRISPR-Cas9 in mice have been reported. Recombinant baculoviral vectors encoding the CRISPR-Cas9 machinery were complexed with magnetic iron oxide nanoparticles and injected either systemically or directly into target organs in mice. The delivery of these vectors to the target tissues was then enhanced by locally applied magnetic fields, resulting in a subset of the transduced population containing the desired genome edit[100].

In conclusion, magnetogenetics has the potential to revolutionize the field of biomedicine and cell therapy by providing a non-invasive and precise method for controlling

cellular behavior. This technology enables researchers to manipulate biological processes in real time and could have significant applications in the development of new therapies for a variety of diseases. However, there are still several challenges that need to be overcome before magnetogenetics can be widely implemented in biomedicine and cell therapy. These challenges include improving the specificity and efficiency of magnetic nanoparticle targeting, optimizing the delivery of these particles to target tissues, and developing new magnetosensitive proteins with improved properties.

Cell encapsulation

Diabetes is a chronic metabolic disease that affects millions of people worldwide. It is characterized by high blood sugar levels, which can lead to a range of complications, including cardiovascular disease, kidney failure, and nerve damage. Diabetes is caused by a deficiency or dysfunction of insulin, a hormone produced by the pancreas that regulates blood sugar levels. Type 1 diabetes, also known as insulin-dependent diabetes, is caused by the destruction of insulin-producing cells in the pancreas, known as pancreatic islets, by the immune system. This results in a complete lack of insulin production, requiring insulin injections or an insulin pump to regulate blood sugar levels. Type 2 diabetes, on the other hand, is caused by a combination of insulin resistance and insufficient insulin production. It is the most common form of diabetes and is strongly associated with lifestyle factors such as diet and exercise.

Islet transplantation is a promising therapy for type 1 diabetes, where isolated pancreatic islets containing β cells, which produce insulin, are transplanted into the liver. This allows for the restoration of insulin production and regulation of blood sugar levels[101]. However, islet transplantation faces several challenges that limit its widespread use as a therapy for type 1 diabetes. One of the main challenges is the need for immunosuppressive drugs to prevent rejection by the recipient's immune system. The immune system recognizes the transplanted islet cells as foreign and attacks them, leading to graft rejection and loss of function[102]. To prevent this, patients receiving islet transplantation must take immunosuppressive drugs for the rest of their lives. These drugs have significant side effects, including an increased risk of infection, and can be costly and difficult to manage[103]. Another challenge of islet transplantation is the limited availability of donor islets. The isolation of islets from donor pancreases is a complex and time-consuming process, and the number of available donor pancreases is limited[104]. This means that only a small number of patients can currently benefit from islet transplantation as a therapy for type 1 diabetes.

Cell encapsulation has emerged as a potential solution to these challenges by providing a protective barrier around the transplanted islet cells, which can prevent immune rejection and allow the use of fewer islets from donor or stem cell differentiation. Encapsulation involves surrounding the islet cells with a protective material, such as a hydrogel[105-107] or polymer matrix[108], to create a semi-permeable barrier that separates the encapsulated cells from their environment while allowing the exchange of nutrients, oxygen, and waste products.

The encapsulating material can be designed to selectively allow the passage of small molecules, such as glucose and insulin, while blocking larger immune cells and molecules. This creates a controlled environment for the transplanted islet cells, allowing them to function optimally and respond to changes in blood glucose levels. Encapsulation can also allow for the use of immune-privileged sites, such as the peritoneal cavity or subcutaneous tissue, for islet transplantation, which can reduce the need for immunosuppressive drugs and improve the long-term survival of the transplanted cells. An ideal islet encapsulation device with following features: 1). provide ample blood supply to sustain survival and function of islet mass for the maintenance of normoglycaemia; 2). exhibit appropriate insulin and glucose kinetics to achieve normoglycaemia; be biocompatible; 3). create an immune barrier to prevent sensitization and rejection; 4). isolate any potentially tumorigenic cells.

Microencapsulation and Macroencapsulation

Microencapsulation and macroencapsulation are two different methods used in the field of β-cell islet transplantation for the treatment of diabetes. Both of them provide a solution to overcome the immune rejection of islet transplantation. Microencapsulation involves the encapsulation of individual islets within a biocompatible material, such as alginate, polyethylene glycol, or chitosan. The encapsulating material forms a protective barrier around the islets, shielding them from the immune system and allowing for the diffusion of nutrients and oxygen. The first described cell microencapsulation applied to diabetes treatment in 1980, by using alginate-polylysine-polyethyleneimine microcapsules which achieved the encapsulated islets survived up to 3 weeks after transplantation[109]. In 1984, O'Shea et al. reported an improved components of the microencapsulation to prolong the islets survival days up to a year by using a modified alginates the outer layer of the microcapsule[110]. In the next several decades, there is still a great motivation to design microencapsulation materials with sufficient durability and biocompatibility[111,112]. For example, after evaluating more than 1000 combinations of polyanion and polycation, they found the combination of sodium alginate, cellulose sulfate, poly(methylene-co-guanidine) hydrochloride, calcium chloride and sodium

chloride was most promising. The formulation of encapsulation to independently adjust the capsule size, wall thickness, mechanical strength, and permeability was developed, which provided great advantages for immunoissolating cells[113]. Duvivier-Kali et al. successfully prolonged the survival of syngeneic and allogeneic transplanted islets in diabetic mice for more than 350 days[114,115].

Macroencapsulation, on the other hand, involves the encapsulation of a larger number of islets within a single device, such as a hollow fiber or a flat membrane. The encapsulating material allows for the diffusion of nutrients and oxygen while blocking larger molecules and immune cells. The first microencapsulation containing transplanted tissue was developed by using extravascular chambers in 1950[116,117]. A typical membrane with pore size of 450 nm was produced for the microencapsulation application, which enabled a nutrient exchange and prevented immune cell direct contact. However, it found that the fibroblastic overgrowth of the graft and chamber, leading to transplant failure[118]. To overcome the limit of oxygen and nutrient exchange, a microencapsulation device was reported to encourage host vascularization and allograft immune protection. The device consists of two membranes sealed at all side with a loading port. Interestingly, they found that the larger pore membrane (5um) had 80-100 fold more vascular structures compared with the one with 0.02 um pore-size[119]. Research has been carried out on big animal species such as dogs and non-human primates. According to a study on Cynomolgus maccacus, optimal alginate encapsulation considerably extended adult pig islet survival in primates for up to 6 months, despite the presence of an antibody response[120].

Strategies to prolong islet viability

Facilitating nutrient and oxygen exchange

It is well known that β-cells is a highly metabolic cell. The insufficient oxygen levels lead to reduce insulin production and even cell apoptosis. One of the key challenges in islet transplantation is the lack of oxygen and nutrients reaching the transplanted islets. This results in islet death and a loss of transplant function. Therefore, methods have been developed to improve nutrient and oxygen transportation to the encapsulated islets.

One approach is the use of highly porous hydrogels that allow for the passage of necessary nutrients and oxygen while still protecting the islets from the immune system. Researchers have developed a variety of hydrogels using various materials such as alginate[115], polyethylene glycol (PEG)[121], and polyvinyl alcohol (PVA)[122]. These hydrogels have been shown to improve the survival and function of transplanted islets in preclinical studies. Another approach is the use of oxygen-releasing biomaterials, such as perfluorocarbons (PFCs) and

oxygen-carrying hemoglobin-based oxygen carriers (HBOCs). These biomaterials can release oxygen in a controlled manner, which can improve the oxygen supply to the encapsulated islets. Studies have shown that the use of PFCs and HBOCs can improve the survival and function of transplanted islets[123,124].

Furthermore, the strategy of rapid vascularization through the delivery of growth factors provides a solution to improve nutrient and oxygen exchange. Andreas et al. reported a poly(ethylene glycol)(PEG) based hydrogel matrices containing vascular endothelial growth factor, leading to completely remodeled into native, vascularized tissue after subcutaneously implanted in rats[125].

Enhancement of immunoprotection

Islet encapsulation is a promising strategy for the treatment of diabetes by protecting transplanted islets from immune rejection. However, immune rejection is still a significant barrier to the success of this technique. Therefore, enhancing immunoprotection is critical for the success of islet encapsulation. The first strategy is to modify the implantation surface by immobilized ligands such as Fas ligand (FasL), TNF-related apoptosis-inducing ligand (TRAIL) and CD200 to manipulate T cell function at the implantation site[126,127]. For example, FasL has been widely studied to eliminate T cell that potentially targets the graft. The release of FasL effectively inhibited FasL overexpressing myoblasts with islet, achieving the restored euglycaemia without the need of continuous immunosuppression[128]. In addition, it has been found that the treatment of islet before transplantation by a engineered FasL protein, yield long-term engraftment of allogeneic and xenogeneic islets[129]. The second strategy is the use of drug-releasing or cytokine-releasing scaffolds. Cytokines such as transforming growth factor- β[130] (TGF β) and IL-10[131], chemokines CXCL12[132], cellular enzymes IDO1[133] and prostaglandins[134] (PGE2) are the among the factors that have been locally delivered either to attenuate the local inflammatory response. The capacity of CXCL12 includes repelling effector T cells while recruiting regulatory T cells (Treg cells), as well as providing a pro-survival signal for β-cells[135]. Similarly, islets that have been transduced to express CCL22 have shown prolonged protection of islet allografts, maintaining euglycemia in 75% of recipients for up to 80 days. This effect was associated with an increased frequency of Treg cells and the absence of antibodies[136]. Thirdly, by modifying the topography of the encapsulation device, it is possible to modulate the immune response at the host-implant interface. It has been proved that porous materials facilitate the neovascularization and reduce the fibrous tissue encapsulation[137]. Modulating the polarization of macrophages to result in fewer foreign body giant cells (FBGCs)

and enhanced tissue repair has been demonstrated by porosity on the scale of 30-40 μm[138]. Additionally, nanotopography has been found to reduce the extent of inflammatory macrophages[139], while surface alignment of nanofibers can generate a thinner fibrous capsule compared to random fibers and films, thus reducing the host immune reaction[140]. The release of pro-inflammatory cytokines can also potentially be modulated by the diameter of the fibers. In the case of microencapsulation capsules, the inflammatory response is influenced by their dimensions. Fourthly, researchers have also explored the use of immune cells to enhance immunoprotection in islet encapsulation[138,141,142]. For example, mesenchymal stromal cells (MSCs) are immune cells that can regulate immune responses through multiple complex pathways. The transplantation of allogeneic cells along with mesenchymal stem cells (MSCs) has been demonstrated to suppress T cell activity and enhance graft survival[143]. Moreover, co-encapsulating MSCs with syngeneic islets and performing intraperitoneal transplantation in murine models has shown improved graft function compared to mice transplanted with encapsulated islets alone[144]. Currently, clinical trials are underway to investigate the safety and tolerability of autologous MSC delivery. The trials aim to infuse MSCs immediately after islet autograft to evaluate whether glycaemic control can be improved. Similarly, regulatory T cells (Tregs) are immune cells that can suppress the immune response[145]. Co-localizing islet antigen-specific regulatory T cells (Tregs) in the kidney capsule has been demonstrated to protect islet grafts from autoimmune destruction in the nonobese diabetic (NOD) model.

Challenges and outlook

Islet encapsulation is a promising approach to achieving long-term insulin independence for individuals with type 1 diabetes. The encapsulation of islets involves enclosing them within a protective barrier that allows for the exchange of insulin and glucose while protecting them from the immune system. However, there are several challenges that need to be addressed before islet encapsulation can become a viable option for widespread clinical use.

One of the main challenges is to improve the immune protection of the encapsulated islets. While encapsulation can provide some level of protection, it is not completely immune-privileged. The immune system can still recognize and attack the encapsulated islets, leading to graft rejection. Several strategies have been explored to improve the immune protection of the encapsulated islets, including the use of immunomodulatory drugs, immune cell therapies, and gene modification techniques. However, there is still a need for further research to develop effective methods for immune protection.

Another challenge is to maintain optimal islet function within the encapsulation device. Islets are highly sensitive to their environment, and any changes in temperature, pH, or oxygen levels can lead to decreased function or even cell death. Therefore, it is important to design encapsulation devices that provide optimal conditions for islet survival and function. This includes finding a suitable method for oxygen and nutrient transport to the islets within the device.

Additionally, there is a need for larger and longer clinical trials to establish the safety and efficacy of islet encapsulation in humans. While several studies have shown promising results in animal models and early clinical trials, more research is needed to fully evaluate the long-term safety and efficacy of the technique. This includes assessing the risk of adverse effects such as infection, inflammation, and the potential for tumorigenicity.

Moreover, the scalability and cost-effectiveness of islet encapsulation for clinical use are also important considerations. Encapsulating large numbers of islets for widespread clinical use can be a challenging and expensive process. There is a need to develop scalable and cost-effective methods for islet encapsulation that can be easily manufactured and distributed.

In conclusion, while islet encapsulation holds great promise for achieving long-term insulin independence for individuals with type 1 diabetes, there are still several challenges that need to be addressed before it can become a viable option for widespread clinical use. Improving the immune protection of the encapsulated islets, maintaining optimal islet function, and finding a suitable method for oxygen and nutrient transport are key challenges that need to be addressed. Additionally, larger and longer clinical trials are needed to establish the safety and efficacy of the technique in humans. Finally, there is a need to develop scalable and cost-effective methods for islet encapsulation to make it accessible for widespread clinical use.

CONTRIBUTION OF THIS WORK

Diabetes is a chronic disease that still heavily rely on daily insulin injection. However, it has a potential risk of severe hypoglycemia resulting from insufficient mimicking of the endogenous insulin secretion pattern. With the rapid development of synthetic biology, many well-designed genetical tools have been developed and applied for diabetic cell-based therapy. In contrast to small molecules, physical cues, such as light, electricity and mechanical force, show great potential to provide a safe, accessible and non-invasive trackless treatment for diabetic patients.

However, current electrogenetic devices require sophisticated electronics and external energy supplies for control and power. Here, in Chapter 2, We designed a self-sufficient subcutaneous push-button-controlled cellular implant to meet several key criteria, namely: (i) bypassing the need of external power source, (ii) having a highly conductive surface for electro-stimulation of cells with a relatively low resistance and energy input, (iii) to be permeable to nutrients and therapeutic protein but shield the implanted cells from the host immune system, (iv) to have good mechanical properties and thus be resilient to repeated finger-pushing, (v) to show good biocompatibility, and (iv) effectively restore normoglycemia in type-1 diabetes.

In Chapter 3, we used synthetic biology principles to engineer human cells to regulate behavior, which could be tuned by music. The constructed music-inducible cellular control device (MUSIC) functionally links music-actuated mechano-transduction of native MscL to depolarization-triggered vesicular biopharmaceutical secretion, thereby sensitizing human cells to release protein therapeutics within minutes in response to music. Our results suggest that listening to specific music tracks to program traceless percutaneous real-time release of biopharmaceuticals from implanted cells could be an interesting and convenient option to increase compliance in some patients.

Reference

1 Mauricio, D., Alonso, N. & Gratacos, M. Chronic Diabetes Complications: The need to move beyond classical concepts. *Trends Endocrinol Metab* **31**, 287-295, doi:10.1016/j.tem.2020.01.007 (2020).

2 Gruessner, A. C. & Gruessner, R. W. Pancreas transplantation of US and non-US cases from 2005 to 2014 as reported to the united network for organ sharing (UNOS) and the International Pancreas Transplant Registry (IPTR). *Rev Diabet Stud* **13**, 35-58, doi:10.1900/RDS.2016.13.35 (2016).

3 Anazawa, T., Okajima, H., Masui, T. & Uemoto, S. Current state and future evolution of pancreatic islet transplantation. *Ann Gastroenterol Surg* **3**, 34-42, doi:10.1002/ags3.12214 (2019).

4 Shapiro, A. M. *et al.* Islet transplantation in seven patients with type 1 diabetes mellitus using a glucocorticoid-free immunosuppressive regimen. *N Engl J Med* **343**, 230-238, doi:10.1056/NEJM200007273430401 (2000).

5 Hering, B. J. *et al.* Single-donor, marginal-dose islet transplantation in patients with type 1 diabetes. *JAMA* **293**, 830-835, doi:10.1001/jama.293.7.830 (2005).

6 Latres, E., Finan, D. A., Greenstein, J. L., Kowalski, A. & Kieffer, T. J. Navigating Two Roads to Glucose Normalization in Diabetes: Automated Insulin Delivery Devices and Cell Therapy. *Cell Metab* **29**, 545-563, doi:10.1016/j.cmet.2019.02.007 (2019).

7 D'Amour, K. A. *et al.* Efficient differentiation of human embryonic stem cells to definitive endoderm. *Nat Biotechnol* **23**, 1534-1541, doi:10.1038/nbt1163 (2005).

8 D'Amour, K. A. *et al.* Production of pancreatic hormone-expressing endocrine cells from human embryonic stem cells. *Nat Biotechnol* **24**, 1392-1401, doi:10.1038/nbt1259 (2006).

9 Kroon, E. *et al.* Pancreatic endoderm derived from human embryonic stem cells generates glucose-responsive insulin-secreting cells in vivo. *Nat Biotechnol* **26**, 443-452, doi:10.1038/nbt1393 (2008).

10 Saxena, P., Bojar, D., Zulewski, H. & Fussenegger, M. Generation of glucose-sensitive insulin-secreting beta-like cells from human embryonic stem cells by incorporating a synthetic lineage-control network. *J Biotechnol* **259**, 39-45, doi:10.1016/j.jbiotec.2017.07.018 (2017).

11 Pagliuca, F. W. *et al.* Generation of functional human pancreatic beta cells in vitro. *Cell* **159**, 428-439, doi:10.1016/j.cell.2014.09.040 (2014).

12 Qadir, M. M. F. *et al.* A Double Fail-Safe Approach to Prevent Tumorigenesis and Select Pancreatic beta Cells from Human Embryonic Stem Cells. *Stem Cell Reports* **12**, 611-623, doi:10.1016/j.stemcr.2019.01.012 (2019).

13 Kuhn, R. & Torres, R. M. Cre/loxP recombination system and gene targeting. *Methods Mol Biol* **180**, 175-204, doi:10.1385/1-59259-178-7:175 (2002).

14 Albanell, J. *et al.* Telomerase activity in germ cell cancers and mature teratomas. *J Natl Cancer Inst* **91**, 1321-1326, doi:10.1093/jnci/91.15.1321 (1999).

15 Siehler, J., Blochinger, A. K., Meier, M. & Lickert, H. Engineering islets from stem cells for advanced therapies of diabetes. *Nat Rev Drug Discov* **20**, 920-940, doi:10.1038/s41573-021-00262-w (2021).

16 Sui, L. *et al.* beta-Cell Replacement in Mice Using Human Type 1 Diabetes Nuclear Transfer Embryonic Stem Cells. *Diabetes* **67**, 26-35, doi:10.2337/db17-0120 (2018).

17 Leite, N. C. *et al.* Modeling Type 1 Diabetes In Vitro Using Human Pluripotent Stem Cells. *Cell Rep* **32**, 107894, doi:10.1016/j.celrep.2020.107894 (2020).

18 Wang, X. *et al.* Point mutations in the PDX1 transactivation domain impair human beta-cell development and function. *Mol Metab* **24**, 80-97, doi:10.1016/j.molmet.2019.03.006 (2019).
19 Dwivedi, O. P. *et al.* Loss of ZnT8 function protects against diabetes by enhanced insulin secretion. *Nat Genet* **51**, 1596-1606, doi:10.1038/s41588-019-0513-9 (2019).
20 Amin, S. *et al.* Discovery of a drug candidate for GLIS3-associated diabetes. *Nat Commun* **9**, 2681, doi:10.1038/s41467-018-04918-x (2018).
21 Millman, J. R. *et al.* Generation of stem cell-derived beta-cells from patients with type 1 diabetes. *Nat Commun* **7**, 11463, doi:10.1038/ncomms11463 (2016).
22 Rezania, A. *et al.* Reversal of diabetes with insulin-producing cells derived in vitro from human pluripotent stem cells. *Nat Biotechnol* **32**, 1121-1133, doi:10.1038/nbt.3033 (2014).
23 Quiskamp, N., Bruin, J. E. & Kieffer, T. J. Differentiation of human pluripotent stem cells into beta-cells: Potential and challenges. *Best Pract Res Clin Endocrinol Metab* **29**, 833-847, doi:10.1016/j.beem.2015.10.011 (2015).
24 Rostovskaya, M., Bredenkamp, N. & Smith, A. Towards consistent generation of pancreatic lineage progenitors from human pluripotent stem cells. *Philos Trans R Soc Lond B Biol Sci* **370**, 20140365, doi:10.1098/rstb.2014.0365 (2015).
25 Thatava, T. *et al.* Intrapatient variations in type 1 diabetes-specific iPS cell differentiation into insulin-producing cells. *Mol Ther* **21**, 228-239, doi:10.1038/mt.2012.245 (2013).
26 Saxena, P. *et al.* A programmable synthetic lineage-control network that differentiates human IPSCs into glucose-sensitive insulin-secreting beta-like cells. *Nat Commun* **7**, 11247, doi:10.1038/ncomms11247 (2016).
27 Bertschi, A. *et al.* Controlling therapeutic protein expression via inhalation of a butter flavor molecule. *Nucleic Acids Res* **51**, e28, doi:10.1093/nar/gkac1256 (2023).
28 Bertschi, A., Wang, P., Galvan, S., Teixeira, A. P. & Fussenegger, M. Combinatorial protein dimerization enables precise multi-input synthetic computations. *Nat Chem Biol*, doi:10.1038/s41589-023-01281-x (2023).
29 Mansouri, M., Ray, P. G., Franko, N., Xue, S. & Fussenegger, M. Design of programmable post-translational switch control platform for on-demand protein secretion in mammalian cells. *Nucleic Acids Res* **51**, e1, doi:10.1093/nar/gkac916 (2023).
30 Galvan, S., Madderson, O., Xue, S., Teixeira, A. P. & Fussenegger, M. Regulation of Transgene Expression by the Natural Sweetener Xylose. *Adv Sci (Weinh)* **9**, e2203193, doi:10.1002/advs.202203193 (2022).
31 Mahameed, M., Wang, P., Xue, S. & Fussenegger, M. Engineering receptors in the secretory pathway for orthogonal signalling control. *Nat Commun* **13**, 7350, doi:10.1038/s41467-022-35161-0 (2022).
32 Mahameed, M., Xue, S., Stefanov, B. A., Hamri, G. C. & Fussenegger, M. Engineering a Rapid Insulin Release System Controlled By Oral Drug Administration. *Adv Sci (Weinh)* **9**, e2105619, doi:10.1002/advs.202105619 (2022).
33 Franko, N., Teixeira, A. P., Xue, S., Charpin-El Hamri, G. & Fussenegger, M. Design of modular autoproteolytic gene switches responsive to anti-coronavirus drug candidates. *Nat Commun* **12**, 6786, doi:10.1038/s41467-021-27072-3 (2021).
34 Teixeira, A. P. *et al.* CelloSelect - A synthetic cellobiose metabolic pathway for selection of stable transgenic CHO cell lines. *Metab Eng* **70**, 23-30, doi:10.1016/j.ymben.2022.01.001 (2022).

35 Arber, C., Young, M. & Barth, P. Reprogramming cellular functions with engineered membrane proteins. *Curr Opin Biotechnol* **47**, 92-101, doi:10.1016/j.copbio.2017.06.009 (2017).
36 Wang, H. *et al.* Identification of sclareol as a natural neuroprotective Ca(v) 1.3-antagonist using synthetic parkinson-mimetic gene circuits and computer-aided drug discovery. *Adv Sci (Weinh)* **9**, e2102855, doi:10.1002/advs.202102855 (2022).
37 Gossen, M. *et al.* Transcriptional activation by tetracyclines in mammalian cells. *Science* **268**, 1766-1769, doi:10.1126/science.7792603 (1995).
38 Weber, W. *et al.* Macrolide-based transgene control in mammalian cells and mice. *Nat Biotechnol* **20**, 901-907, doi:10.1038/nbt731 (2002).
39 Liu, Y., Charpin-El Hamri, G., Ye, H. & Fussenegger, M. A synthetic free fatty acid-regulated transgene switch in mammalian cells and mice. *Nucleic Acids Res* **46**, 9864-9874, doi:10.1093/nar/gky805 (2018).
40 Scheller, L., Strittmatter, T., Fuchs, D., Bojar, D. & Fussenegger, M. Generalized extracellular molecule sensor platform for programming cellular behavior. *Nat Chem Biol* **14**, 723-729, doi:10.1038/s41589-018-0046-z (2018).
41 Ye, H., Daoud-El Baba, M., Peng, R. W. & Fussenegger, M. A synthetic optogenetic transcription device enhances blood-glucose homeostasis in mice. *Science* **332**, 1565-1568, doi:10.1126/science.1203535 (2011).
42 Shao, J. *et al.* Smartphone-controlled optogenetically engineered cells enable semiautomatic glucose homeostasis in diabetic mice. *Sci Transl Med* **9**, doi:10.1126/scitranslmed.aal2298 (2017).
43 Gomelsky, M. Photoactivated cells link diagnosis and therapy. *Sci Transl Med* **9**, doi:10.1126/scitranslmed.aan3936 (2017).
44 Stefanov, B. A., Mansouri, M., Charpin-El Hamri, G. & Fussenegger, M. Sunlight-Controllable Biopharmaceutical Production for Remote Emergency Supply of Directly Injectable Therapeutic Proteins. *Small* **18**, e2202566, doi:10.1002/smll.202202566 (2022).
45 Mansouri, M. *et al.* Smartphone-Flashlight-Mediated Remote Control of Rapid Insulin Secretion Restores Glucose Homeostasis in Experimental Type-1 Diabetes. *Small* **17**, e2101939, doi:10.1002/smll.202101939 (2021).
46 Mansouri, M. *et al.* Smart-watch-programmed green-light-operated percutaneous control of therapeutic transgenes. *Nat Commun* **12**, 3388, doi:10.1038/s41467-021-23572-4 (2021).
47 Strittmatter, T., Argast, P., Buchman, P., Krawczyk, K. & Fussenegger, M. Control of gene expression in engineered mammalian cells with a programmable shear-stress inducer. *Biotechnol Bioeng* **118**, 4751-4759, doi:10.1002/bit.27939 (2021).
48 Strittmatter, T. *et al.* Mechano-regulation of Wnt/beta-Catenin signaling to control paraxial versus lateral mesoderm lineage bifurcation. *Biotechnol Prog* **39**, e3312, doi:10.1002/btpr.3312 (2023).
49 Stefanov, B. A. *et al.* Genetically Encoded Protein Thermometer Enables Precise Electrothermal Control of Transgene Expression. *Adv Sci (Weinh)* **8**, e2101813, doi:10.1002/advs.202101813 (2021).
50 Krawczyk, K. *et al.* Electrogenetic cellular insulin release for real-time glycemic control in type 1 diabetic mice. *Science* **368**, 993-1001, doi:10.1126/science.aau7187 (2020).
51 Stanley, S. A., Sauer, J., Kane, R. S., Dordick, J. S. & Friedman, J. M. Remote regulation of glucose homeostasis in mice using genetically encoded nanoparticles. *Nat Med* **21**, 92-98, doi:10.1038/nm.3730 (2015).

52 Madderson, O., Teixeira, A. P. & Fussenegger, M. Emerging mammalian gene switches for controlling implantable cell therapies. *Curr Opin Chem Biol* **64**, 98-105, doi:10.1016/j.cbpa.2021.05.012 (2021).
53 Han, X. *et al.* Millisecond-timescale optical control of neural dynamics in the nonhuman primate brain. *Neuron* **62**, 191-198, doi:10.1016/j.neuron.2009.03.011 (2009).
54 Bi, A. *et al.* Ectopic expression of a microbial-type rhodopsin restores visual responses in mice with photoreceptor degeneration. *Neuron* **50**, 23-33, doi:10.1016/j.neuron.2006.02.026 (2006).
55 Jain, P. K. *et al.* Development of Light-Activated CRISPR Using Guide RNAs with Photocleavable Protectors. *Angew Chem Int Ed Engl* **55**, 12440-12444, doi:10.1002/anie.201606123 (2016).
56 Nihongaki, Y., Kawano, F., Nakajima, T. & Sato, M. Photoactivatable CRISPR-Cas9 for optogenetic genome editing. *Nat Biotechnol* **33**, 755-760, doi:10.1038/nbt.3245 (2015).
57 Zhou, Y. *et al.* A small and highly sensitive red/far-red optogenetic switch for applications in mammals. *Nat Biotechnol* **40**, 262-272, doi:10.1038/s41587-021-01036-w (2022).
58 Zhou, X. X., Chung, H. K., Lam, A. J. & Lin, M. Z. Optical control of protein activity by fluorescent protein domains. *Science* **338**, 810-814, doi:10.1126/science.1226854 (2012).
59 Konermann, S. *et al.* Optical control of mammalian endogenous transcription and epigenetic states. *Nature* **500**, 472-476, doi:10.1038/nature12466 (2013).
60 Mansouri, M., Strittmatter, T. & Fussenegger, M. Light-Controlled Mammalian Cells and Their Therapeutic Applications in Synthetic Biology. *Adv Sci (Weinh)* **6**, 1800952, doi:10.1002/advs.201800952 (2019).
61 Pan, Y. *et al.* Mechanogenetics for the remote and noninvasive control of cancer immunotherapy. *Proc Natl Acad Sci U S A* **115**, 992-997, doi:10.1073/pnas.1714900115 (2018).
62 Wang, J. H., Thampatty, B. P., Lin, J. S. & Im, H. J. Mechanoregulation of gene expression in fibroblasts. *Gene* **391**, 1-15, doi:10.1016/j.gene.2007.01.014 (2007).
63 Tyler, W. J. The mechanobiology of brain function. *Nat Rev Neurosci* **13**, 867-878, doi:10.1038/nrn3383 (2012).
64 Eyckmans, J., Boudou, T., Yu, X. & Chen, C. S. A hitchhiker's guide to mechanobiology. *Dev Cell* **21**, 35-47, doi:10.1016/j.devcel.2011.06.015 (2011).
65 Gu, Y. & Gu, C. Physiological and pathological functions of mechanosensitive ion channels. *Mol Neurobiol* **50**, 339-347, doi:10.1007/s12035-014-8654-4 (2014).
66 Coste, B. *et al.* Piezo1 and Piezo2 are essential components of distinct mechanically activated cation channels. *Science* **330**, 55-60, doi:10.1126/science.1193270 (2010).
67 Coste, B. *et al.* Piezo1 ion channel pore properties are dictated by C-terminal region. *Nat Commun* **6**, 7223, doi:10.1038/ncomms8223 (2015).
68 Clapham, D. E. TRP channels as cellular sensors. *Nature* **426**, 517-524, doi:10.1038/nature02196 (2003).
69 Qiu, Z. *et al.* The Mechanosensitive ion channel piezo1 significantly mediates in vitro ultrasonic stimulation of neurons. *iScience* **21**, 448-457, doi:10.1016/j.isci.2019.10.037 (2019).
70 Bass, R. B., Strop, P., Barclay, M. & Rees, D. C. Crystal structure of Escherichia coli MscS, a voltage-modulated and mechanosensitive channel. *Science* **298**, 1582-1587, doi:10.1126/science.1077945 (2002).

71 Zhang, Y. *et al.* Visualization of the mechanosensitive ion channel MscS under membrane tension. *Nature* **590**, 509-514, doi:10.1038/s41586-021-03196-w (2021).
72 Liu, Z., Gandhi, C. S. & Rees, D. C. Structure of a tetrameric MscL in an expanded intermediate state. *Nature* **461**, 120-124, doi:10.1038/nature08277 (2009).
73 Sukharev, S. I., Blount, P., Martinac, B., Blattner, F. R. & Kung, C. A large-conductance mechanosensitive channel in E. coli encoded by mscL alone. *Nature* **368**, 265-268, doi:10.1038/368265a0 (1994).
74 Sun, J., Chen, J., Mohagheghian, E. & Wang, N. Force-induced gene up-regulation does not follow the weak power law but depends on H3K9 demethylation. *Sci Adv* **6**, eaay9095, doi:10.1126/sciadv.aay9095 (2020).
75 ten Berge, D. *et al.* Embryonic stem cells require Wnt proteins to prevent differentiation to epiblast stem cells. *Nat Cell Biol* **13**, 1070-1075, doi:10.1038/ncb2314 (2011).
76 Wu, Y. *et al.* Control of the activity of CAR-T cells within tumours via focused ultrasound. *Nat Biomed Eng* **5**, 1336-1347, doi:10.1038/s41551-021-00779-w (2021).
77 Sengupta, P. & Garrity, P. Sensing temperature. *Curr Biol* **23**, R304-307, doi:10.1016/j.cub.2013.03.009 (2013).
78 Bai, P. *et al.* A fully human transgene switch to regulate therapeutic protein production by cooling sensation. *Nat Med* **25**, 1266-1273, doi:10.1038/s41591-019-0501-8 (2019).
79 Narberhaus, F. Translational control of bacterial heat shock and virulence genes by temperature-sensing mRNAs. *RNA Biol* **7**, 84-89, doi:10.4161/rna.7.1.10501 (2010).
80 Rossmanith, J., Weskamp, M. & Narberhaus, F. Design of a Temperature-Responsive Transcription Terminator. *ACS Synth Biol* **7**, 613-621, doi:10.1021/acssynbio.7b00356 (2018).
81 Neupert, J., Karcher, D. & Bock, R. Design of simple synthetic RNA thermometers for temperature-controlled gene expression in Escherichia coli. *Nucleic Acids Res* **36**, e124, doi:10.1093/nar/gkn545 (2008).
82 Zadeh, J. N. *et al.* NUPACK: Analysis and design of nucleic acid systems. *J Comput Chem* **32**, 170-173, doi:10.1002/jcc.21596 (2011).
83 Hoynes-O'Connor, A., Hinman, K., Kirchner, L. & Moon, T. S. De novo design of heat-repressible RNA thermosensors in E. coli. *Nucleic Acids Res* **43**, 6166-6179, doi:10.1093/nar/gkv499 (2015).
84 Cheng, H., Huang, Y., Yue, H. & Fan, Y. Electrical Stimulation Promotes Stem Cell Neural Differentiation in Tissue Engineering. *Stem Cells Int* **2021**, 6697574, doi:10.1155/2021/6697574 (2021).
85 Oh, B. *et al.* Modulating the Electrical and Mechanical Microenvironment to Guide Neuronal Stem Cell Differentiation. *Adv Sci (Weinh)* **8**, 2002112, doi:10.1002/advs.202002112 (2021).
86 Du, J. *et al.* Optimal electrical stimulation boosts stem cell therapy in nerve regeneration. *Biomaterials* **181**, 347-359, doi:10.1016/j.biomaterials.2018.07.015 (2018).
87 Park, J. S., Oh, D. H., Hwang, N. K. & Lee, J. H. Effects of neuromuscular electrical stimulation in patients with Parkinson's disease and dysphagia: A randomized, single-blind, placebo-controlled trial. *NeuroRehabilitation* **42**, 457-463, doi:10.3233/NRE-172306 (2018).
88 Pascual-Valdunciel, A., Rajagopal, A., Pons, J. L. & Delp, S. Non-invasive electrical stimulation of peripheral nerves for the management of tremor. *J Neurol Sci* **435**, 120195, doi:10.1016/j.jns.2022.120195 (2022).
89 Chen, C., Bai, X., Ding, Y. & Lee, I. S. Electrical stimulation as a novel tool for regulating cell behavior in tissue engineering. *Biomater Res* **23**, 25, doi:10.1186/s40824-019-0176-8 (2019).

90 Rajendran, S. B., Challen, K., Wright, K. L. & Hardy, J. G. Electrical Stimulation to Enhance Wound Healing. *J Funct Biomater* **12**, doi:10.3390/jfb12020040 (2021).
91 Hronik-Tupaj, M., Rice, W. L., Cronin-Golomb, M., Kaplan, D. L. & Georgakoudi, I. Osteoblastic differentiation and stress response of human mesenchymal stem cells exposed to alternating current electric fields. *Biomed Eng Online* **10**, 9, doi:10.1186/1475-925X-10-9 (2011).
92 Bogdan, C. Nitric oxide and the regulation of gene expression. *Trends Cell Biol* **11**, 66-75, doi:10.1016/s0962-8924(00)01900-0 (2001).
93 Carter, C. S. *et al.* Exposure to Static Magnetic and Electric Fields Treats Type 2 Diabetes. *Cell Metab* **32**, 561-574 e567, doi:10.1016/j.cmet.2020.09.012 (2020).
94 Weber, W. *et al.* Gas-inducible transgene expression in mammalian cells and mice. *Nat Biotechnol* **22**, 1440-1444, doi:10.1038/nbt1021 (2004).
95 Mansouri, M. & Fussenegger, M. Electrogenetics: Bridging synthetic biology and electronics to remotely control the behavior of mammalian designer cells. *Curr Opin Chem Biol* **68**, 102151, doi:10.1016/j.cbpa.2022.102151 (2022).
96 Huang, H., Delikanli, S., Zeng, H., Ferkey, D. M. & Pralle, A. Remote control of ion channels and neurons through magnetic-field heating of nanoparticles. *Nat Nanotechnol* **5**, 602-606, doi:10.1038/nnano.2010.125 (2010).
97 Shin, W. *et al.* Magnetogenetics with Piezo1 Mechanosensitive Ion Channel for CRISPR Gene Editing. *Nano Lett* **22**, 7415-7422, doi:10.1021/acs.nanolett.2c02314 (2022).
98 Nimpf, S. & Keays, D. A. Is magnetogenetics the new optogenetics? *EMBO J* **36**, 1643-1646, doi:10.15252/embj.201797177 (2017).
99 Zhu, L., Wu, Y., Yoon, C. W. & Wang, Y. Mechanogenetics for cellular engineering and cancer immunotherapy. *Curr Opin Biotechnol* **66**, 88-94, doi:10.1016/j.copbio.2020.06.008 (2020).
100 Zhu, H. *et al.* Spatial control of in vivo CRISPR-Cas9 genome editing via nanomagnets. *Nat Biomed Eng* **3**, 126-136, doi:10.1038/s41551-018-0318-7 (2019).
101 Matsumoto, S. Islet cell transplantation for Type 1 diabetes. *J Diabetes* **2**, 16-22, doi:10.1111/j.1753-0407.2009.00048.x (2010).
102 Tahbaz, M. & Yoshihara, E. Immune Protection of Stem Cell-Derived Islet Cell Therapy for Treating Diabetes. *Front Endocrinol (Lausanne)* **12**, 716625, doi:10.3389/fendo.2021.716625 (2021).
103 Takaki, T. & Shimoda, M. Pancreatic islet transplantation: toward definitive treatment for diabetes mellitus. *Glob Health Med* **2**, 200-211, doi:10.35772/ghm.2020.01057 (2020).
104 McCall, M. & Shapiro, A. M. Update on islet transplantation. *Cold Spring Harb Perspect Med* **2**, a007823, doi:10.1101/cshperspect.a007823 (2012).
105 Duin, S. *et al.* 3D Bioprinting of Functional Islets of Langerhans in an Alginate/Methylcellulose Hydrogel Blend. *Adv Healthc Mater* **8**, e1801631, doi:10.1002/adhm.201801631 (2019).
106 Huang, L. *et al.* Regulation of Blood Glucose Using Islets Encapsulated in a Melanin-Modified Immune-Shielding Hydrogel. *ACS Appl Mater Interfaces* **13**, 12877-12887, doi:10.1021/acsami.0c23010 (2021).
107 Jiang, K. *et al.* 3-D physiomimetic extracellular matrix hydrogels provide a supportive microenvironment for rodent and human islet culture. *Biomaterials* **198**, 37-48, doi:10.1016/j.biomaterials.2018.08.057 (2019).
108 Dimitrioglou, N., Kanelli, M., Papageorgiou, E., Karatzas, T. & Hatziavramidis, D. Paving the way for successful islet encapsulation. *Drug Discov Today* **24**, 737-748, doi:10.1016/j.drudis.2019.01.020 (2019).

109 Lim, F. & Sun, A. M. Microencapsulated islets as bioartificial endocrine pancreas. *Science* **210**, 908-910, doi:10.1126/science.6776628 (1980).
110 O'Shea, G. M., Goosen, M. F. & Sun, A. M. Prolonged survival of transplanted islets of Langerhans encapsulated in a biocompatible membrane. *Biochim Biophys Acta* **804**, 133-136, doi:10.1016/0167-4889(84)90107-1 (1984).
111 Sawhney, A. S., Pathak, C. P. & Hubbell, J. A. Interfacial photopolymerization of poly(ethylene glycol)-based hydrogels upon alginate-poly(l-lysine) microcapsules for enhanced biocompatibility. *Biomaterials* **14**, 1008-1016, doi:10.1016/0142-9612(93)90194-7 (1993).
112 Klock, G. *et al.* Production of purified alginates suitable for use in immunoisolated transplantation. *Appl Microbiol Biotechnol* **40**, 638-643, doi:10.1007/BF00173321 (1994).
113 Wang, T. *et al.* An encapsulation system for the immunoisolation of pancreatic islets. *Nat Biotechnol* **15**, 358-362, doi:10.1038/nbt0497-358 (1997).
114 Duvivier-Kali, V. F., Omer, A., Lopez-Avalos, M. D., O'Neil, J. J. & Weir, G. C. Survival of microencapsulated adult pig islets in mice in spite of an antibody response. *Am J Transplant* **4**, 1991-2000, doi:10.1111/j.1600-6143.2004.00628.x (2004).
115 Duvivier-Kali, V. F., Omer, A., Parent, R. J., O'Neil, J. J. & Weir, G. C. Complete protection of islets against allorejection and autoimmunity by a simple barium-alginate membrane. *Diabetes* **50**, 1698-1705, doi:10.2337/diabetes.50.8.1698 (2001).
116 Algire, G. H., Weaver, J. M. & Prehn, R. T. Growth of cells in vivo in diffusion chambers. I. Survival of homografts in immunized mice. *J Natl Cancer Inst* **15**, 493-507 (1954).
117 Prehn, R. T., Weaver, J. M. & Algire, G. H. The diffusion-chamber technique applied to a study of the nature of homograft resistance. *J Natl Cancer Inst* **15**, 509-517 (1954).
118 Scharp, D. W. & Marchetti, P. Encapsulated islets for diabetes therapy: history, current progress, and critical issues requiring solution. *Adv Drug Deliv Rev* **67-68**, 35-73, doi:10.1016/j.addr.2013.07.018 (2014).
119 Brauker, J. H. *et al.* Neovascularization of synthetic membranes directed by membrane microarchitecture. *J Biomed Mater Res* **29**, 1517-1524, doi:10.1002/jbm.820291208 (1995).
120 Dufrane, D., Goebbels, R. M., Saliez, A., Guiot, Y. & Gianello, P. Six-month survival of microencapsulated pig islets and alginate biocompatibility in primates: proof of concept. *Transplantation* **81**, 1345-1353, doi:10.1097/01.tp.0000208610.75997.20 (2006).
121 Knobeloch, T., Abadi, S. E. M., Bruns, J., Zustiak, S. P. & Kwon, G. Injectable Polyethylene Glycol Hydrogel for Islet Encapsulation: an in vitro and in vivo Characterization. *Biomed Phys Eng Express* **3**, doi:10.1088/2057-1976/aa742b (2017).
122 Qi, M. *et al.* PVA hydrogel sheet macroencapsulation for the bioartificial pancreas. *Biomaterials* **25**, 5885-5892, doi:10.1016/j.biomaterials.2004.01.050 (2004).
123 Farris, A. L., Rindone, A. N. & Grayson, W. L. Oxygen Delivering Biomaterials for Tissue Engineering. *J Mater Chem B* **4**, 3422-3432, doi:10.1039/C5TB02635K (2016).
124 Sen Gupta, A. Hemoglobin-based Oxygen Carriers: Current State-of-the-art and Novel Molecules. *Shock* **52**, 70-83, doi:10.1097/SHK.0000000000001009 (2019).
125 Zisch, A. H. *et al.* Cell-demanded release of VEGF from synthetic, biointeractive cell ingrowth matrices for vascularized tissue growth. *FASEB J* **17**, 2260-2262, doi:10.1096/fj.02-1041fje (2003).
126 Falschlehner, C., Schaefer, U. & Walczak, H. Following TRAIL's path in the immune system. *Immunology* **127**, 145-154, doi:10.1111/j.1365-2567.2009.03058.x (2009).

127 Miller, S. D., Turley, D. M. & Podojil, J. R. Antigen-specific tolerance strategies for the prevention and treatment of autoimmune disease. *Nat Rev Immunol* **7**, 665-677, doi:10.1038/nri2153 (2007).
128 Lau, H. T., Yu, M., Fontana, A. & Stoeckert, C. J., Jr. Prevention of islet allograft rejection with engineered myoblasts expressing FasL in mice. *Science* **273**, 109-112, doi:10.1126/science.273.5271.109 (1996).
129 Yolcu, E. S. *et al.* Pancreatic islets engineered with SA-FasL protein establish robust localized tolerance by inducing regulatory T cells in mice. *J Immunol* **187**, 5901-5909, doi:10.4049/jimmunol.1003266 (2011).
130 Cuff, C. A., Martiney, J. A., Berman, J. W. & Brosnan, C. F. Differential effects of transforming growth factor-beta 1 on interleukin-1-induced cellular inflammation and vascular permeability in the rabbit retina. *J Neuroimmunol* **70**, 21-28, doi:10.1016/s0165-5728(96)00103-8 (1996).
131 Martinez, F. O., Sica, A., Mantovani, A. & Locati, M. Macrophage activation and polarization. *Front Biosci* **13**, 453-461, doi:10.2741/2692 (2008).
132 Sanchez-Martin, L. *et al.* The chemokine CXCL12 regulates monocyte-macrophage differentiation and RUNX3 expression. *Blood* **117**, 88-97, doi:10.1182/blood-2009-12-258186 (2011).
133 Chen, G. *et al.* Intragraft CD11b(+) IDO(+) cells mediate cardiac allograft tolerance by ECDI-fixed donor splenocyte infusions. *Am J Transplant* **12**, 2920-2929, doi:10.1111/j.1600-6143.2012.04203.x (2012).
134 Wang, L. *et al.* Neural stem/progenitor cells modulate immune responses by suppressing T lymphocytes with nitric oxide and prostaglandin E2. *Exp Neurol* **216**, 177-183, doi:10.1016/j.expneurol.2008.11.017 (2009).
135 Chen, T. *et al.* Alginate encapsulant incorporating CXCL12 supports long-term allo- and xenoislet transplantation without systemic immune suppression. *Am J Transplant* **15**, 618-627, doi:10.1111/ajt.13049 (2015).
136 Montane, J. *et al.* CCL22 Prevents Rejection of Mouse Islet Allografts and Induces Donor-Specific Tolerance. *Cell Transplant* **24**, 2143-2154, doi:10.3727/096368914X685249 (2015).
137 Madden, L. R. *et al.* Proangiogenic scaffolds as functional templates for cardiac tissue engineering. *Proc Natl Acad Sci U S A* **107**, 15211-15216, doi:10.1073/pnas.1006442107 (2010).
138 Yan, Z., Zhuansun, Y., Chen, R., Li, J. & Ran, P. Immunomodulation of mesenchymal stromal cells on regulatory T cells and its possible mechanism. *Exp Cell Res* **324**, 65-74, doi:10.1016/j.yexcr.2014.03.013 (2014).
139 Lee, S. *et al.* Analysis on migration and activation of live macrophages on transparent flat and nanostructured titanium. *Acta Biomater* **7**, 2337-2344, doi:10.1016/j.actbio.2011.01.006 (2011).
140 Cao, H., McHugh, K., Chew, S. Y. & Anderson, J. M. The topographical effect of electrospun nanofibrous scaffolds on the in vivo and in vitro foreign body reaction. *J Biomed Mater Res A* **93**, 1151-1159, doi:10.1002/jbm.a.32609 (2010).
141 Barbeau, D. J. *et al.* Early growth response-2 signaling mediates immunomodulatory effects of human multipotential stromal cells. *Stem Cells Dev* **23**, 155-166, doi:10.1089/scd.2013.0194 (2014).
142 Luz-Crawford, P. *et al.* Mesenchymal stem cells generate a CD4+CD25+Foxp3+ regulatory T cell population during the differentiation process of Th1 and Th17 cells. *Stem Cell Res Ther* **4**, 65, doi:10.1186/scrt216 (2013).

143 Ding, Y. *et al.* Mesenchymal stem cells prevent the rejection of fully allogenic islet grafts by the immunosuppressive activity of matrix metalloproteinase-2 and -9. *Diabetes* **58**, 1797-1806, doi:10.2337/db09-0317 (2009).

144 Kerby, A., Jones, E. S., Jones, P. M. & King, A. J. Co-transplantation of islets with mesenchymal stem cells in microcapsules demonstrates graft outcome can be improved in an isolated-graft model of islet transplantation in mice. *Cytotherapy* **15**, 192-200, doi:10.1016/j.jcyt.2012.10.018 (2013).

145 Graham, J. G. *et al.* PLG scaffold delivered antigen-specific regulatory T cells induce systemic tolerance in autoimmune diabetes. *Tissue Eng Part A* **19**, 1465-1475, doi:10.1089/ten.TEA.2012.0643 (2013).

CHAPTER 2: Diabetes therapy at the push of a button – Autonomous push-button-controlled rapid insulin release from a piezoelectrically activated subcutaneous cell implant

Haijie Zhao[1], Shuai Xue[1], Marie-Didiée Hussherr[1], Ana Palma Teixeira[1], Martin Fussenegger[1,2,*]

[1]Department of Biosystems Science and Engineering, ETH Zurich, Mattenstrasse 26, CH-4058 Basel, Switzerland.

[2]Faculty of Science, University of Basel, Mattenstrasse 26, CH-4058 Basel, Switzerland

[*]Corresponding author. E-mail: fussenegger@bsse.ethz.ch

The work presented in this chapter has been published in the peer reviewed journal "Science Advances". DOI: 10.1126/sciadv.abm4389

Traceless physical cues are desirable for remote control of the in-situ production and real-time dosing of biopharmaceuticals in cell-based therapies. However, current optogenetic, magnetogenetic or electrogenetic devices require sophisticated electronics, complex AI-assisted software, and external energy supplies for power and control. Here, we describe a self-sufficient subcutaneous push-button-controlled cellular implant powered and activated to release a biopharmaceutical simply by repeated gentle finger pressure exerted on the overlying skin. Pushing the button causes transient percutaneous deformation of the implant's embedded piezoelectric membrane, which produces sufficient low-voltage energy inside a semi-permeable platinum-coated cell chamber to mediate rapid release of a biopharmaceutical from engineered electro-sensitive human cells. Release is fine-tuned by varying the frequency and duration of finger-pressing stimulation. As proof-of-concept, we show that finger-pressure activation of the subcutaneous implant can restore normoglycemia in a mouse model of type-1 diabetes. Self-sufficient push-button devices may provide a new level of convenience for patients to control their cell-based therapies.

Introduction

Engineered cell-based therapies hold great promise for the treatment of a wide range of chronic diseases. Advances in the field of synthetic biology have made it possible to engineer cells with reliable sense-and-response therapeutic programs, which, upon implantation in mouse models, can treat chronic pain[1], obesity[2], gouty arthritis[3], liver disease[4], and diabetes[5-8], and can reverse muscle atrophy[9]. Early synthetic gene switches relied on soluble small molecules e.g., antibiotics[10,11] or food components[1,5,12] as external input signals to control cellular behavior. The development of genetic switches responsive to traceless physical cues, such as light[13-15], magnetic fields[16], ultrasound[17] and more recently electrical signals[8], overcame the challenges associated with systemic delivery of chemical inducers and improved the spatiotemporal resolution of therapeutics delivery. Among currently available types of physically triggered gene switches, electrogenetic switches have the advantage of simplifying the process of energy conversion, enabling direct electrical control of cellular functions.

Electrical signals regulate a variety of processes in human physiology, such as contraction of cardiomyocytes[18], secretion of hormones by endocrine cells, and release of neurotransmitters by neurons[19-21]. These actions are mediated by many proteins in the plasma membrane, including ion channels that allow ions to flow across the membrane. Inspired by the action potentials in electrically active cells, we recently engineered non-excitable cells to perceive externally applied electrical signals by overexpression of specific ion channels and to react by secreting insulin[8]. In the first proof-of-concept application of electrogenetics to control cell-based therapies, we showed that an implant containing these cells could successfully treat type-1 diabetic mice[8]. However, the cell encapsulation device required sophisticated electronics and relied on an external power supply to electrically stimulate the implanted therapeutic cells. Instead, encapsulation devices independent of an external power source would have great practical significance for disease therapy.

The ability of piezoelectric materials to generate voltage upon mechanical deformation has attracted considerable attention for biomedical applications, such as health monitoring[22,26] and tissue engineering[27-29]. Advances in the nanofabrication of piezoelectric materials have improved various properties, including flexibility[24], higher voltage supply[30] and stretchability[31]. Biocompatible piezoelectric polyvinylidene difluoride (PVDF)-based films[32,33] have been employed as power sources in many implantable devices, serving to convert the mechanical forces from heart, diaphragm or muscles[34-36] into electricity. We considered that combining piezoelectric materials with electrogenetics could enable self-powered and self-controlled, voltage-based systems for programming electro-inductive designer cells. However, the low

amplitude and frequency of mechanical forces generated by organs restricts the voltage generated by piezoelectric materials to a level below the voltage required for triggering these cells by direct coupling stimulation[8,37]. In this work, we aimed to develop and test a cellular encapsulation device that can efficiently utilize the low voltage generated by gentle finger-pushing a PVDF film-based piezoelectric module in order to trigger encased electro-sensitive human designer cells to produce a therapeutic output. As a proof of concept, we show that finger-push-triggered insulin secretion from the developed subcutaneously implanted button-like devices could successfully restore normoglycemia in type-1 diabetic mice.

Results

Toward piezo-triggered electro-inducible vesicular secretion

First, we evaluated the suitability of piezoelectric PVDF films for electrical stimulation of electro-sensitive cells derived from the pancreatic beta cell line 1.1E7[8], which was engineered to express proinsulin, as well as for constitutive expression of $Ca_V1.2$ and $K_{ir}2.1$ channels. Indeed, we found that the piezoelectrically generated electric charge stimulated the opening of the voltage-gated $Ca_V1.2$ channels, triggering the release of insulin stored in secretory vesicles (**Fig. 1A**). We initially tested the most common electrical stimulation method, which is direct coupling using electrodes placed in the culture medium[37,38], connected to each side of the PVDF-based piezoelectric module to provide the positive and negative charges (**Fig. 1B**). The electrodes were arranged in two configurations in relation to the cell monolayer, generating an electric field above (**Fig. 1C, E**) or across (**Fig. 1D, F**) the monolayer. However, although KCl-induced membrane depolarization activated insulin secretion in electro-sensitive cells, they did not respond to the voltage generated by finger-pushing a 52 μm thick piezoelectric module for 3 min at 1 Hz in either of the electrode arrangements, as similar reporter insulin levels were secreted by stimulated and non-stimulated cells (**Fig. 1G, H**).

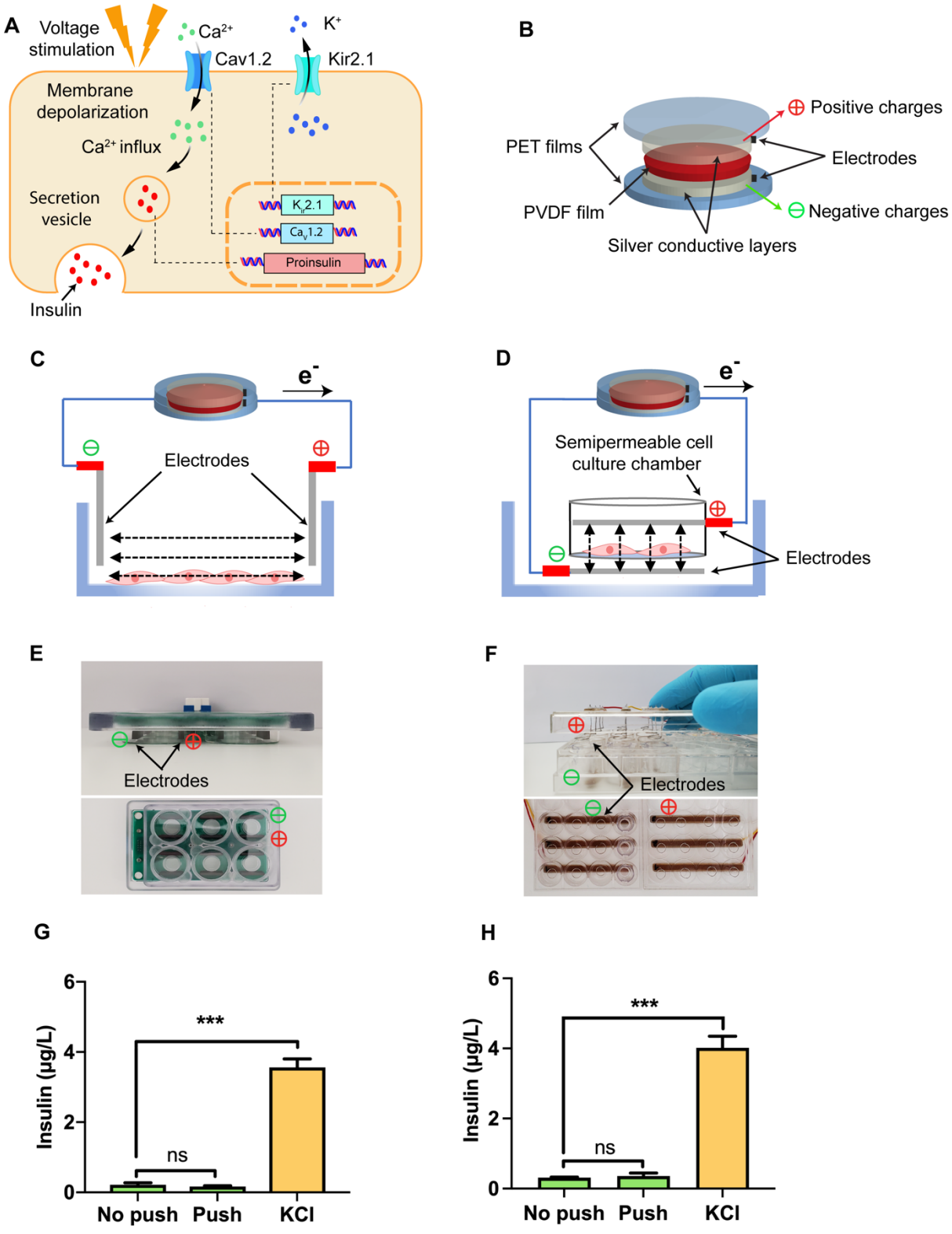

Figure 1. Stimulation of electro-sensitive cells with piezoelectric pulses. **(A)** Upon membrane depolarization of engineered electro-sensitive cells constitutively expressing the channels Cav1.2 and $K_{ir}2.1$ and a synthetic Proinsulin construct, the intracellular calcium concentration is increased, which drives the release of vesicle-stored insulin. **(B)** Illustration of the prototypic

piezoelectric module. The electrodes are connected to the top and bottom sides of a silver-coated PVDF film, providing positive and negative charges, respectively. (**C**, **E**) Scheme and image of the stimulation cell culture multiwell plate with electrodes aligned vertically in relation to the cell monolayer. (**D**, **F**) Scheme and image of stimulation cell culture inserts and multiwell plate with electrodes aligned horizontally in relation to the cell monolayer. Cells were cultured on a porous membrane inside inserts, with one electrode placed above and one below the cell monolayer to generate an electric field across it. For both vertical (**G**) and horizontal (**H**) electrode configurations, piezoelectrical pulses were produced for 3 min at 1 Hz by finger-pressing a piezoelectric module with a 52 μm PVDF film placed on human skin to allow sufficient deformation. Cells were also either non stimulated or treated with 40 mM KCl (chemical depolarization) as negative and positive controls, respectively. Insulin expression level was measured in culture supernatant samples collected after 3 min of stimulation. Data are means ± SEM; n = 4. Statistical analysis was done with a two-tailed t-test. ns not significant, ***P < 0.001.

Design of a piezoelectrically powered implant

We hypothesized that a more conductive cell-culture chamber might enable the low voltage generated from the piezoelectric material to trigger electro-sensitive cells. Therefore, we modified commercially available cell culture inserts (**Fig. 1D**) by coating their entire surface with a thin platinum layer (**Fig. 2A**), including the semipermeable membrane, which retained an average pore diameter of 0.4 μm (**Fig. 2B**), and connected two electrodes on opposite sides of the cell chamber. To test the conductive chamber for low-voltage electrostimulation, we applied unipolar square pulses with alternate polarization to electro-sensitive cell cultures and measured the insulin responses to different voltages, stimulation frequencies and stimulation periods. Indeed, the conductive chamber significantly improved the efficiency of electrostimulation, with secretion of insulin peaking at 1 V (**Fig. 2C**), 1 Hz (**Fig. 2D**) and after 3 min of stimulation (**Fig. 3E**). There is no observed false activation from electro-sensitve cells (**Fig. S2**). The electro-sensitive cells had released all of their stored insulin after 10 min of stimulation, reaching levels similar to those obtained with KCl stimulation (**Fig. 2C, E**). Indeed, the highest level of insulin production is achieved with 10-15 min stimulation, without affecting the cell viability. Nevertheless, 3 min stimulation provides also significant insulin induction levels, which are only about 20% lower than the maximum achieved levels. Therefore, we selected 3 min for follow up experiments because shorter

stimulation times are preferred for patient's convenience. Importantly, the cell viability was not impacted at these voltages (**Fig. 2F)** and frequencies (**Fig. 2G**). Next, we tested whether the PVDF-based piezoelectric module (**Fig. 1A**) connected to the electrodes in the conductive cell chamber could stimulate the electro-sensitive cells. For this purpose, the piezoelectric module was placed above human skin and gently finger-pressed for 3 min, which showed maximum insulin secretion at frequencies over 1 Hz (**Fig. 2H**). The pressure generated by finger-pushing corresponds to 1 kPa (0.1 N/cm^2), which is lower than typing on a keyboard[39]. The electrosensitive cells could also be stimulated by an electric toothbrush (E-toothbrush), which vibrates with 50 Hz vibration and produces 1 V when placed on top of the piezoelectric module (**Fig. S1**). The use of an E-toothbrush also activated insulin secretion within 3 min of stimulation and reached similar levels as achieved by finger pushing at 1 Hz (**Fig. 2H**). E-toothbrush control of insulin expression could be a highly convenient and straightforward and compliant way to trigger insulin secretion after each meal, simply by brushing the teeth for three minutes.

We also evaluated how long it would take for the cells to replenish their insulin pool in secretory vesicles, by performing a second stimulation 1 to 4 h after the first stimulation. As expected, the amount of secreted insulin increased as the interval between stimulations became longer, with the insulin response to the second stimulation reaching that of the first stimulation when the interval was 4 h (**Fig. 2I**). The cells responded repeatedly with reproducible insulin secretion kinetics to two consecutive stimulations within 4 h (**Fig. 2J**). Together, these data demonstrate that the electricity generated by transient deformation of the piezoelectric module can stimulate the electro-sensitive cells in the conductive chamber, matching the stimulation achieved by an external power source (**Fig. 2C**, **2D**, **2E**) which shows piezoelectric module can be employed as a reliable self-sufficient power source for electro-stimulation.

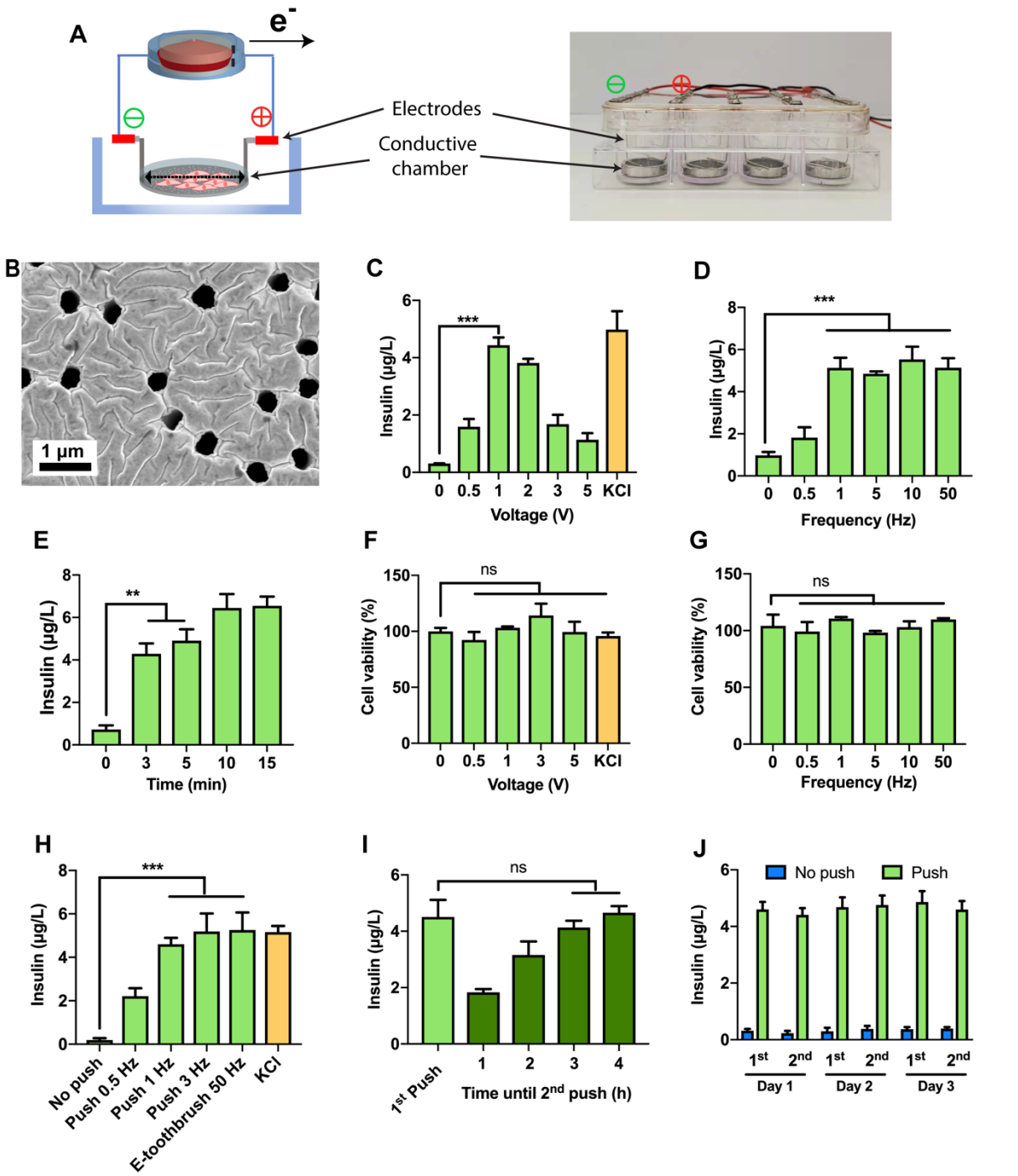

Figure 2. Design and *in vitro* characterization of the conductive chamber. (**A**) Schematic representation and picture of the conductive cell culture chamber containing a porous membrane for cell attachment and two electrodes connected on opposite sides of the chamber. The whole chamber, including the porous membrane, is coated with a thin platinum (Pt) layer. (**B**) Scanning electron microscopy (SEM) image of the porous membrane, showing that the Pt deposition had no effect on the average pore size of 0.4 µm (shown in black). (**C-E**) Insulin secretion level upon stimulation of electro-sensitive cells by a pulse generator. (**C**) Voltage

dependence. Electrical stimulation was performed for 3 min at 1 Hz, at the indicated voltages. (**D**) Frequency effect. Electrical stimulation was performed at the indicated frequencies for 3 min at 1 V. (**E**) Stimulation time dependence. Electrical stimulation was performed for the indicated time periods at 1 V and 1 Hz. (**F-G**) Cell viability after electrical stimulation for 30 min at (**F**) 1 Hz and the indicated voltages, or (**G**) 1 V and the indicated frequencies. (**H**) Insulin secretion level upon stimulation of electro-sensitive cells with voltage generated by finger pressure or E-toothbrush on a 28 μm thick piezoelectric module for 3 min at the indicated frequencies. (**I**) Reload kinetics of vesicular insulin. Cells were stimulated twice during 3 min with the indicated time intervals between stimulations. (**J**) Reversibility assay. Electro-sensitive cells were stimulated twice for 3 min with a 4 h interval between the first and second electrostimulation on each day in period of 3 days. Data are means ± SEM. Statistical analysis was done with a two-tailed t-test (n = 3). ns not significant, *P < 0.05, **P < 0.01, ***P < 0.001.

Optimization and validation of the push-button implant design in vitro

To make a compact, subcutaneously implantable piezoelectric-based device, we sandwiched a semipermeable platinum-coated cell chamber and a piezoelectric module with a reinforcement ring between them (**Fig. 3A**). The bottom membrane of the cell culture chamber allows exchange of oxygen, nutrients and therapeutic proteins, and protects the cells from the host's immune system. This conductive chamber is linked by platinum wires to the piezoelectric module for voltage transfer. The reinforcement ring, 3D-printed in FDA-licensed polylactide, protects the top membrane from the mechanical force of pressing and provides space for deformation of the piezoelectric module. The resulting button-like implant device is smaller than a 1-cent Euro coin and smaller than a U.S. dime (**Fig. 3B**). The magnitude of the voltage generated on the surface of piezoelectric module when a mechanical force is applied depends on the thickness of the film. Finger-pushing a 28 or 52 μm thick PVDF film-based piezoelectric module placed on human skin with pressures around 1 kPa provides voltages of 1 V or 2 V, respectively (**Fig. 3C**). We also characterized the voltages generated by the piezoelectric module on top of the cell culture chamber using reinforcement rings of different thicknesses (0.5, 1 and 2 mm) to determine the minimum thickness (for a more compact design) that would provide enough space for deformation of the module by finger-pushing. Rings of 1 or 2 mm were sufficient to generate 1 V or 2 V from 28 or 52 μm PVDF films, respectively (**Fig. 3D-F**). Thus, we chose 28 μm as the optimal thickness of the PVDF film to deliver 1 V

upon deformation and 1 mm as the minimum thickness of the reinforcement ring to provide sufficient space for film deformation. To validate the button-like device *in vitro*, electro-sensitive cells were loaded inside the cell culture chamber and the piezoelectric module on top was finger-pressed for 3 min at 1 Hz. The stimulated cells secreted 20-fold more insulin than non-stimulated cells, and the amount was comparable to that released by cells depolarized with 40 mM KCl (**Fig. 3G**). When the stimulation time was extended to 30 min, the level of secreted insulin plateaued (**Fig. 3H**), suggesting that cells released all of their vesicle-stored insulin during this period.

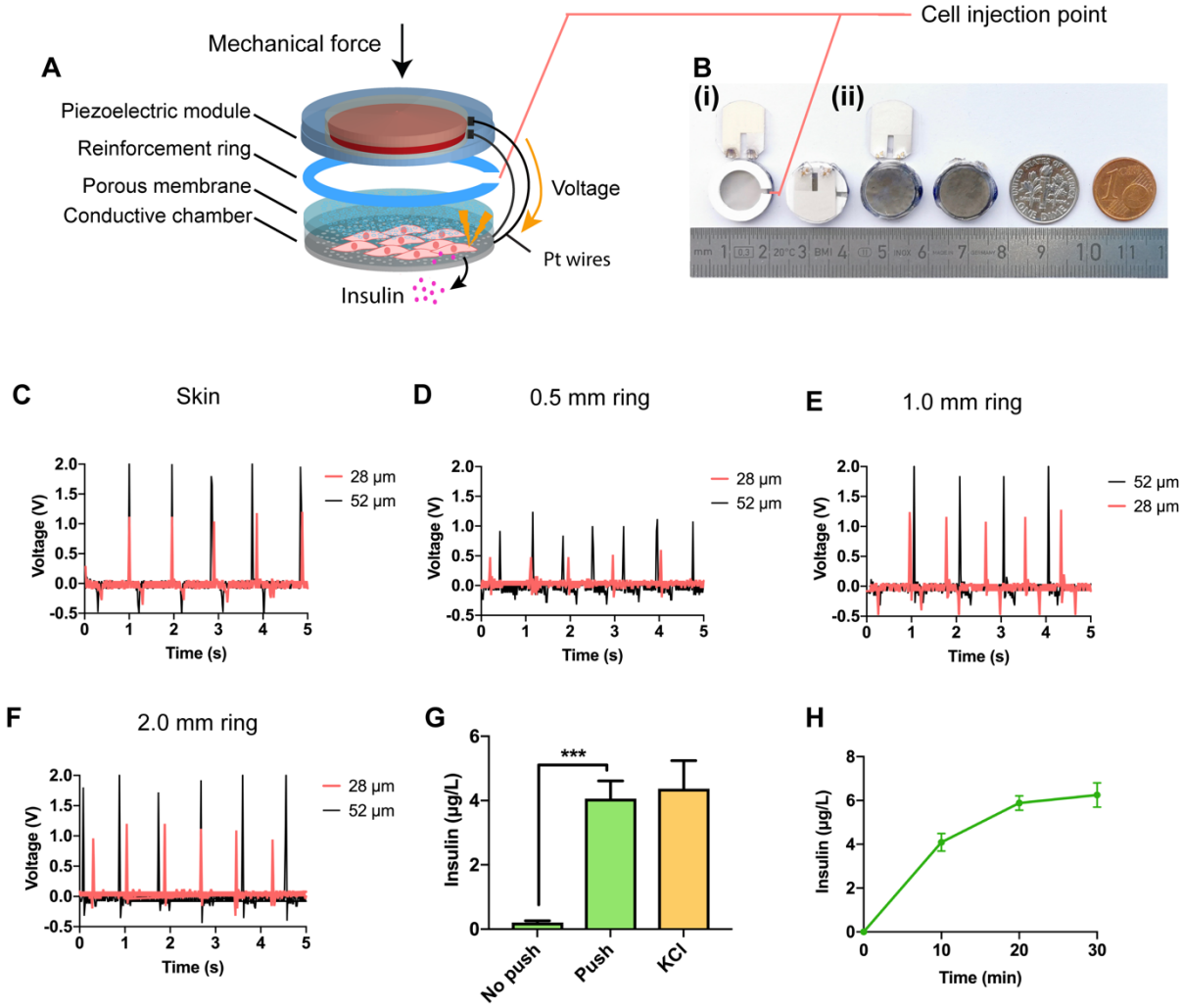

Figure 3. Design and *in vitro* characterization of the button-like cellular device. (**A**) Schematic representation of the device. The cell chamber is delimited by two porous membranes, with the bottom one also coated with platinum (Pt). A reinforcement ring is placed between the piezoelectric module and the conductive cell chamber. The piezoelectric module is linked by Pt wires to the conductive cell chamber, which encases engineered electro-sensitive cells. The conductive chamber allows diffusion of nutrients and therapeutic protein in and out of the device, as well as protecting the cells from immune system attack. (**B**) Pictures of the (i) top

and (ii) bottom sides of unfolded and folded devices. The cells are injected into the cell culture chamber via a port in the reinforcement ring, followed by heat sealing of the porous membrane. Piezoelectric voltage output generated by finger-pushing the piezoelectric module on different materials. (**C**) Output voltage generated by periodically finger-pressing PVDF film-based piezoelectric modules of 28 and 52 μm thickness on top of human skin (applied pressure: around 1 kPa). (**D-F**) Voltage generated from piezoelectric module placed above 0.5 mm (**D**), 1 mm (**E**), and 2 mm (**F**) reinforcement rings. (**G**) Insulin secretion by electro-sensitive cells upon electrostimulation by finger-pushing the button-like implant for 3 min at 1 Hz. Non-stimulated and KCl-stimulated cells were used as negative and positive controls, respectively (**H**) Insulin secretion kinetics. Electro-sensitive cells were stimulated for 30 min by finger-pushing and insulin levels in the cell chamber were analyzed by ELISA. Data are means ± SEM. Statistical analysis was done with a two-tailed t-test (n = 3). *P < 0.05, **P < 0.01, ***P < 0.001.

Biocompatibility and longevity of the push-button implant in vivo

The biocompatibility of the button-like implant was assessed at 30 days after subcutaneous implantation in the dorsal back of mice. We observed no systemic toxicity of the kidneys or liver of treated animals (**Table S1**) and no local immune cell infiltration of the implant, as validated according to ISO 10993. Histological images of a middle section of the cell culture chamber (**Fig. 4A**) and a section at the electrode side (**Fig. 4J**) of explanted devices revealed no apparent difference between the well-vascularized fibrous capsule surrounding cell-free (**Fig. 4B, 4C, 4K, 4L, Table S2**) and cell-containing (**Fig. 4F, 4G**) implants. Likewise, there was no apparent difference in immune cell infiltration in the fibrotic tissue around the cell-free (**Fig. 4D and 4E**) and cell-containing (**Fig. 4H and 4I**) implants. Finally, a functionality assessment of the explanted devices showed that they could still produce about 1 V in response to finger-pushing the piezoelectric module at 30 days after implantation (**Fig. 4M**), and there was no decline in performance compared with before implantation (**Fig. 3E**).

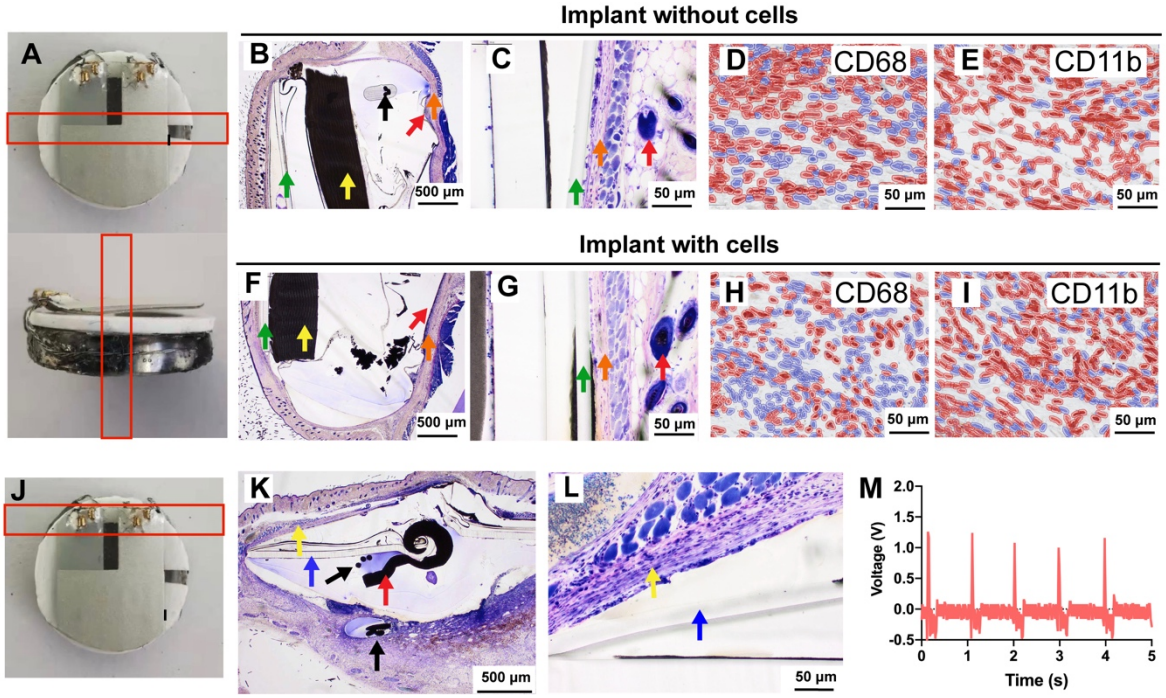

Figure 4. Biocompatibility of the piezoelectrical cell implants (**A**) Images of the implant sections (red frames) analyzed for histopathology and immunohistochemistry. The button-like implants were placed subcutaneously on the dorsal side of mice for 30 days. The samples were stained with Paragon (toluidine blue and basic fuchsin) for assessment of fibrotic capsule formation. Overview of the cell culture chamber section **(B)** without and **(F)** with cells. Green arrow – piezoelectric module; yellow arrow – reinforcement ring; black arrow – platinum wires; red arrow – membrane of conductive chamber; orange arrow - fibrotic tissue. (**C,G**) Magnified view of the chamber section. Red arrow - blood vessel; orange arrow – fibrocytes; green arrow – piezoelectric module. (**D, H**) The adherent tissues around the implant were immunostained with anti-CD68 antibodies. CD68-positive cells are red-circled and mark activated macrophages and fibroblasts. (**E, I**) CD11b-positive cells are red-circled and indicate macrophages, neutrophils and NK cells. Histopathology of electrode section. (**J**) Image of the electrode section (red frame) analyzed for histopathology. (**K**) Overview of the electrode section. yellow arrow - fibrotic tissue; blue arrow - piezoelectric module; black arrow - platinum wires; red arrow - electrodes. (**L**) Magnification of the chamber section. Blue arrows - piezoelectric module; yellow arrow - fibrocytes. (**M**) Functionality of the explanted devices at 30 days after implantation. Representative output voltage generated by periodically finger-pressing an explanted piezoelectrical cell implant.

Push-button therapeutic control of experimental type-1 diabetes

The mechanoelectrical actuation of engineered electro-sensitive cells enabled by piezoelectric materials has several advantages for implementation of cell-based therapies, as it enables traceless control, can be easily activated by gentle finger-pushing without the need for external power sources to apply the electrical stimulation, and provides an extremely compact design not requiring any electronic parts or batteries (**Fig. 5A**). For pre-clinical proof-of-concept, the button-like devices loaded with electro-sensitive insulin-producing cells were subcutaneously transplanted into type-1-diabetic mice. Mice stimulated by finger-pushing the skin immediately above the implant showed a rapid decrease in fasting blood-glucose levels, while non-stimulated mice showed continued hyperglycemia (**Fig. 5B**), confirming the effectiveness of finger-push-mediated remote control of insulin release by the implanted cells. Peak blood insulin levels were reached 2 h after initiating the stimulation (**Fig. 5C**). The button-like cellular device could also provide sufficient insulin to rapidly attenuate postprandial blood-glucose levels during glucose-tolerance tests (**Fig. 5D**). In contrast, blood glucose levels remained high in mice without the implant and in implanted animals that were not stimulated with finger-pushing. Blood insulin levels were monitored during one week, and mice stimulated by finger-pushing consistently showed significantly higher insulin levels compared with those of non-stimulated mice (**Fig. 5E**). Furthermore, it should be noted that all mice (finger-push treated and controls) are freely moving inside the cages and occasionally bump into each other or in the cage walls. For the real-time blood glucose monitoring experiments and glucose tolerance tests (**Figs. 5B-D**), the mice were anesthetized during the finger-pushing period, but then were in normal activation during the 2 h monitoring period. Therefore, we believe our device does not have potential risk for false activation. Altogether, these results indicate that simply pushing the skin above the subcutaneously implanted button-like cellular device can activate insulin secretion by encapsulated electro-sensitive designer cells to control type-1 diabetes.

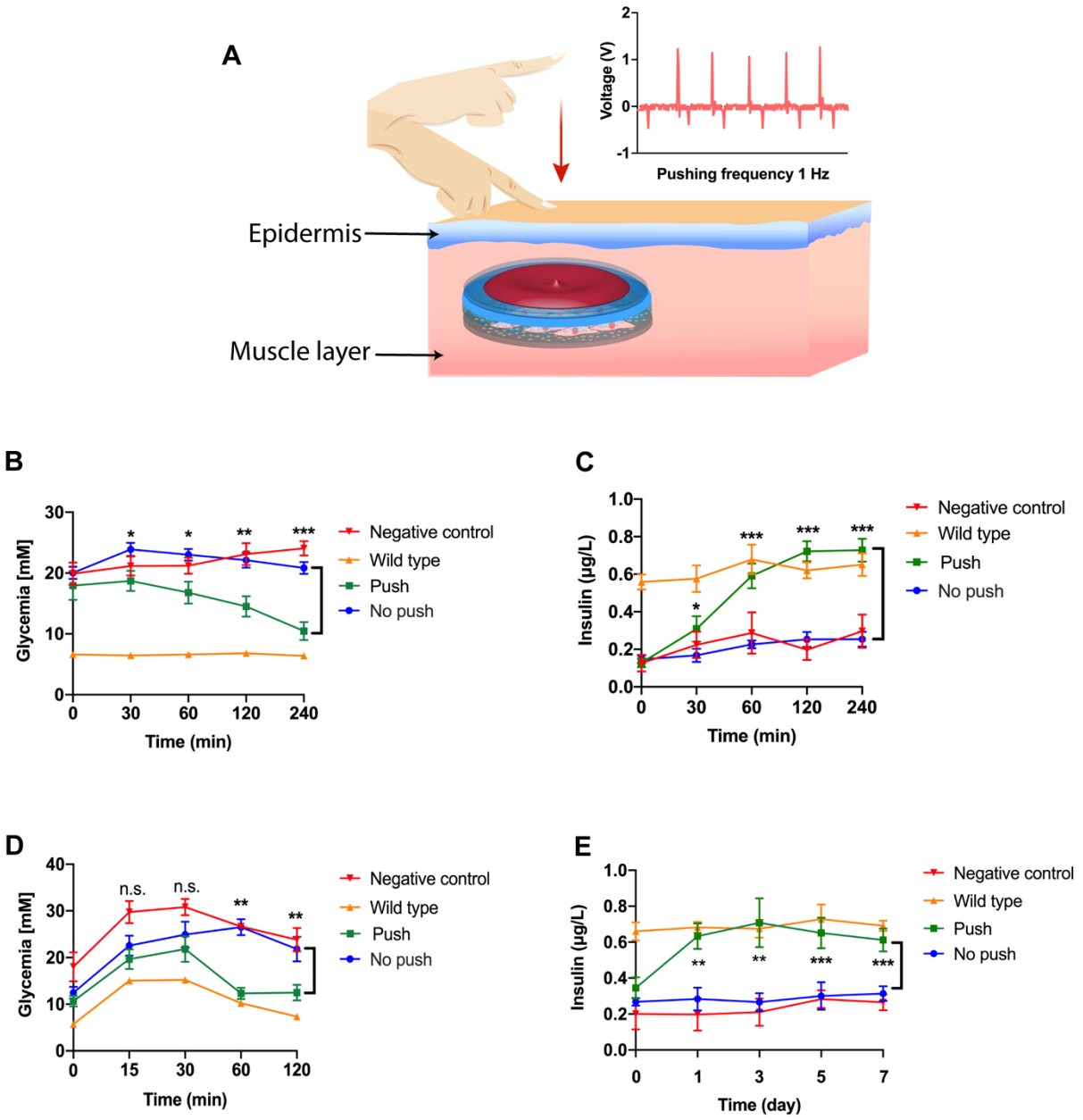

Figure 5. *In vivo* performance of the button-like cellular implant. (**A**) Electric pulses are generated by finger-pushing the skin above a subcutaneously implanted cellular device incorporating a piezoelectric module. (**B-C**) Wild-type or type 1 diabetic mice with subcutaneously implanted devices were fasted for 4 h before finger-push stimulation at around 1 Hz frequency. Blood samples were collected at indicated time points. Non-stimulated mice were used as controls. Time courses of blood (**B**) glucose and (**C**) insulin levels. (**D**) Glucose tolerance test. Wild-type or type 1 diabetic mice were treated by finger-pressing the skin above the cellular implant, and then injected intraperitoneally with 1.25 g of glucose per kg body weight. (**E**) The button-like devices were subcutaneously implanted into type 1 diabetic mice and insulin levels were recorded every 2 days after of finger-push stimulation, over a period of

7 days. The statistical significance of the difference between the finger-push and no push groups was calculated. Data are means ± SEM. Statistical analysis was done with a two-tailed t-test (n = 5). ns not significant, *P < 0.05, **P < 0.01, ***P < 0.001.

Discussion

Engineered cell-based therapies are changing the treatment landscape of life-threatening diseases, constituting an important pillar in modern medicine[40,41]. The first translational successes were recently achieved with chimeric antigen receptor (CAR) T cell therapies approved for blood cancers[42], and an increasing number in clinical development. In these cell immunotherapies, patient's own T cells are modified with anti-tumor synthetic receptors to trigger their killing activity upon recognition of tumor cells displaying the target antigens. However, cytokine release syndrome or off-tumor toxicity are common safety concerns, which are being addressed by applying multiple synthetic biology approaches[43,44]. Beyond cancer, other diseases requiring chronic administration of precisely dosed therapeutic proteins could benefit greatly from cell therapy approaches relying on synthetic gene switches to enable the required control. Engineered cell therapies based on allogeneic cell sources are at early stages of pre-clinical development, targeting numerous diseases, such as metabolic diseases[4], infections[45], and autoimmunity[46], among others. They have been tested in animal models by implantation subcutaneously or intraperitoneally, using some form of encapsulation to protect the cells from the host's immune system. While chemically induced gene switches were initially used, recent developments have focused mainly on regulation by traceless physical stimuli such as light (optogenetics)[13-15], magnetic fields (magnetogenetics)[16], ultrasound (sonogenetics)[17] and electrical stimulation (electrogenetics)[8]. Physical triggers are particularly attractive for chronic disease management as the stimulus can be controlled both temporally and spatially, enabling precise control over the cellular therapeutic response. In the present work, we have developed a new traceless way to activate transplanted therapeutic cells, which is as simple as pushing a button. Our piezoelectrically-based button-like cellular implant acts as voltage generator when the button is pushed and can trigger encased electro-sensitive cells to secrete an effector protein, bypassing the need for an external power source for activation and electronics for control. We designed the cell culture chamber to meet several key criteria, namely: (i) to have a highly conductive surface for electro-stimulation of cells with a relatively low resistance and energy input, (ii) to be permeable to nutrients and therapeutic protein but shield the implanted cells from the host immune system, (iii) to have good

mechanical properties and thus be resilient to repeated finger-pushing, and (iv) to show good biocompatibility. For in vitro and in vivo testing, the device was loaded with engineered cells that can sense electrical signals and respond in a calcium-dependent signaling pathway by releasing vesicle-stored proteins. The piezoelectrically generated electrical charge produced by pressing the button is efficiently transmitted to the cells via the platinum-coated semipermeable cell chamber. As piezoelectric material, we selected PVDF films, based on their high flexibility, easy processability, semipermeability and biocompatibility. Such films have been widely explored for applications in biomedicine and tissue engineering[34-36]. The voltage generated is dependent on the thickness of the PVDF film employed, and we found that 28 μm thick films deliver sufficient voltage (1 V) to maximally stimulate the electro-sensitive cells used here. The push-button device could either be activated by gentle finger pushing at 1 Hz or by using an electric toothbrush vibrating at 50 Hz, which represents a particularly attractive medical intervention to release the insulin after each meal simply by brushing one's teeth.

Furthermore, we confirmed that the cellular response in terms of secreted protein levels can be tuned by the duration of the stimulation period to deliver the energy required for the conductive cell chamber to be active for long enough. Importantly, the activation of the implant through pulsatile mechanoelectrical signals allows for more compact implants, as there is no need for electronic switchboards or batteries, which would increase the size, complexity and susceptibility to errors of the implant.

As an in vivo proof-of-principle, we implanted the device subcutaneously in type-1 diabetic mice. Repeated gentle finger-pressing of the skin above the implantation site, which is reminiscent of the pulsatile nature of hormone secretion[47], was effective to program fast insulin release by electro-sensitive cells in the button-like cellular implant, resulting in the restoration of normoglycemia. Notably, the implant was also able to decrease short-term postprandial high blood-glucose levels with fast kinetics. Although 0.4 μm pore size facilitates nutrient and insulin permeability to keep therapeutic cells viable and functional, it also allows the escape of extracellular vesicles eventually produced by the therapeutic cells, including exosomes (size up to 0.1 μm)[48]. Several cell types have been shown to release exosomes packed with nucleic acids, lipids and proteins, that in a cell transplantation scenario can be transferred to the host cells. The impact of the exosomes released by donor cells on triggering a host immune response in diabetic patients is still unclear[49]. Nevertheless, exosomes have been extensively explored as promising therapeutic delivery vehicles due to their low toxicity, safety profile and ability to easily diffuse through plasma membranes[50,51]. The finger-pressing was so

gentle like typing on a keyboard that treated animals did no show any signs of skin rashes or hepatoma and the need for repeated pushing prevented inadvertent biopharmaceutical release by accidental touches.

For clinical translation, it will be important to confirm the longevity of the piezoelectric device. Implanted PVDF membranes have been validated for up to six months and over seven thousand bending cycles[33] while cells have been shown to remain responsive inside implanted semi-permeable microcontainers for several months[48,52,53] or even years[54]. All of our piezoelectric implants showed a high degree of biocompatibility and remained functional in providing a reliable power soure for electrically triggered biopharmaceutical release over the entire experimental period of thirty days. At the meantime, the encased engineered pancreatic cells are protected by a permeable membrane which allows free diffusion of nutrients for cell survival and functionality. Nevertheless, the decrease in insulin production in relation to in vitro studies might reflect some oxygen or nutrient limitations due to insufficient vascularization of the implantation site. To address these issues, some strategies have been proposed. For instance, implanting empty (cell-free) push-button devices to allow for pre-vascularization before introducing the therapeutic cells inside[48], or incorporating oxygen delivery systems to reduce exposure of the therapeutic cells to hypoxia[55].

For scaling up the push-button device to treat human diabetes, we could take as size reference the Viacyte patch (27 cm^2) encasing stem cell-derived pancreatic progenitors recently used in phase I/II clinical trials[56,57]. The fabrication method employing 3D-printing technology and porous scaffolds[58] should easily allow to attain larger push-button devices with effective conductive surface area to stimulate the therapeutic cells. For human use, the immortalized pancreatic cells used in this study would need to be replaced by more clinically relevant cells, such as primary mesenchymal stem cells[59], engineered with the necessary components to produce insulin (or other therapeutic proteins) in response to electrical stimulation[8].

In a clinical context, such a device could not only greatly simplify the treatment regime of T1D patients who are dependent on frequent insulin injections and could be expected to increase compliance, it may also serve as a blueprint for the treatment of other medical conditions requiring sequenctial secretion of therapeutic peptides such as severe osteoporosis where daily injections of the parathyroid hormone is used to stimulate bone formation[60]. We believe this simple, compact device also has great potential for the implementation of electrogenetics in other next-generation cell-based therapies targeting many currently intractable diseases.

Materials and Methods

Cell culture

Electro-sensitive cells were previously established in our lab by engineering the human pancreatic cell line 1.1E7 (cat. no. 10070101-1VL, Sigma-Aldrich, Saint Louis, MO, USA) to stably co-express the $Ca_v1.2$ and $K_{ir}2.1$ channels, as well as proinsulin containing nano luciferase in C-peptide portion[8]. These cells were routinely cultured in Roswell Park Memorial Institute 1640 medium (RPMI; cat. no. 72400-021, Thermo Fischer Scientific) supplemented with 10% (v/v) fetal bovine serum (FBS; cat. no. 022M3395, Sigma-Aldrich) and 1% (v/v) penicillin/streptomycin solution (PenStrep; Biowest, Nuaillé, France) at 37 °C in a humidified atmosphere containing 5% CO_2. For passaging, cells were detached by incubation in 0.05% trypsin-EDTA (Life Technologies, Carlsbad, California, USA; cat. no. 25300-054) for 5 min at 37 °C, resuspended in cell culture medium and centrifuged for 1 min at 200 x g. Then the supernatant was discarded, and the cells were resuspended in fresh medium and seeded at a density of 1.5 x 10^5 cells/mL. Cell number was quantified using an electric field multichannel cell counting device (Casy Cell Counter and Analyzer Model TT, Roche Diagnostics GmbH, Rotkreuz, Switzerland). For electrostimulation, electro-sensitive cells were cultured in RPMI 1640 medium supplemented with 10% FBS, 1% PenStrep and 2.0 mM $CaCl_2$.

Recording of voltage from PVDF film-based piezoelectric module

PVDF films of 28 μm (cat. no. 1-1002608-0, TE Connectivity, USA) and 52 μm (cat. no. 2-1002608-0-M, TE Connectivity, USA) were placed on top of human skin or reinforcement rings and finger-pushed. The output voltage was recorded on a digital oscilloscope (Rigol DS1052E, Rigol Tehnologies, Inc., PRC). The pressure generated by finger-pushing was measured with a digital force gauge (cat. no. 123946-AW, Sauter FK 50, Sauter, Switzerland).

Preparation of the conductive cell culture chamber

The conductive chamber was customized from Corning Transwell® cell culture inserts (cat.no. 353095, VWR, Switzerland), which were cut to have a height of around 2.5 mm, followed by a sputter process to deposit 200 nm of platinum (Ionfab300, Oxford Instruments, Abingdon, UK) on a PET semipermeable membrane with pore size of 0.4 μm. The resulting conductive layer was imaged using a scanning electron microscope (SEM, JSM-7100F, JOEL, Japan).

Electrostimulation through the culture medium

(a) Electrodes placed vertically in relation to the cell monolayer: a C-dish (Ionoptix, Dublin, Ireland) containing a pair of vertical carbon electrodes that fit into the wells of standard

6-well culture plate was used for transferring the voltage provided by PVDF films. The electro-sensitive cells were seeded at a density of 35,000 cells/cm^2 in 1.4 mL of medium. (b) Electrodes placed horizontally in relation to the cell monolayer: a customized 24-well plate containing a pair of 0.5 mm Pt electrodes (cat. no. HXA 050, Cooksongold Ltd., Birmingham, United Kingdom) placed above and below the cell monolayer was used. Cells were cultured in an insert with a semipermeable membrane (cat. no. 353095, Falcon) at a seeding density of 35,000 cells/cm^2 in 1.7 mL medium. (c) Electrical stimulation applied through the conductive cell chamber: a customized cover contains a pair of 0.5 mm Pt electrodes that fit in individual wells of a standard 24-well plate. The electrodes were connected to the Pt conductive chamber on opposite sides. Cell culture chambers were pretreated with poly-L-lysine to promote cell adhesion (cat. no. P4832, Sigma-Aldrich) before seeding 35,000 cells/cm^2 in 0.5 mL medium. The cells were stimulated by a HP3245A Universal Source function generator or by pressing the piezoelectric module with a finger or using an electric toothbrush (ProtectiveClean 4300, Philips Sonicare).

Insulin quantification

Insulin quantification was measured by mouse ELISA kits or correlation with nano luciferase NLuc. Mouse insulin ELISA kits were used to quantify recombinant mouse insulin levels in culture supernatants (cat. no. 10-1247-01; Mercodia, Uppsala, Sweden) and mouse serum (cat. no. 10-1249-01, Mercodia)**,** according to the manufacturer's instructions. Optical density was measured at 450 nm on a Tecan Infinite® M1000 Pro plate reader and the corresponding concentrations were calculated based on the measured absorbances of manufacturer-provided standard solutions. The concentration of NLuc in cell culture supernatants was measured by using the Nano-Glo Luciferase Assay System (Promega, Madison, Wisconsin, USA, cat. no. N1110). In brief, 10 µL of each supernatant sample was mixed with 10 µL Nano-Glo® substrate-containing buffer (in a ratio of 1:50) in black 384-well plates (cat. no. 781900, Greiner, Germany) and incubated at room temperature for 10 min. Total luminescence was measured with a Tecan Infinite® M1000 Pro plate reader (Tecan Group AG, Maennedorf, Switzerland).

Resazurin-based cell viability analysis

To assess the percentage of viable cells with active metabolism, cells were incubated with 60 µg/mL of resazurin (cat. no. R7017, Sigma-Aldrich, USA) for 2 hours. Fluorescence was then measured with a Tecan Infinite® M1000 Pro plate reader at excitation and emission

wavelengths of 560/9 nm and 590/20 nm, respectively. To calculate the relative cell viability, the fluorescence of non-electrically stimulated cells was set to 100 %.

Preparation of the button-like implant device

The device contains a conductive cell culture chamber, a 28 μm PVDF film-based piezoelectric module (cat. no. 11028362-00, TE Connectivity) and a 3D-printed polylactide reinforcement ring. The PVDF film was glued to a PET film (cat. no. GF98750021-2EA, Sigma) on the back with light-curing silicone adhesive (cat. no. 1212167, Loctite 5055^{TM}, Henkel, USA) and cured under UV light (365 nm wavelength) for 30 seconds to increase the mechanical strength, and then trimmed to match the size of the reinforcement ring. Platinum (Pt) wires were used to link the conductive chamber to the electrodes of the PVDF film. They were connected to the bottom of the conductive chamber by applying electrical conductive gel (cat. no. SKU-0018, Bare Conductive), which was then covered with light-curing silicone adhesive and cured for 30 seconds. Light-curing silicone adhesive was also used to fix the wires to the electrodes in the PVDF film, using the same procedure mentioned above. After connection, the implants were washed in 500 mL ddH_2O for 2 days and sterilized by immersion in 70% ethanol. The bottom conductive membrane of the culture chamber was treated with 0.01% poly-L-lysine solution (cat. no. 25988-63-0, Sigma, Switzerland) for 1 hour and dried at room temperature. Then, porous polycarbonate (PC) membrane (cat. no. 110637, Whatman^{TM}, USA) with a pore size of 0.4 μm was sealed onto the conductive chamber, sparing a region surrounding the port for cell injection. The reinforcement ring was bonded to the cell culture chamber using Epo-Tek 301-2 (cat. no. 301-2; Epoxy Technology Inc., Billerica, MA, USA), followed by washing in 500 mL ddH_2O for 2 days and UV disinfection. For seeding, a cell suspension of 2 x 10^6 cells in 200 μL medium was injected into the conductive chamber via the entry port, and afterwards the PC membrane was fully sealed by heating.

Animal experiments

Type 1 diabetic (T1D) mouse model. Wild-type 8-week-old male C57BL/6J mice were fasted for 4 h and injected with daily doses of freshly diluted streptozocin (STZ; cat. no. S0130, Sigma, Switzerland; 50 mg/kg of body weight in ice-cold 0.1 M citrate buffer) for five consecutive days. Blood glucose levels were measured with a commercial glucometer (Contour® Next; Bayer HealthCare, Levekusen, Germany). Five days after STZ treatment, the animals were anesthetized with inhaled isoflurane and the button-like devices were subcutaneously implanted in their backs. For the glucose tolerance test (GTT), treated mice were fasted for 8 h and then finger-pressing was done above the implantation site, followed by injection of 1.25 g/kg D-glucose and collection of blood samples from the tail vein for glucose

measurement. Fasting blood glucose and insulin levels were measured after 4 hours of food restriction at the indicated time points of finger-pressing stimulation. All experiments involving animals were performed according to the directive of the European Community Council (2010/63/EU) and carried out by Shuai Xue and Marie-Didiée Hussherr (license number: 2997/30779) at ETH Zurich in Basel, Switzerland.

Histology

For hematoxylin and eosin (H&E) staining, liver and kidneys from mice implanted with cell-free and cell-containing devices were collected at 30 days after device implantation. Tissue around the implants was excised, embedded in paraffin, and cut into 2-4 µm slices, followed by staining with H&E. Explanted devices and surrounding tissue were processed by methyl methacrylate resin embedding. The chamber of each device was diamond-sawed (EXAKT 300 CP System; EXAKT Technologies Inc., Oklahoma City, OK, USA) at its central position in the transverse direction at a thickness of approximately 400 µm. The sections were ground to a thickness of approximately 40-60 µm (EXAKT Technologies Inc., Oklahoma City, OK, USA), and stained with Paragon (toluidine blue and basic fuchsin).

Immunohistochemistry (IHC)

IHC was performed using the rabbit monoclonal antibodies anti-CD11b (Ab133357; Lot no.GR3209213-2; Abcam, Cambridge, United Kingdom) and anti-CD68 (ab125212; LotGR300628-28; Abcam, Cambridge, United Kingdom) for all samples. The optimal dilutions for the anti-CD11b and anti-CD68 were established to be 1:7500 and 1:1500, respectively. Epitope retrieval was performed with Bond™ Epitope Retrieval Solution 1 (citrate-based buffer, pH: 5.9-6.1; Leica Biosystems, Wetzlar, Germany) for 20 min at 100°C, before the staining protocol was started.

Histopathology

Histopathology evaluation was performed by AnaPath GmbH using a scoring system according to ISO 10993-6:2016(E). The images were taken by an Olympus UC30 camera.

Image Analysis

Quantitative analyses of immunohistochemistry sections were performed using the image analysis software QuPath (https://qupath.github.io).

Statistical analysis

All in vitro data represent means ± SEM of three independent experiments (n = 3 to 4). For mouse experiments, each treatment group was composed of five mice (n = 5). Comparisons between groups were analyzed using Student's t tests, and the values are expressed as means ±

SEM. Differences were considered statistically significant at $P < 0.05$. Prism 6 software (version 8.0.0, GraphPad Software Inc.) was used for statistical analysis.

Acknowledgments

We would like to thank P. Rimpf for support with platinum deposition, C. Alampi for taking scanning electron microscope images, P. Buchmann for help in the initial stage of the project, S. Cao for support with 3D printing, and M. Xie as well M. Mansouri and H. Zulewski for generous advice. This work was supported by a European Research Council (ERC) advanced grant (ElectroGene; grant no. 785800) and in part by the Swiss National Science Foundation NCCR Molecular Systems Engineering.

Author contributions

H.Z. and M.F. designed the project; H.Z. performed all the cell culture experiments and H.Z. and S.X. designed the implants, H.Z., S.X. and M.D.H. performed the animal experiments; H.Z., S.X., A.P.T. and M.F. designed the experiments and analysed the results; H.Z., S.X., A.P.T. and M.F. wrote the manuscript.

Competing interest

the authors declare no competing interests.

Data and materials availability

All data are available in the main text or the supplementary materials. Requests for materials should be made to the corresponding author.

Supplementary Materials

Diabetes therapy at the push of a button – Autonomous push-button-controlled rapid insulin release from a piezoelectrically activated subcutaneous cell implant

Haijie Zhao[1], Shuai Xue[1], Marie-Didiée Hussherr[1], Ana Palma Teixeira[1], Martin Fussenegger[1,2,*]

[1]Department of Biosystems Science and Engineering, ETH Zurich, Mattenstrasse 26, CH-4058 Basel, Switzerland.

[2]Faculty of Science, University of Basel, Mattenstrasse 26, CH-4058 Basel, Switzerland

[*]Corresponding author. E-mail: fussenegger@bsse.ethz.ch

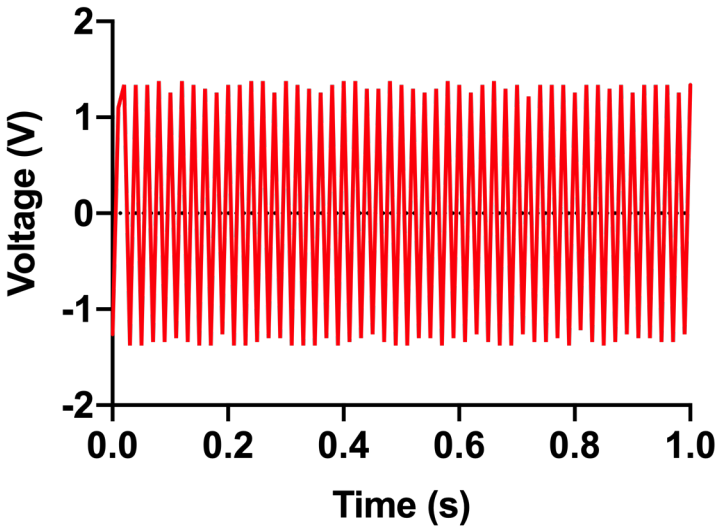

Figure S1. Toothbrush activation of the piezoelectrical device. Output voltage generated by a PVDF film-based piezoelectrical module of 28 μm thickness on top of human skin, mechanically stimulated by a vibrating electric toothbrush.

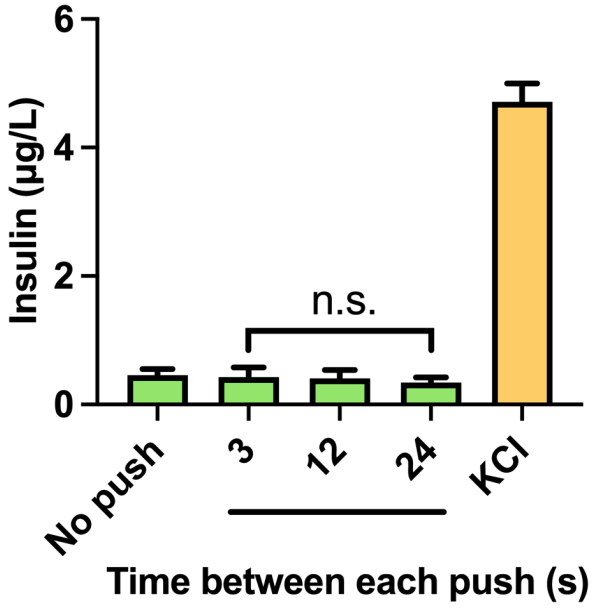

Figure S2. Insulin secretion by electro-sensitive cells upon electrostimulation by finger-pushing the button-like implant for 15 min at intervals of 3, 12 and 24 sec between pushes. "No-push" and KCl-treated cells were used as negative and positive controls, respectively. Data are means ± SEM. Statistical analysis was done with a two-tailed t-test (n = 4). ns: not statistically significant versus "No push" control.

Table S1: Microscopic Findings in Organs Sampled for Systemic Toxicity

Group	Animal Number	Organ	Findings
Implant without cells	1	Kidney	Mononuclear cell foci, unilateral, minimal
		Liver	Hepatocellular glycogen deposits, slight
	2	Kidney	Tubular cell vacuolation, proximal tubules, multifocal, bilateral, minimal; Hyaline casts, focal, unilateral, minimal; Pyelitis, chronic, unilateral, minimal
		Liver	Hepatocellular glycogen deposits, slight
	3	Kidney	Tubular cell vacuolation, proximal tubules, multifocal, bilateral, slight; Mononuclear cell foci, bilateral, minimal
		Liver	Hepatocellular glycogen deposits, slight; Inflammatory cell foci, minimal
Implant with cells	4	Kidney	Pyelitis, chronic, unilateral, minimal; Mononuclear cell foci, unilateral, minimal
		Liver	Hepatocellular glycogen deposits, slight; Inflammatory cell foci, minimal
	5	Kidney	Tubular cell vacuolation, proximal tubules, multifocal, bilateral, slight; Hyaline casts, focal, unilateral, minimal; Mononuclear cell foci, unilateral, minimal
		Liver	Hepatocellular glycogen deposits, slight; Inflammatory cell foci, minimal
	6	Kidney	Tubular cell vacuolation, proximal tubules, multifocal, bilateral, slight
		Liver	Hepatocellular glycogen deposits, slight; Hemopoietic cell foci, minimal

Table S2. Biocompatibility – individual sample data of chamber and sections scores according to the adapted ISO 10993-6:2016(E) Scoring System.

	Implant without cells			**Implant with cells**					
	Chamber Section			**Chamber Section**			**PVDF film**		
Animal No.	**1**	**2**	**3**	**4**	**5**	**6**	**4**	**5**	**6**
Polymorphonuclear	3	2	2	3	3	2	2	3	1
Lymphocytes	1	1	1	1	1	1	1	1	1
Plasma cells	0	0	0	0	0	0	0	0	0
Mast cells	1	1	1	1	1	1	1	1	1
Macrophages	2	3	2	3	3	3	2	2	1
Giant cells	1	1	0	1	1	2	1	1	0
Necrosis	0	0	0	0	0	0	0	0	0
Subtotal (x2)	**16**	**16**	**12**	**18**	**18**	**18**	**14**	**16**	**8**
Neovascularisation	2	3	2	2	2	2	1	2	1
Fibrosis	2	2	2	2	2	3	1	3	1
Edema	1	1	0	1	0	0	0	1	1
Hemosiderin deposits	1	1	1	0	1	2	0	1	0
Fatty infiltrate	0	0	0	0	0	0	0	0	0
Detritus	2	1	3	2	1	2	1	1	0
Subtotal	**8**	**8**	**8**	**7**	**6**	**9**	**3**	**8**	**3**
Total	**24**	**24**	**20**	**25**	**24**	**27**	**17**	**24**	**11**

References

1 Wang, H., Xie, M., Charpin-El Hamri, G., Ye, H. & Fussenegger, M. Treatment of chronic pain by designer cells controlled by spearmint aromatherapy. *Nat Biomed Eng* **2**, 114-123, doi:10.1038/s41551-018-0192-3 (2018).

2 Rossger, K., Charpin-El-Hamri, G. & Fussenegger, M. A closed-loop synthetic gene circuit for the treatment of diet-induced obesity in mice. *Nat Commun* **4**, 2825, doi:10.1038/ncomms3825 (2013).

3 Kemmer, C. *et al.* Self-sufficient control of urate homeostasis in mice by a synthetic circuit. *Nat Biotechnol* **28**, 355-360, doi:10.1038/nbt.1617 (2010).

4 Bai, P. *et al.* A synthetic biology-based device prevents liver injury in mice. *J Hepatol* **65**, 84-94, doi:10.1016/j.jhep.2016.03.020 (2016).

5 Bojar, D., Scheller, L., Hamri, G. C., Xie, M. & Fussenegger, M. Caffeine-inducible gene switches controlling experimental diabetes. *Nat Commun* **9**, 2318, doi:10.1038/s41467-018-04744-1 (2018).

6 Ye, H. *et al.* Self-adjusting synthetic gene circuit for correcting insulin resistance. *Nat Biomed Eng* **1**, 0005, doi:10.1038/s41551-016-0005 (2017).

7 Xie, M. *et al.* beta-cell-mimetic designer cells provide closed-loop glycemic control. *Science* **354**, 1296-1301, doi:10.1126/science.aaf4006 (2016).

8 Krawczyk, K. *et al.* Electrogenetic cellular insulin release for real-time glycemic control in type 1 diabetic mice. *Science* **368**, 993-1001, doi:10.1126/science.aau7187 (2020).

9 Bai, P. *et al.* A fully human transgene switch to regulate therapeutic protein production by cooling sensation. *Nat Med* **25**, 1266-1273, doi:10.1038/s41591-019-0501-8 (2019).

10 Gossen, M. *et al.* Transcriptional activation by tetracyclines in mammalian cells. *Science* **268**, 1766-1769, doi:10.1126/science.7792603 (1995).

11 Weber, W. *et al.* Macrolide-based transgene control in mammalian cells and mice. *Nat Biotechnol* **20**, 901-907, doi:10.1038/nbt731 (2002).

12 Gitzinger, M., Kemmer, C., El-Baba, M. D., Weber, W. & Fussenegger, M. Controlling transgene expression in subcutaneous implants using a skin lotion containing the apple metabolite phloretin. *Proc Natl Acad Sci U S A* **106**, 10638-10643, doi:10.1073/pnas.0901501106 (2009).

13 Ye, H., Daoud-El Baba, M., Peng, R. W. & Fussenegger, M. A synthetic optogenetic transcription device enhances blood-glucose homeostasis in mice. *Science* **332**, 1565-1568, doi:10.1126/science.1203535 (2011).

14 Shao, J. *et al.* Smartphone-controlled optogenetically engineered cells enable semiautomatic glucose homeostasis in diabetic mice. *Sci Transl Med* **9**, doi:10.1126/scitranslmed.aal2298 (2017).

15 Gomelsky, M. Photoactivated cells link diagnosis and therapy. *Sci Transl Med* **9**, doi:10.1126/scitranslmed.aan3936 (2017).

16 Stanley, S. A., Sauer, J., Kane, R. S., Dordick, J. S. & Friedman, J. M. Remote regulation of glucose homeostasis in mice using genetically encoded nanoparticles. *Nat Med* **21**, 92-98, doi:10.1038/nm.3730 (2015).

17 Pan, Y. *et al.* Mechanogenetics for the remote and noninvasive control of cancer immunotherapy. *Proc Natl Acad Sci U S A* **115**, 992-997, doi:10.1073/pnas.1714900115 (2018).

18 Lee, S. *et al.* Ultrasoft electronics to monitor dynamically pulsing cardiomyocytes. *Nat Nanotechnol* **14**, 156-160, doi:10.1038/s41565-018-0331-8 (2019).

19 Cho, S. & von Gersdorff, H. Ca(2+) influx and neurotransmitter release at ribbon synapses. *Cell Calcium* **52**, 208-216, doi:10.1016/j.ceca.2012.06.004 (2012).

20 Ashcroft, F. M. & Rorsman, P. K(ATP) channels and islet hormone secretion: new insights and controversies. *Nat Rev Endocrinol* **9**, 660-669, doi:10.1038/nrendo.2013.166 (2013).
21 Gribble, F. M. & Reimann, F. Function and mechanisms of enteroendocrine cells and gut hormones in metabolism. *Nat Rev Endocrinol* **15**, 226-237, doi:10.1038/s41574-019-0168-8 (2019).
22 Park, D. Y. *et al.* Self-Powered Real-Time Arterial Pulse Monitoring Using Ultrathin Epidermal Piezoelectric Sensors. *Adv Mater* **29**, doi:10.1002/adma.201702308 (2017).
23 Park, K. I. *et al.* Highly-efficient, flexible piezoelectric PZT thin film nanogenerator on plastic substrates. *Adv Mater* **26**, 2514-2520, doi:10.1002/adma.201305659 (2014).
24 Dagdeviren, C. *et al.* Conformal piezoelectric systems for clinical and experimental characterization of soft tissue biomechanics. *Nat Mater* **14**, 728-736, doi:10.1038/nmat4289 (2015).
25 Dagdeviren, C. *et al.* Flexible piezoelectric devices for gastrointestinal motility sensing. *Nat Biomed Eng* **1**, 807-817, doi:10.1038/s41551-017-0140-7 (2017).
26 Boutry, C. M. *et al.* Biodegradable and flexible arterial-pulse sensor for the wireless monitoring of blood flow. *Nat Biomed Eng* **3**, 47-57, doi:10.1038/s41551-018-0336-5 (2019).
27 Bhang, S. H. *et al.* Zinc Oxide Nanorod-Based Piezoelectric Dermal Patch for Wound Healing. *Advanced Functional Materials* **27**, 1603497, doi:10.1002/adfm.201603497 (2017).
28 Zhang, X. *et al.* Piezoelectric Nanotopography Induced Neuron-Like Differentiation of Stem Cells. *Advanced Functional Materials* **29**, 1900372, doi:10.1002/adfm.201900372 (2019).
29 Liu, L. *et al.* Wireless Manipulation of Magnetic/Piezoelectric Micromotors for Precise Neural Stem-Like Cell Stimulation. *Advanced Functional Materials* **30**, 1910108, doi:10.1002/adfm.201910108 (2020).
30 Persano, L. *et al.* High performance piezoelectric devices based on aligned arrays of nanofibers of poly(vinylidenefluoride-co-trifluoroethylene). *Nat Commun* **4**, 1633, doi:10.1038/ncomms2639 (2013).
31 Park, S. *et al.* Stretchable energy-harvesting tactile electronic skin capable of differentiating multiple mechanical stimuli modes. *Adv Mater* **26**, 7324-7332, doi:10.1002/adma.201402574 (2014).
32 Yu, Y. *et al.* Biocompatibility and in vivo operation of implantable mesoporous PVDF-based nanogenerators. *Nano Energy* **27**, 275-281, doi:10.1016/j.nanoen.2016.07.015 (2016).
33 Li, J. *et al.* Study of Long-Term Biocompatibility and Bio-Safety of Implantable Nanogenerators. *Nano Energy* **51**, 728-735, doi:10.1016/j.nanoen.2018.07.008 (2018).
34 Dagdeviren, C. *et al.* Conformal piezoelectric energy harvesting and storage from motions of the heart, lung, and diaphragm. *Proc Natl Acad Sci U S A* **111**, 1927-1932, doi:10.1073/pnas.1317233111 (2014).
35 Kim, D. H. *et al.* In Vivo Self-Powered Wireless Transmission Using Biocompatible Flexible Energy Harvesters. *Advanced Functional Materials* **27**, 1700341, doi:10.1002/adfm.201700341 (2017).
36 Han, M. *et al.* Three-dimensional piezoelectric polymer microsystems for vibrational energy harvesting, robotic interfaces and biomedical implants. *Nature Electronics* **2**, 26-35, doi:10.1038/s41928-018-0189-7 (2019).
37 Balint, R., Cassidy, N. J. & Cartmell, S. H. Electrical stimulation: a novel tool for tissue engineering. *Tissue Eng Part B Rev* **19**, 48-57, doi:10.1089/ten.TEB.2012.0183 (2013).

38 Ercan, B. & Webster, T. J. The effect of biphasic electrical stimulation on osteoblast function at anodized nanotubular titanium surfaces. *Biomaterials* **31**, 3684-3693, doi:10.1016/j.biomaterials.2010.01.078 (2010).
39 Dennerlein, J. T., Diao, E., Mote, C. D., Jr. & Rempel, D. M. In vivo finger flexor tendon force while tapping on a keyswitch. *J Orthop Res* **17**, 178-184, doi:10.1002/jor.1100170205 (1999).
40 Fischbach, M. A., Bluestone, J. A. & Lim, W. A. Cell-based therapeutics: the next pillar of medicine. *Sci Transl Med* **5**, 179ps177, doi:10.1126/scitranslmed.3005568 (2013).
41 Tan, X., Letendre, J. H., Collins, J. J. & Wong, W. W. Synthetic biology in the clinic: engineering vaccines, diagnostics, and therapeutics. *Cell* **184**, 881-898, doi:10.1016/j.cell.2021.01.017 (2021).
42 Wang, M. *et al.* KTE-X19 CAR T-Cell Therapy in Relapsed or Refractory Mantle-Cell Lymphoma. *N Engl J Med* **382**, 1331-1342, doi:10.1056/NEJMoa1914347 (2020).
43 Roybal, K. T. *et al.* Engineering T Cells with Customized Therapeutic Response Programs Using Synthetic Notch Receptors. *Cell* **167**, 419-432 e416, doi:10.1016/j.cell.2016.09.011 (2016).
44 Allen, M. E. *et al.* An AND-Gated Drug and Photoactivatable Cre-loxP System for Spatiotemporal Control in Cell-Based Therapeutics. *ACS Synth Biol* **8**, 2359-2371, doi:10.1021/acssynbio.9b00175 (2019).
45 Liu, Y. *et al.* Immunomimetic Designer Cells Protect Mice from MRSA Infection. *Cell* **174**, 259-270 e211, doi:10.1016/j.cell.2018.05.039 (2018).
46 Saxena, P., Charpin-El Hamri, G., Folcher, M., Zulewski, H. & Fussenegger, M. Synthetic gene network restoring endogenous pituitary-thyroid feedback control in experimental Graves' disease. *Proc Natl Acad Sci U S A* **113**, 1244-1249, doi:10.1073/pnas.1514383113 (2016).
47 Keenan, D. M. & Veldhuis, J. D. Pulsatility of Hypothalamo-Pituitary Hormones: A Challenge in Quantification. *Physiology (Bethesda)* **31**, 34-50, doi:10.1152/physiol.00027.2015 (2016).
48 Bose, S. *et al.* A retrievable implant for the long-term encapsulation and survival of therapeutic xenogeneic cells. *Nat Biomed Eng* **4**, 814-826, doi:10.1038/s41551-020-0538-5 (2020).
49 Mattke, J. *et al.* Role of Exosomes in Islet Transplantation. *Front Endocrinol (Lausanne)* **12**, 681600, doi:10.3389/fendo.2021.681600 (2021).
50 Kojima, R., Scheller, L. & Fussenegger, M. Nonimmune cells equipped with T-cell-receptor-like signaling for cancer cell ablation. *Nat Chem Biol* **14**, 42-49, doi:10.1038/nchembio.2498 (2018).
51 Rahman, M. J., Regn, D., Bashratyan, R. & Dai, Y. D. Exosomes released by islet-derived mesenchymal stem cells trigger autoimmune responses in NOD mice. *Diabetes* **63**, 1008-1020, doi:10.2337/db13-0859 (2014).
52 Soon-Shiong, P. Treatment of type I diabetes using encapsulated islets. *Adv Drug Deliv Rev* **35**, 259-270, doi:10.1016/s0169-409x(98)00076-3 (1999).
53 Bochenek, M. A. *et al.* Alginate encapsulation as long-term immune protection of allogeneic pancreatic islet cells transplanted into the omental bursa of macaques. *Nat Biomed Eng* **2**, 810-821, doi:10.1038/s41551-018-0275-1 (2018).
54 Jacobs-Tulleneers-Thevissen, D. *et al.* Sustained function of alginate-encapsulated human islet cell implants in the peritoneal cavity of mice leading to a pilot study in a type 1 diabetic patient. *Diabetologia* **56**, 1605-1614, doi:10.1007/s00125-013-2906-0 (2013).

55 Evron, Y. *et al.* Long-term viability and function of transplanted islets macroencapsulated at high density are achieved by enhanced oxygen supply. *Sci Rep* **8**, 6508, doi:10.1038/s41598-018-23862-w (2018).
56 Ramzy, A. *et al.* Implanted pluripotent stem-cell-derived pancreatic endoderm cells secrete glucose-responsive C-peptide in patients with type 1 diabetes. *Cell Stem Cell* **28**, 2047-2061 e2045, doi:10.1016/j.stem.2021.10.003 (2021).
57 Shapiro, A. M. J. *et al.* Insulin expression and C-peptide in type 1 diabetes subjects implanted with stem cell-derived pancreatic endoderm cells in an encapsulation device. *Cell Rep Med* **2**, 100466, doi:10.1016/j.xcrm.2021.100466 (2021).
58 Kelly, C. N., Miller, A. T., Hollister, S. J., Guldberg, R. E. & Gall, K. Design and Structure-Function Characterization of 3D Printed Synthetic Porous Biomaterials for Tissue Engineering. *Adv Healthc Mater* **7**, e1701095, doi:10.1002/adhm.201701095 (2018).
59 Squillaro, T., Peluso, G. & Galderisi, U. Clinical Trials With Mesenchymal Stem Cells: An Update. *Cell Transplant* **25**, 829-848, doi:10.3727/096368915X689622 (2016).
60 Wein, M. N. & Kronenberg, H. M. Regulation of Bone Remodeling by Parathyroid Hormone. *Cold Spring Harb Perspect Med* **8**, doi:10.1101/cshperspect.a031237 (2018).

CHAPTER 3: Tuning of cellular insulin release by music for real-time diabetes control

Haijie Zhao[1], Shuai Xue[1], Marie-Didiée Hussherr[1], Peter Buchmann[1], Ana Palma Teixeira[1], Martin Fussenegger[1,2,*]

[1]Department of Biosystems Science and Engineering, ETH Zurich, Mattenstrasse 26, CH-4058 Basel, Switzerland; [2]Faculty of Science, University of Basel, Mattenstrasse 26, CH-4058 Basel, Switzerland; [*]Corresponding author. E-mail: fussenegger@bsse.ethz.ch

The work presented in this chapter has been published in the peer reviewed journal "The Lancet Diabetes & Endocrinology". DOI: 10.1016/S2213-8587(23)00153-5

Music is well known to impact on human emotions, and is clinically used for relieving insomnia symptoms and for rehabilitation of patients with cognitive disorders. However, the molecular mechanisms involved remain largely elusive. Here, capitalising on synthetic biology-inspired engineering of human cells, we have established a direct molecular link between music and cellular behaviour by constructing a music-inducible cellular control device (MUSIC) consisting of human cells ectopically expressing the native *Escherichia coli* large-conductance mechanosensitive channel (MscL). Cell membrane deformation induced by exposure to music played through an off-the-shelf loudspeaker stimulates MscL, activates rewired endogenous calcium signalling, and triggers immediate vesicular release of protein cargo, such as insulin. Music-programmed cellular biopharmaceutical release was specifically stimulated in the low-bass frequency range (50 – 250 Hz) with an optimal loudspeaker membrane acceleration of 50 m/s^2, corresponding to a sound level of 55 - 85 decibels (dB). MUSIC control had no effect on cell viability and was insensitive to a range of natural sounds (wind, rain and bird songs), as well as to speech (BBC news, talk shows and conversations). However, different selections of popular music, movie soundtracks, and classical music as well as guitar music triggered different levels of biopharmaceutical release. In an in vivo study, type-1 diabetic mice implanted with microencapsulated cells engineered for MUSIC-controlled vesicular insulin release (MUSIC$_{INS}$ cells) and exposed to Queen's "We Will Rock You" for just three minutes received a full insulin dose within 15 minutes. Postprandial glycaemic excursions were attenuated and normoglycemia was restored by just a single music session per day. Importantly, MUSIC$_{INS}$ cells required only 4 h to accumulate a

full insulin refill after vesicular release, reducing the risk of hypoglycaemia while providing capability for regular postprandial insulin shots. Listening to specific music tracks as a means to program traceless percutaneous real-time release of biopharmaceuticals from implanted cells might be a promising approach to drive compliance with cell-based therapies to a new level.

Introduction

Music, consisting of vocal and instrumental sounds with melody, harmony, rhythm and timbre, is an integral part of all human societies, and is used to express, share and control emotions[1-3]. It is important both as entertainment and as a way to tune out and relax from our hectic lives[4]. Music has been shown to affect emotions by regulating the dopaminergic limbic reward pathway[2,5-7] and modulating mood-associated hormones (cortisol, estrogen, testosterone) [8], neurotransmitters (norepinephrine, endogenous opioids, GABA) [9,10], neuropeptides (oxytocin, brain-derived neurotrophic factor, nerve growth factor) [11,12] and other biochemical mediators (endorphins, endocannabinoid, nitric oxide) [13]. These empirical molecular links provide a basis for the clinical use of music therapy to relieve insomnia symptoms[14,15] and cognitive disorders such as anxiety, depression and Parkinson's, Huntington's and Alzheimer's diseases[2,16,17]. Nevertheless, the specific molecular activities underlying music-based treatment strategies remain largely unknown.

Music consists of physically propagated acoustic waves, which humans typically notice in the frequency range of 20 Hz to 20 kHz[18]. These air pressure variations are converted by the bony ossicles in the middle ear into mechanical vibrations that reach the organ of Corti in the inner ear. There, the basilar membrane motion activates mechanosensitive ion channels of the hair cells, which depolarize and release neurotransmitters that relay the musical information via the nervous system to the brain for perception[19]. Similar mechanical-to-neural transduction pathways are involved in other processes, such as touch sensation[20], blood-pressure management[21] and mechano-electric feedback of the heart[22]. Indeed, mechanosensitive ion channels have been found across the entire animal kingdom. Prominent examples include the transient receptor potential channels[23,24] (TRPs), the piezo-type mechanosensitive ion channel[25-28] (Piezo1/2,) and the small[29,30] (MscS), and large[31,32] (MscL) conductance mechanosensitive channels of bacteria. The basic unifying principle of all these mechanosensitive ion channels consists of membrane tension-triggered ion-specific channel

opening, which results in membrane depolarization and ion-triggered activation of intracellular signalling cascades that modulate the expression of target genes[33,34].

Modified *Escherichia coli* MscL has previously been expressed in mammalian cells, [35] where it enabled tension-controlled loading with small-molecular compounds and small peptides such as phalloidin and trigger-inducible release of the model cargoes by [2-(trimethylammonium)ethyl]methanethiosulfonate bromide-mediated MscL gating[35,36]. Small-molecular switches[37-45] enabling trigger-inducible dosing of expression or release of protein pharmaceuticals by engineered cells also provide a basis for next-generation therapies[46,47]; indeed, cell-based therapies for the treatment of gouty arthritis[48], psoriasis[49], obesity[50], chronic pain[51], cancer[52,53], muscle atrophy[54], diabetes[41,45,55,56], and even infectious diseases[43] are being developed. Because the systemic delivery of small-molecular trigger compounds often suffers from pharmacokinetic challenges and side effects, attention has turned toward non-molecular traceless trigger cues such as light[57-64], ultrasound[65], magnetic fields[66-69], radio waves, [68,70,71] electricity[55] and heat[72]**.** However, physically triggered gene switches may require high energy input, [62,63,73] may involve unphysiological chemical or inorganic co-factors with side effects[62,64,66,68,69,71], poor bioavailability[74] or short half-lives[41,75], may suffer from illumination-based cytotoxicity[76], may be confounded by any fever-associated medical condition[72,77] and may require complex bioelectronic implants[55,57,60,61,78] or other specialised non-wearable equipment[66,68,70,79].

Inspired by the mechanosensitive process underlying human hearing, we used synthetic biology principles to engineer human cells the expression behaviour of which could be tuned by music. The constructed music-inducible cellular control device (MUSIC) functionally links music-actuated mechano-transduction of ectopically expressed MscL to depolarization-triggered vesicular biopharmaceutical secretion, thereby sensitising human cells to release protein therapeutics within minutes in response to music. Interestingly, we found that different selections of popular music, movie soundtracks, and classical music as well as guitar music triggered different levels of insulin release in type-1-diabetic mice implanted with microencapsulated cells engineered for MUSIC-controlled vesicular insulin release, whereas a wide range of natural sounds such as wind, rain and bird songs, as well as speech, including BBC news, talk shows and human conversation, had no effect. Our results suggest that listening to specific music tracks to program traceless percutaneous real-time release of biopharmaceuticals from implanted cells could be an interesting and convenient option to increase compliance in some patients.

Results

Engineering human cells to listen to music

The design concept of the music-inducible cellular control device (MUSIC) consists of rewiring the intracellular calcium surge actuated by calcium-permeable mechanosensitive channels in response to music to drive immediate calcium-triggered vesicular release of biopharmaceuticals **(Fig. 1A)**. For this purpose, we generated stably-transgenic clonal MUSIC-controlled insulin-releasing cell lines constitutively expressing either the mammalian mechanosensitive receptor PIEZO1[80,81] or the bacterial small[82] (MscS), or large[35] (MscL) conductance mechanosensitive channel, together with a pro-insulin expression unit in glucose-insensitive human pancreatic beta cells. The engineered cells were cultivated in standard 6-well plates with a flexible rubber bottom[83] placed on top of a customised box containing off-the-shelf loudspeakers wired to a pulse generator and a standard high-fidelity amplifier to control frequency and output voltage, respectively (**Fig. 1B**, **Fig. S1**). The impact of acoustic air-pressure waves, especially in the low-bass range, on the cell membrane was expected to increase membrane tension, activate the mechanosensitive channels and trigger vesicular secretion of insulin. To evaluate whether music could activate mechanosensitive channels in human cells in a real-world listening scenario, we correlated loudspeaker membrane acceleration with decibels (dB), a widely used relative unit of sound levels. A sound level of 60 dB at 50 Hz, which is within the safe range for the human ear[84,85], effectively activated the channels (**Fig. S2**). All cell lines containing mechanosensitive channels were responsive to real-world acoustic bass stimulation at 50 Hz and 60 dB (50 m/s^2) for 15 min, and among them, MscL-transgenic cells ($MUSIC_{INS}$) showed the best response, characterised by the highest maximum and fold induction of insulin release combined with the lowest basal expression (not exceeding that of the music-insensitive parental pancreatic cell line used as a negative control) (**Fig. 1C**). $MUSIC_{INS}$ cells cultivated as suspension microtissues were insensitive to acoustic stimulation because they neutralised mechanical actuation by rotation. Thus, music-responsive cells need to be immobilised, for example in adherent monolayers or implanted in host tissues (**Fig. S3**; see **Fig. 2** below). The mechanistic connection between sound stimulation and insulin release by $MUSIC_{INS}$ is likely mediated by calcium. Indeed, imaging of MscL-positive and MscL-negative cells expressing the fluorescent calcium indicator GCaMP6s showed significantly higher intracellular calcium levels in the former cell population after both had been sound-stimulated (**Fig. S4**). Furthermore, sound-stimulated $MUSIC_{INS}$ cells showed increased insulin release when incubated in higher calcium chloride concentrations (**Fig. S5)**. Finally, mechanical stimulation by piston-induced shear forces also triggered significantly

higher insulin secretion by MUSIC$_{INS}$ cells (**Fig. S6**). Taken together, these results support the idea that the sound waves act as mechanical forces to open the MscL channels and initiate calcium influx (**Figs. S4-S6**).

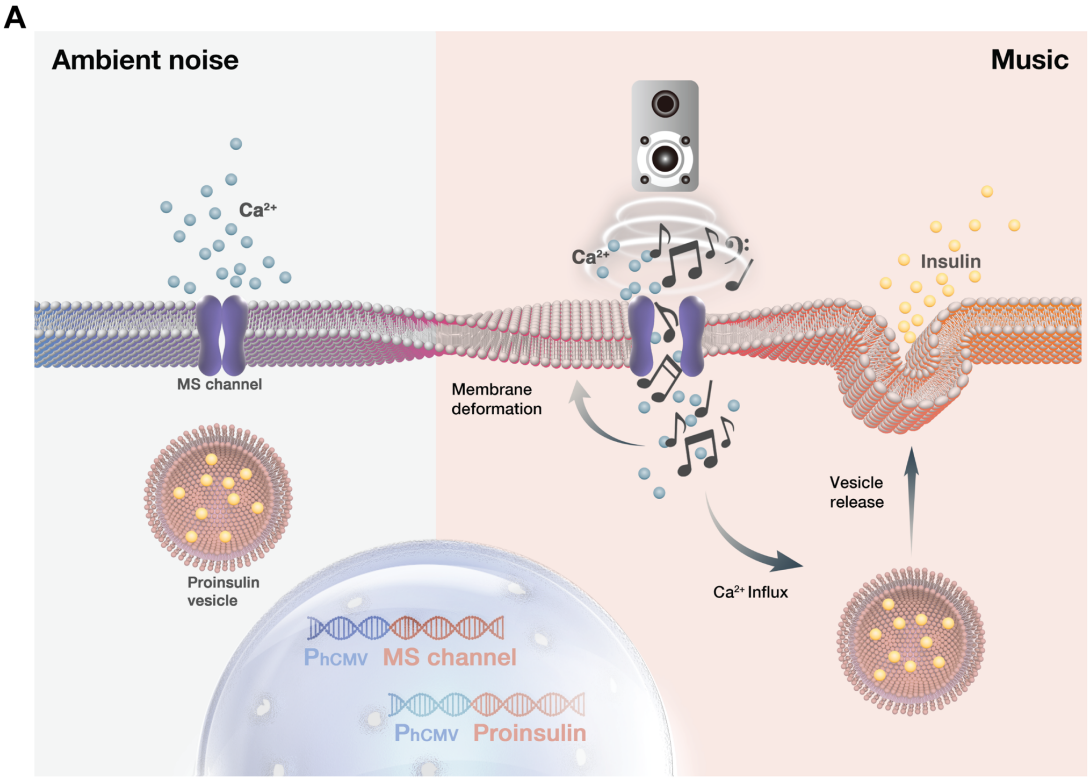

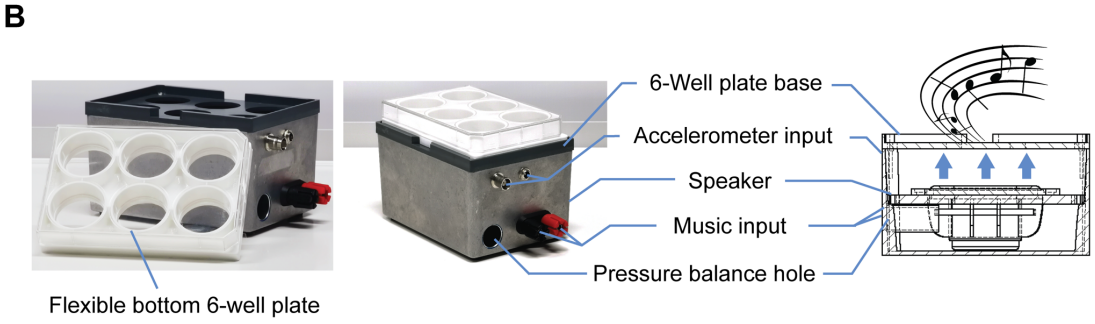

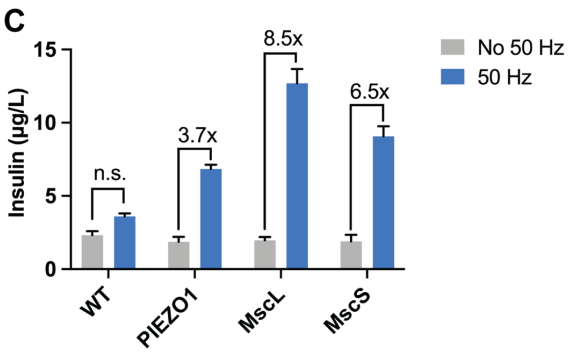

Figure 1. Design of the music-sensitive inducible cell system ($MUSIC_{INS}$ cells). (**A**) Sound waves induce membrane deformation of engineered β cells constitutively expressing a mechanosensitive (MS) channel and a synthetic proinsulin construct, triggering intracellular Ca^{2+} increase due to opening of the MS channel, which initiates the release of insulin from the secretory vesicles. (**B**) Image and illustration of the sound exposure device used for in vitro studies. The compact setup includes a speaker, pressure-balancing hole and 6-well plate base, which generates pressure on the flexible bottom 6-well plate. (**C**) Insulin secretion levels by engineered cells stably expressing three different MS channels, not exposed to sound or exposed to 50 Hz at 60 dB (50 m/s^2) during 15 min. Cells transfected with an empty plasmid were used as the control (n = 4).

Acoustic characterization and validation of MUSIC

In order to identify MUSIC's most efficient frequency range, we profiled the vesicular insulin release of MUSIC-transgenic $MUSIC_{INS}$ cells within 15 minutes over the human hearing range of 20 Hz to 20 kHz while keeping the membrane acceleration of the loudspeaker at 50 m/s^2 (55 - 85 dB) for the bass range (20 - 250 Hz) and below 25 m/s^2 (85 dB) for the midrange and treble (0.5 - 20 kHz). $MUSIC_{INS}$-mediated insulin release was particularly effective in the low-bass range between 50 to 100 Hz, even exceeding the release of the biopharmaceutical in response to KCl, used as the gold-standard positive chemical depolarization control (**Fig. 2A**). Beyond 100 Hz, the insulin release gradually decreased, becoming insignificant compared to unstimulated cells at 1 kHz and higher (**Fig. 2A**).

None of the acoustic trigger frequencies within the human hearing spectrum had any negative impact on the cell viability after acoustic stimulation for 15 min, and it appeared that MscL expressed in human cells was specifically responsive the low-bass range of 50 to 100 Hz (**Fig. 2B**). Further analysis of the loudspeaker membrane acceleration confirmed that $MUSIC_{INS}$ cells showed maximum viability while providing the highest insulin release within 15 min at 50 Hz and 50 m/s^2 (60 dB) (**Fig. 2C**, **Fig. 2D**). Based on all these data, we settled on values of 50 Hz and 50 m/s^2 (60 dB) for follow-up experiments.

Since music consists of sequential sound pulses, we were curious to establish what intervals of low-bass frequency activation would maximally stimulate insulin release by $MUSIC_{INS}$. Therefore, we acoustically stimulated $MUSIC_{INS}$ at 50 Hz and 60 dB for 15 min while setting the stimulation to 5 s ON / 2 s OFF with the OFF period gradually increasing to 120 s (**Fig. 2E**). The acoustic interval profiles revealed that low-bass acoustic insulin release gradually decreased with increasing length of the OFF intervals, which suggested that the

insulin dose could in principle be tuned depending on the frequency of the low-bass content of the composition, and that pieces of music with fewer low-bass signals per 120 s would not significantly trigger insulin release (**Fig. 2E**). Importantly, MUSIC activation requires at least three seconds of continuous music stimulation to activate insulin release, and this should serve to insulate the device against inadvertent activation during many everyday activities (**Fig. 2F**).

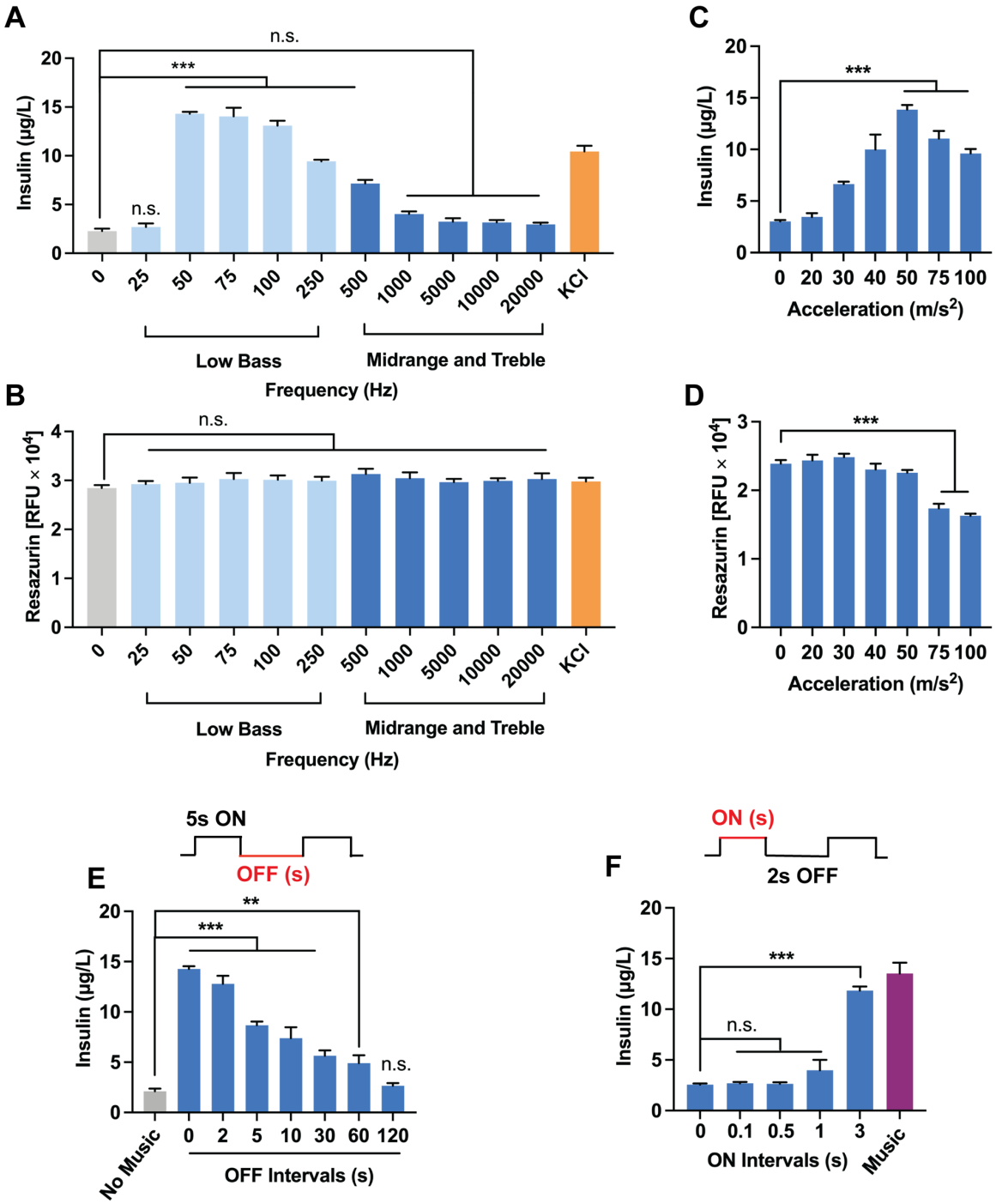

Figure 2. Characterization of the responses of MUSIC$_{INS}$ cells to different sound programs. (**A**) Frequency dependence. Insulin release by cells stimulated during 15 min at the indicated sound

frequencies (n = 6). (**B**) Cell viability after sound stimulation at the indicated frequencies (n = 6). (**C**) Voltage effect. Sound stimulation was performed at the indicated voltages for 15 min at 60 dB. (**D**) Cell viability after sound stimulation at the indicated voltages (n = 6). (**E**) Cells were stimulated at 60 dB (50 m/s^2) and 50 Hz for 15 min, using programmed sound patterns with 5 s on and the indicated time off (n = 6). (**F**) Cells were stimulated at 60 dB (50 m/s^2) and 50 Hz for 15 min, programming sound patterns with 2 s off and the indicated time on (n = 6). The cells were cultured on flexible-bottom 6-well plates and exposed to 60 dB, 50 Hz sound from the speaker for 15 min. Data are means ± SEM. Statistical analysis was done with a two-tailed t-test. ns not significant, **P < 0.01, ***P < 0.001.

$MUSIC_{INS}$ in concert

Capitalizing on our comprehensive acoustic profiling, we next validated $MUSIC_{INS}$' insulin-release performance in response to a 15 min exposure to different genres of music (**Fig. S7**), including popular music (**Fig. 3A**), movie soundtracks (**Fig. 3B**), classical music (**Fig. 3C**) and guitar music (**Fig. 3D**) set to 85 dB, which corresponds to the average sound level when listening to music[86] and is lower than that during a typical live concert[87] (105-110 dB). As expected from their low-bass content, popular music (**Fig. 3A**) and movie soundtracks (**Fig. 3B**) induced maximum levels of insulin release, while the response to classical music and guitar music was more diverse and specific to the composition (**Fig. 3C, Fig. 3D**). While Beethoven's "Sonata no. 6" and the guitar compositions " Chôros No.1" and "Asturias" induced some insulin release, Beethoven's "Für Elise", Mozart's "Alla Turca" and the guitar piece "Recuerdos" did not induce substantial insulin release (**Fig. 3C**, **Fig. 3D**), supporting the idea that insulin levels could in principle be tuned by a particular composition and that patients might still be able to enjoy listening to certain categories of music without triggering a shot of insulin. Since Beethoven's "Für Elise" and Mozart's "Alla Turca" are piano classics, we considered that $MUSIC_{INS}$ might be insensitive to instruments generating low acoustic pressure waves. Indeed, piano or guitar interpretations of original compositions by the Beatles (She Loves You), Queen (We Will Rock You) and Michael Jackson (Heal The World) showed substantially decreased insulin secretion (**Fig. 3E**, **Fig. 3F**), suggesting that music-lovers could still enjoy their entire music library using non-therapeutic instrumental interpretations (**Fig. 3A**), while preserving specific tracks for therapy (**Fig. 3E**, **Fig. 3F**). Environmental noises such as wind, rain and bird songs or speech, including BBC news, talk shows and normal conversations also did not trigger any insulin release (**Fig. 3G**, **Fig. 3H**), suggesting that $MUSIC_{INS}$ might not be triggered inadvertently in normal daily life. In short, our results suggest that insulin release can be

intentionally triggered and tuned to specific levels by listening to specific compositions containing distinct low-bass frequency patterns for 15 min at 85 dB (**Fig. 3I**).

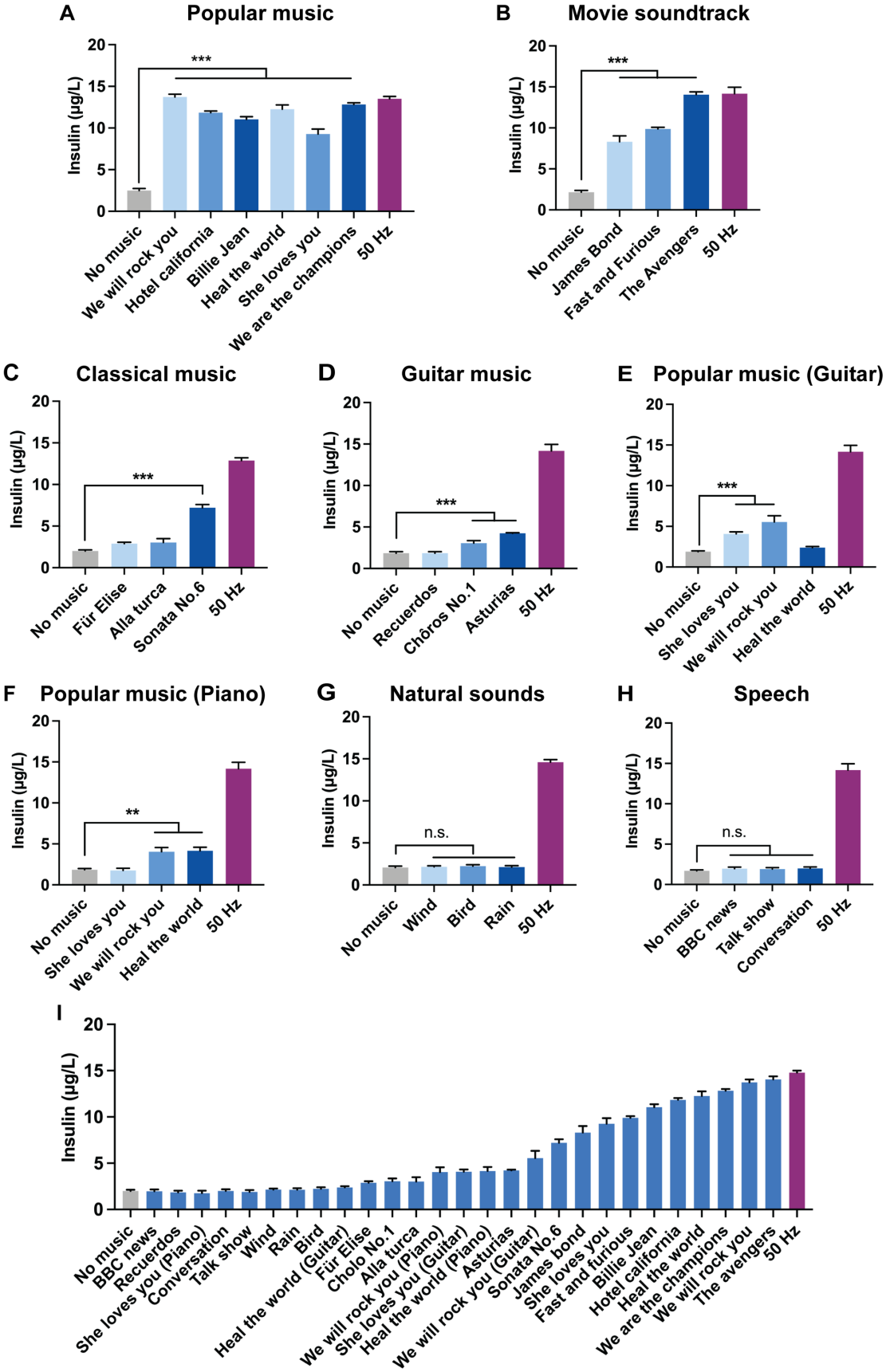

Figure 3. In vitro characterization of the responses of $MUSIC_{INS}$ cells to different songs. $MUSIC_{INS}$ cells were stimulated during 15 min with (**A**) Popular music, including "We Will Rock You", "Hotel California", "Billie Jean", "Heal the World", "She Loves You" and "We are the Champions", (**B**) Movie soundtracks, including James Bond ("James Bond Theme"), Fast and Furious ("See you again") and The Avengers ("Live to rise"), (**C**) Classical music, including Beethoven's "Für Elise", Mozart's "Alla Turca" and Beethoven's "Sonata No.6", (**D**) Guitar music, including Francisco Tárrega's "Recuerdos de la Alhambra", Heitor Villa-Lobos's " Chôros No.1", Isaac Albeniz's "Asturias", and popular music interpretations of original compositions on (**E**) guitar and (**F**) piano, (**G**) recorded naturals sounds such as wind, bird song and the sound of rain, (**H**) speech including "BBC news", "talk show" and "conversation". Stimulation with sound waves at 50 Hz was used as a positive control. (**I**) Summary of insulin secretion levels after exposure of $MUSIC_{INS}$ cells to different music. Data are means ± SEM. Statistical analysis was done with a two-tailed t-test (n = 6). ns not significant, $^{**}P < 0.01$, $^{***}P < 0.001$.

MUSIC-controlled insulin-release dynamics

Since vesicular secretion is characterised by rapid release of proteins stored in cytosolic vesicles, which is particularly important to match the dynamics required for the treatment of blood-glucose levels in diabetes, we also comprehensively analysed the dynamics of music-triggered insulin release from $MUSIC_{INS}$. Profiling of insulin levels in the culture supernatant of $MUSIC_{INS}$ stimulated by Queen's "We Will Rock You" showed that almost 70% of insulin is released within the first 5 minutes of music exposure, while complete release occurs within 15 minutes, which is even faster than in the case of KCl-mediated depolarization, and is comparable with glucose-triggered insulin release by human pancreatic islets[88] **(Fig. 4A)**. Most importantly, specific insulin release kinetics following music exposure for 3 to 5 min confirmed that $MUSIC_{INS}$ was able to release clinically relevant insulin levels within minutes, which would be essential for real-world diabetes therapy (**Fig. 4A**).

Another key parameter of native beta cells is the time required to refill their vesicular insulin storage. We exposed insulin-depleted $MUSIC_{INS}$ cells to a second music session after different periods of time and observed that $MUSIC_{INS}$ cells are gradually replenished their insulin stores, achieving a full insulin refill ready for the next music-triggered insulin release within 4 h (**Fig. 4B**). This refill time was consistent over several days (**Fig. 4C**), and would provide the capability for timely insulin release to attenuate glycaemic excursions associated with typical dietary habits[89].

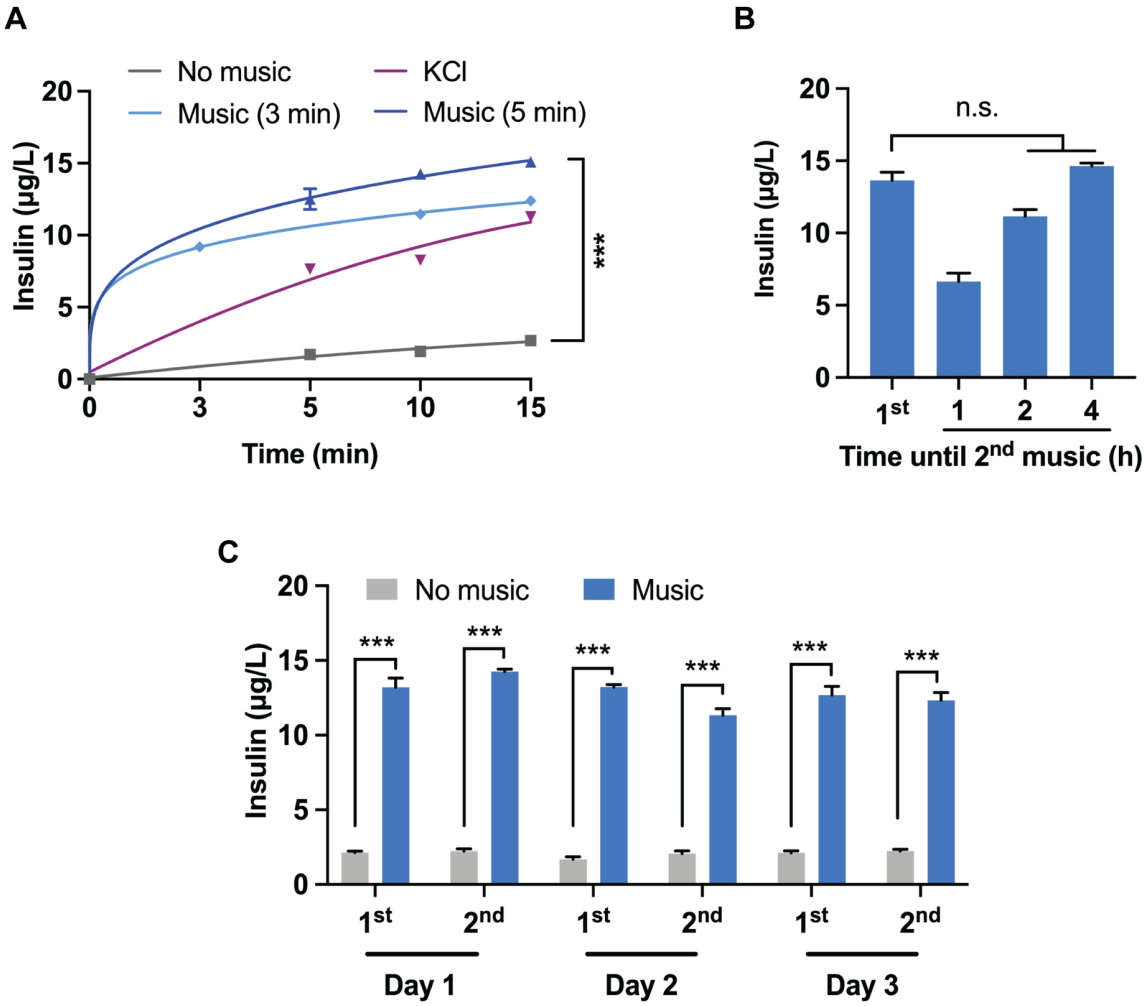

Figure 4. In vitro functionality of $MUSIC_{INS}$ cells. The track "We Will Rock You" was used for this study. (**A**) Music-stimulated insulin secretion kinetics. $MUSIC_{INS}$ cells were stimulated with music for 3 and 5 min by the speaker setup. $MUSIC_{INS}$ cells without music stimulation or treated with KCl were used as negative control and positive controls, respectively. (**B**) Reloading kinetics of vesicular insulin. Cells were stimulated twice for 15 min with the indicated time interval. (**C**) Reversibility assay. Electro-sensitive cells were stimulated twice daily for 15 min with a four-hour interval for a period of 3 days. Data are means ± SEM. Statistical analysis was done with a two-tailed t-test (n = 6). ns not significant, ***P < 0.001.

Tuning experimental type-1 diabetes to normoglycemia by MUSIC

For our mouse experiment, we developed a special loudspeaker box containing two off-the-shelf loudspeakers; this box fully immerses the entire body of the animal in the acoustic waves via a deflector (**Fig. 5A**, **Fig. S8**, **Fig. S9**). In order to enable efficient music transmission and encapsulate $MUSIC_{INS}$ for therapeutic applications, we immobilised the implanted $MUSIC_{INS}$ cells in coherent hydrogel microcontainers whose persistence, efficacy and

immuno-protection have been clinically validated for human islet transplantation[90], and we confirmed music-sensitive insulin release by the microencapsulated $MUSIC_{INS}$ cells (**Fig. S10**). Type-1 diabetic mice subcutaneously implanted with microencapsulated $MUSIC_{INS}$ cells and listening to low-bass acoustic waves at 60 dB (50 m/s^2) for 15 min reached near wild-type blood insulin levels, while untreated animals and treatment groups without acoustic stimulation continued to exhibit severe hyperglycaemia associated with type-1 diabetes-specific insulin deficiency (**Fig. 5B**). Treatment groups listening to Queen's "We Will Rock You" reached sufficient insulin levels to rapidly attenuate postprandial glycaemic excursions during glucose tolerance tests, while animals without implants or with implants but without music immersion showed consistent hyperglycaemia **(Fig. 5C).** Due to the rapid vesicular insulin release by implanted $MUSIC_{INS}$, the blood-insulin levels of music-immersed animals rose within minutes, reached wild-type levels and peaked within only 90 min (**Fig. 5D**). With just a single 15 min music session per day, wild-type blood insulin levels could be restored and normoglycemia reinstated in type-1 diabetic mice (**Fig. 5E**). Importantly, commercial headphones or ear plugs such as AirPods®) are not sufficiently powerful to trigger $MUSIC_{INS}$, which would enable patients to continue enjoying their favourite music in a non-therapeutic context (**Fig. S11**). $MUSIC_{INS}$ cells are triggered only if the sound waves directly impinge on the skin just above the implantation site for at least 15 minutes (**Fig. S12A** and **Fig. S12B**). Various loud environmental noises such as low flying aircraft, lawn mower, fire trucks and horns did not result in undesired insulin secretion when perceived from different distances and directions (**Fig. S12C**).

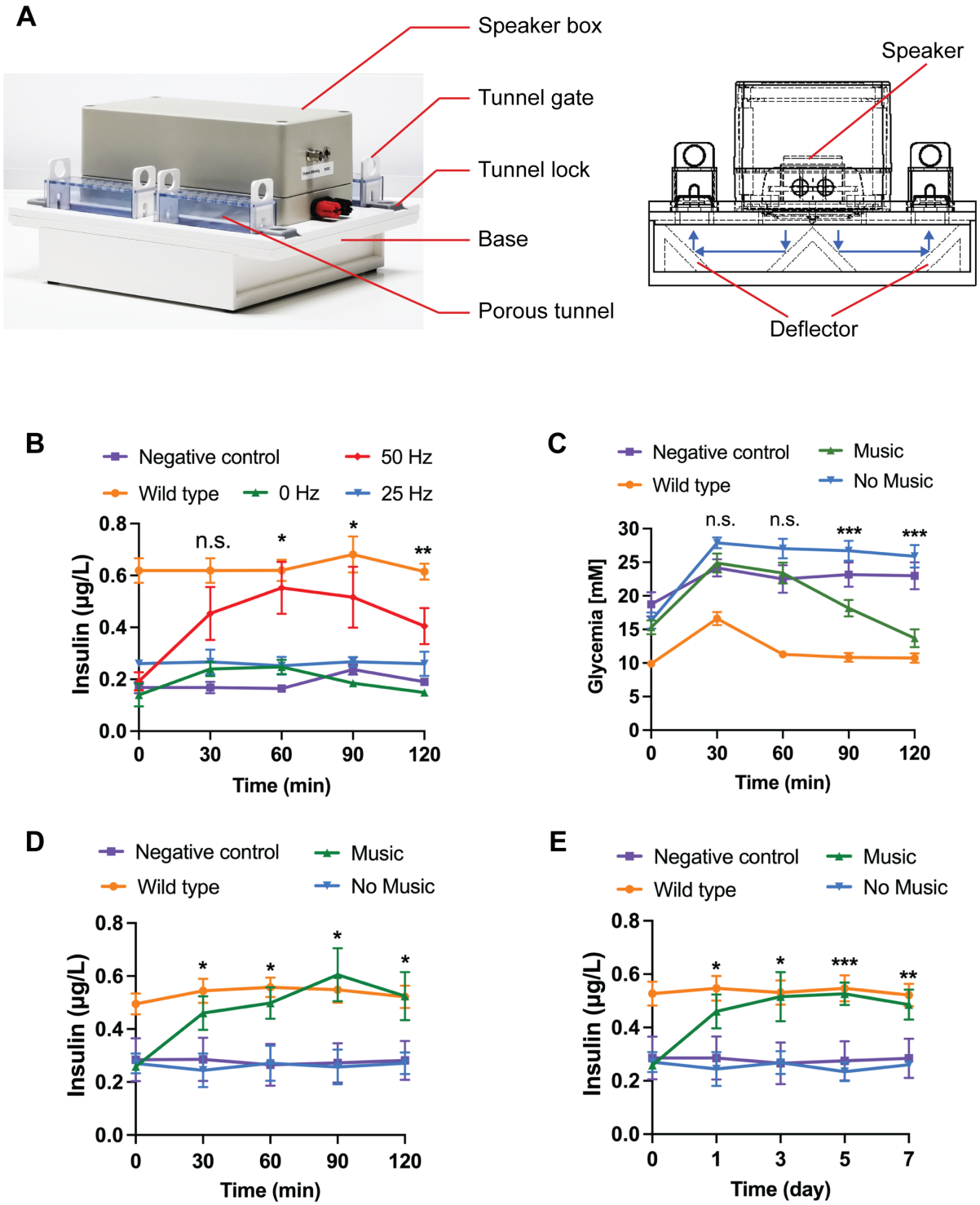

Figure 5. Design of the in vivo sound stimulation setup and in vivo characterization of $MUSIC_{INS}$ cells. **(A)** Picture **(left)** and illustration **(right)** of the speaker setup for the in vivo study. **(B)** Frequency. The type-1 diabetic mice were exposed to different frequencies at 50 m/s^2 for 15 min after subcutaneous implantation of encapsulated $MUSIC_{INS}$ cells (n = 5). **(C)** Glucose tolerance test. Wild-type or type-1 diabetic mice were exposed to music for 15 min after intraperitoneal injection of 1.5 g of glucose per kg body weight. **(D)** Time course of blood insulin levels. Wild-type or type-1 diabetic mice implanted intraperitoneally with alginate-

based hollow microcontainers were fasted for 4 h before music stimulation for 15 min. Blood samples were collected at the indicated time points. Non-stimulated mice were used as controls. **(E)** The microcontainers were intraperitoneally implanted into type-1 diabetic mice and insulin levels were recorded every 2 days after 15 min of music stimulation, over a period of 7 days. Non-implanted type-1 diabetic mice were used as negative control. The statistical significance of the difference between the 50 Hz/music stimulation group and the no 50 Hz/music stimulation group was calculated. Data are means ± SEM. Statistical analysis was done with a two-tailed t-test (n = 8). ns not significant, *P < 0.05, **P < 0.01, ***P < 0.001.

Discussion

With cell-based therapies beginning to provide opportunities for novel precision treatments[46,47,91,92], the Paracelsus paradigm that the dose makes the drug is shifting from pill-based administration of small-molecular drugs toward gene switches that dynamically tune therapeutic gene expression and in-situ biopharmaceutical production[41,43,45,48-51,54-56,92,93]. However, the quest for optimal gene switches combining specific, tuneable and reversible expression of therapeutic transgenes with traceless triggering, appropriate dosing dynamics, and convenient operation is still ongoing[57,58,60,62-64,68,72,92]. Since chemical control is often limited by the side effects[94,95], bioavailability[96] or pharmacodynamics[97,98] of the trigger compounds, technologies to enable remote-control of somatic cellular behaviour from outside the body using traceless cues such as electromagnetic waves (including light), [57,59-64] or temperature change electro-induced by heat pads[72], magnetic fields[66,67,69,99,100] or radio waves[68,70,71,99,100] seem particularly promising. However, optogenetics continues to struggle with issues such as high energy consumption[62,63,73] and illumination-based cytotoxicity[76]. Electro-induced heat generation shares similar challenges, and may be confounded by the homeostatic restriction of temperature fluctuations in endothermic species such as humans[72]; furthermore, there is controversy as to whether these systems function as intended[99,100].

Focused ultrasound can travel for long distances in thin bone and deep soft tissues, and has also been evaluated for focal actuation of genetically sensitized neurons to treat experimental neurodegenerative disorders[101,102]. However, since sonogenetics operates between 0.2 and 10 MHz[101,103], it requires specialized equipment operated by trained personnel, which may preclude its use for the routine treatment of metabolic disorders requiring frequent changes in the dosing regimens of specific protein therapeutics.

Listening to music is a common cultural denominator of all human societies. Inspired by the human hearing process in which air-pressure waves trigger membrane deformation, activation of mechanosensitive channels, and depolarization-mediated neurotransmitter release by hair cells in the inner ear to enable music perception in the brain[19], we set out to design a synthetic music-responsive gene switch by rewiring music-based membrane deformation via depolarization by mechanosensitive channels to vesicular release of protein therapeutics. Several methods have been devised to sensitize cell genetic behaviour to membrane deformation, such as atomic force microscopy[104], blunt probes[105,106], pipette pressure[25] and shear flow[107,108], but none is sufficiently sensitive to capture typical audio frequencies between 20 Hz and 20 kHz. Here, we selected the large-conductance mechanosensitive channel MscL, which opened in response to increased plasma membrane tension following audible acoustic stimulation. This results in calcium ion influx and membrane depolarization, which could in principle either be rewired via synthetic signalling cascades to synthetic promoters[41,43,45,48-51,54-56,92,93] for transcriptional control of therapeutic transgenes or, as shown here, linked to vesicular release of protein pharmaceuticals. In its novel mammalian cellular context, MscL captured music in the low-bass audible frequency spectrum of 50 to 500 Hz at a typical music-listening sound level of 55 – 85 dB, which made the constructed music-inducible cellular control device (MUSIC) insensitive to natural sounds such as wind, rain and bird songs, as well as conversations, news and talk shows. Activation required continuous rhythmic low-bass stimulation for at least three minutes, so that MUSIC was non-responsive to inadvertent incidental stimulation or shorter acoustic input. In other words, MUSIC can specifically tune cellular behaviour and biopharmaceutical release dependent on exposure to music with a rhythmic low-bass profile. Notably, while low-bass-heavy music tunes the cellular device to maximum levels, music with intermittent low-bass sequences adjusts the cellular response to intermediate levels, and piano and guitar compositions with little low-bass content have only minor or no impact on MUSIC. This seems to apply to all music styles from classical to pop and rock. Thus, therapeutic MUSIC sessions would still be compatible with listening to other types of music, as well as with listening to all types of music via headphones.

We chose to connect MUSIC to vesicular protein secretion, which is capable of rapidly providing several daily doses of specific protein therapeutics. This rapid-release design was inspired by neurotransmitter and hormone release mechanisms, and could easily be linked to MUSIC's calcium signalling via a common membrane depolarization interface. Compared to classical transcription-based transgene-control modalities[41,43,45,48-51,54-56,92,93], vesicular secretion is not only much faster, but also enables a discontinuous peak delivery of protein

therapeutics that is more appropriate for metabolic interventions, and is compatible with standard drug administration schemes[109,110]. MUSIC-stimulated peak dosing is followed by a refill time, during which the cellular system synthesizes the biopharmaceutical and stores it for the next release. The all-in-one rapid release and refill characteristics ensure full reversibility of the system. Most importantly, with only four hours required for a full refill, MUSIC can provide several therapeutic doses a day in the absence of medical equipment or staff, simply by having the patient listen to the "prescribed" music.

Most sophisticated medical interventions, including cell-based therapies and the administration of biopharmaceuticals, require advanced infrastructure, specialised medical equipment and trained medical specialists, making it infeasible to provide several treatments per day outside medical centres. In contrast, MUSIC-transgenic cells can simply be stimulated by portable battery-powered commercial loudspeakers, making multiple daily dosing of biopharmaceuticals straightforward even in the absence of medical infrastructure. As a proof-of-concept to validate MUSIC's potential for future applications we focused on diabetes, which shows dramatically increasing global prevalence and is a dynamic metabolic disease that is very challenging to treat. Indeed, in an experimental type-1 diabetes setting, MUSIC-driven insulin release stimulated by off-the-shelf loudspeakers was able to attenuate postprandial glycemic excursions and restore normoglycemia. This finding, combined with the safety feature offered by the "refill" period, suggests that therapeutic cell implants "listening" to specific music and releasing critical biopharmaceuticals in response could be an interesting option for extending the range of cell-based therapies for certain patients, especially those suffering from metabolic disorders, where the need for frequent dosing raises issues of compliance.

Material and Methods

Cell culture and transfection

Human pancreatic 1.1E7 cells (cat. no. 10070101-1VL, Sigma-Aldrich) were cultured in Roswell Park Memorial Institute 1640 medium (RPMI, cat. no. 72400-021, Thermo Fischer Scientific) supplemented with 10 % foetal bovine serum (FBS, cat. no. F7524, lot no. 022M3395, Sigma-Aldrich), 100 U/mL penicillin and 100 µg/mL 100x penicillin-streptomycin solution (cat. no. L0022, Biowest). Cells were cultivated at 37 ˚C in a humidified atmosphere containing 5% CO_2. For passaging, cells were detached by incubation for 3 min at 37 °C in 0.05% trypsin-EDTA (cat. no. 25300-054, Life Technologies), collected by centrifugation for 1 min at 200 x g and resuspended in FBS-containing RPMI at 1.5 x 10^5 cells/mL. Cell densities

were quantified using an automated cell counter (CellDrop™, DeNOVIX). For transfection, the cells were seeded at a density of 3.5 x 10^5 per cm^2 and cultivated for 24 h before adding a lipofectamine (Lipofectamine™ 3000, Thermo Fisher Scientific) transfection mixture containing a total of 0.5 µg of plasmid DNA per cm^2 of transfected cells for another 24 h.

Establishment of stable MUSIC$_{INS}$ cells

Human pancreatic 1.1E7 cells (2 x 10^6 cells/mL) were co-transfected as described above with (i) pLX304 (P_{hCMV}-Proinsulin-NanoLuc-pA, 4.5 µg), encoding constitutive expression of insulin and nanoluciferase, (ii) pHZ10 (ITR-P_{hCMV}-MscL-P2A-PuroR-pA:P_{RPBSA}-BFP-P2A-Zeo-pA-ITR; 5.5 µg) encoding, besides the reporter gene (BFP) and selection markers (PuroR, Zeo), the constitutive expression of the *Escherichia coli* large-conductance mechanosensitive channel (MscL), and (iii) 0.5 µg of pCMV-T7-SB100 (P_{hCMV}-SB100X-pA) containing the constitutive expression unit for the Sleeping Beauty transposase SB100X. The cells were cultivated for clonal selection in culture medium containing 25 µg/mL of puromycin (cat. no. A1113803, Thermo Fisher Scientific) or 25 µg/mL of zeocin (cat. no. R25005, Thermo Fisher Scientific). For isogenic cell lines expressing the mammalian mechanosensitive receptor PIEZO1 or the prokaryotic small-conductance mechanosensitive channel MscS, pHZ10 was replaced by pTS391 (ITR-P_{hCMV}-PIEZO1-pA:P_{RPBSA}-mRubby-P2A-PuroR-pA-ITR) or pTS414 (ITR-P_{hCMV}-MscS-pA:P_{RPBSA}-BFP-P2A-Zeo-pA-ITR), respectively. For the assembly of β-cell organoids, MUSIC$_{INS}$ were detached as described above, washed twice in RPMI medium, and 5 x 10^5 cells/mL were seeded in 24-well ultra-low attachment plates (cat. no. CLS3473-24EA, Corning Inc.) for 12 hours. The spontaneously assembled MUSIC$_{INS}$ microtissues were collected by centrifugation for 5 min at 200 x g and used in stimulation experiments.

Analytical assays

Cell viability. Cell viability was quantified by incubating the cells for 2 hours with resazurin (50 µg/mL, cat. no. R7017, Sigma-Aldrich) before recording the fluorescence at 540/590 nm (Tecan Infinite 200 PRO plate reader, Tecan Group AG). **NanoLuc luciferase.** NanoLuc luciferase was quantified in cell culture supernatants using the Nano-Glo® Luciferase Assay System (cat. no. N1110, Promega). In brief, 10 µL of cell culture supernatant was added per well of a black 384-well plate and mixed with 10 µL of substrate-containing assay buffer. Total luminescence was quantified at 460/20 nm (Tecan GENios PRO plate reader, Tecan Group AG). **Insulin.** Insulin was quantified by an ELISA kit (cat. no. 10-1247-01, Mercordia).

Glucose. Blood-glucose levels were quantified using the clinically licensed Contour®Next test strips and Contour®Next ONE reader (Ascensia Diabetes Care).

Music stimulation

Cell culture. Engineered cells were cultivated in flexible-bottomed 6-well BioFlex® culture plates (cat. no. BF-3001C, Flexcell) at a density of 3.5 x 10^5 cells/cm^2 for 48 h before the plate was fixed onto a customised speaker set-up that directly exposes the monolayer cultures to the soundwaves generated by the speaker (cat. no. W3-1750S, TB-Speakers). The customised speaker set-up contains six holes matching the size of the individual wells of a 6-well plate base, thereby locating the flexible rubber membrane of the BioFlex® culture plate above the loudspeaker. To maintain the pressure balance inside the device, an additional hole was made in the side of the loudspeaker device. The frequency was set by a pulse generator (JT-JDS6600-LITE, JOYIT) and the output intensity was controlled by a 2 x 50 W stereo amplifier (T21, Renkforce). Speaker acceleration was monitored by an accelerometer (ADXL326, Adafruit Industries) and an oscilloscope (DS1052E, Rigol Technologies). The sound level (dB) was measured with a sound level meter (SL-10, Voltcraft). To set the exposure times and intervals, the speaker system was programmed using a software-controlled switchboard (cat. no. MEGA 2560, Arduino, software version 1.8.11, Arduino). **Mice.** The speaker box for music stimulation of mice implanted with microencapsulated $MUSIC_{INS}$ cells was handmade with polyvinyl chloride (PVC) by an external workshop (G+B PLEX AG, Switzerland), and contains two speakers (cat. no. W3-1750S, TB-Speakers), a centering base, a deflector shelf, a tunnel lock and a tunnel gate. The animals were exposed to music for 15 min at 50 Hz and 60 dB.

Calcium imaging

Human embryonic kidney (HEK-293) cells were transfected with the genetically encoded calcium indicator GCaMP6s (P_{hCMV}-GCaMP6s-pA) in the presence or absence of constitutive expression of the MscL channel (P_{hCMV}-MscL-pA). A 3D-printed customized adapter for a 6-well BioFlex® culture plate was used in a Nikon Eclipse Ti2-E wide-field microscope. Before music stimulation, the cell culture medium was replaced by phenol red-free DMEM (cat. no. 21063029, Thermo Fisher Scientific). During music stimulation, the speaker is buckled upside down on the 6-well plate. Images were collected via a 10x objective lens with 100 ms exposure time and 1 s duration.

Microencapsulation and implantation of $MUSIC_{INS}$ cells

To protect the human $MUSIC_{INS}$ cells from the mouse immune system while enabling free diffusion of nutrients and therapeutic proteins such as insulin, we used clinical trial-

validated, FDA-licensed alginate-based encapsulation technology. $MUSIC_{INS}$ were microencapsulated into coherent alginate-poly(L-lysine) (PLL)-alginate microcapsules of 400 µm in diameter by mixing 7.5 x 10^7 $MUSIC_{INS}$ with 12 mL alginate (cat. no. 11061528; Büchi, Switzerland), 200 mL 0.05 % PLL solution (cat. no. PLKB50, Alamanda Polymers). The encapsulator (B-395 Pro, Büchi, Switzerland) was set to the following parameters: 200 µm nozzle with a vibration frequency of 1025 Hz, a 25 mL syringe operated at a flow rate of 20 mL/min and 1.1 kV voltage for bead dispersion. Then 5 x 10^6 microencapsulated cells in 0.5 mL of serum-free DMEM (500 cells/capsule) were intraperitoneally (i.p.) implanted through a standard 5 mL syringe equipped with a 21-gauge needle.

Animal experimentation

Type-1 diabetic mice were established by fasting 8-week-old C57BL/6J mice (Janvier Labs) for 4 h per day for five consecutive days while injecting a single dose per day of freshly diluted streptozotocin (STZ, cat. no. S0130, Sigma-Aldrich; 50 mg/kg in 300 µL sodium citrate buffer adjusted to pH 4.3). Type-1 diabetes-associated persistent fasting hyperglycemia was confirmed after six days by blood-glucose profiling. Fasting glycemia was measured after 8 h. For glucose-tolerance tests, treated animals were intraperitoneally injected with 1.5 g/kg glucose and blood glucose levels were recorded at regular intervals. Insulin was quantified in blood serum collected using Microtainer® serum separator tubes (cat. no. 365967, Becton Dickinson). All animal experiments were approved by the authorities of the Canton of Basel-Stadt, Switzerland (license number: 2996/30779) and conducted by Shuai Xue and Marie-Didiée Hussherr at the Department of Biosystems Science and Engineering (D-BSSE) of the ETH Zurich in Basel.

Statistical analysis

For the in vitro experiments, all the cell monolayers were derived from the same cell source, which was used across all replicates and conditions in order to reduce biological variation. Our unit of analysis is a monolayer of cells cultivated in a well of a standard 6-well cell culture plate. For each treatment group (no stimulation, different sound/music stimulation), we simultaneously performed at least 3 biological replicates consisting of cell monolayers seeded from the same cell batch. Each of these experiments was independently repeated three times using batches of cells with different passage numbers. For the in vivo experiments, each animal represents an independent unit of analysis, and each treatment group consists of at least 5 mice. The relative fluorescence (indicative of the resazurin levels) is the dependent variable in the cell viability experiment. The glycemia level is the dependent variable in the GTT experiment. The concentration of insulin is the dependent variable in other experiments. Data

are means ± SEM. Statistical analysis was done with a two-tailed Mann-Whitney non-parametric test or student t test (n = 6). Confidence interval (CI) = 95%. n.s. not significant, *P < 0.05, **P < 0.01, ***P < 0.001.

Acknowledgments

We thank Paul Argast, Nik Franko, Tobias Strittmatter and Henryk Zulewski for generous advice and Tobias Strittmatter and Jinbo Huang for sharing plasmids prior to publication. Haijie Zhao acknowledges support by the Chinese Scholarship Council (CSC, no. 201806780020). This work was supported by a European Research Council advanced grant (ElectroGene, grant no.785800) and in part by the Swiss National Science Foundation NCCR Molecular Systems Engineering.

Author contributions

H.Z. and M.F. designed the project; H.Z. performed all the cell culture experiments, P. B. designed the speaker setup, H.Z., S.X. and M.D.H. performed the animal experiments; H.Z., S.X., A.P.T. and M.F. designed the experiments and analysed the results; H.Z., S.X., A.P.T. and M.F. wrote the manuscript.

Competing interest.

The authors declare no competing interests.

Data and materials availability

The authors declare that all the data supporting the findings of this study are available within the paper and its supplementary materials. All materials and original plasmids listed in Supplementary Table S1 are available upon request.

Supplementary Materials

Tuning of cellular insulin release by music for real-time diabetes control

Haijie Zhao[1], Shuai Xue[1], Marie-Didiée Hussherr[1], Peter Buchmann, Paul Argast, Ana Palma Teixeira[1], Martin Fussenegger[1,2,*]

[1]Department of Biosystems Science and Engineering, ETH Zurich, Mattenstrasse 26, CH-4058 Basel, Switzerland.

[2]Faculty of Science, University of Basel, Mattenstrasse 26, CH-4058 Basel, Switzerland

[*]Corresponding author. E-mail: fussenegger@bsse.ethz.ch

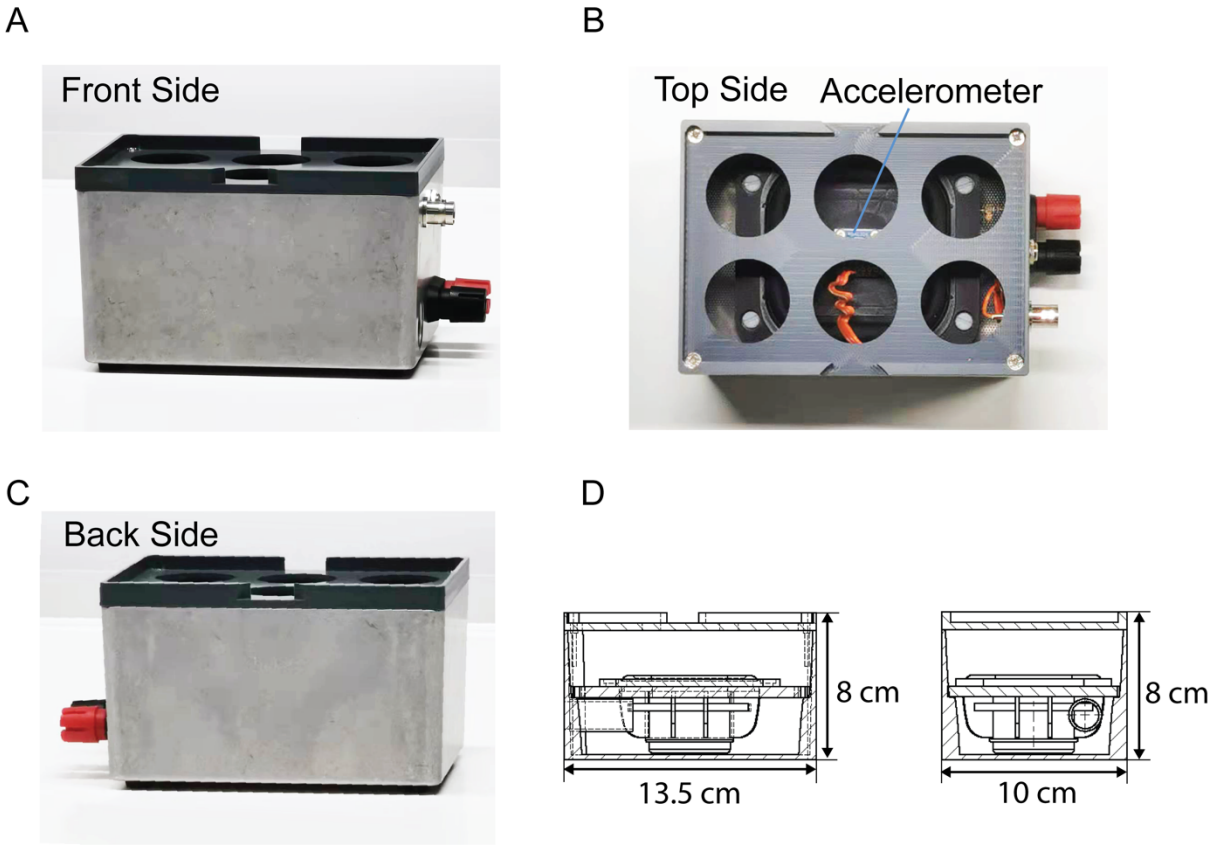

Fig. S1. (A - C) Three-dimensional and perspective views of the speaker system used for in vitro study, **(D)** with scale details.

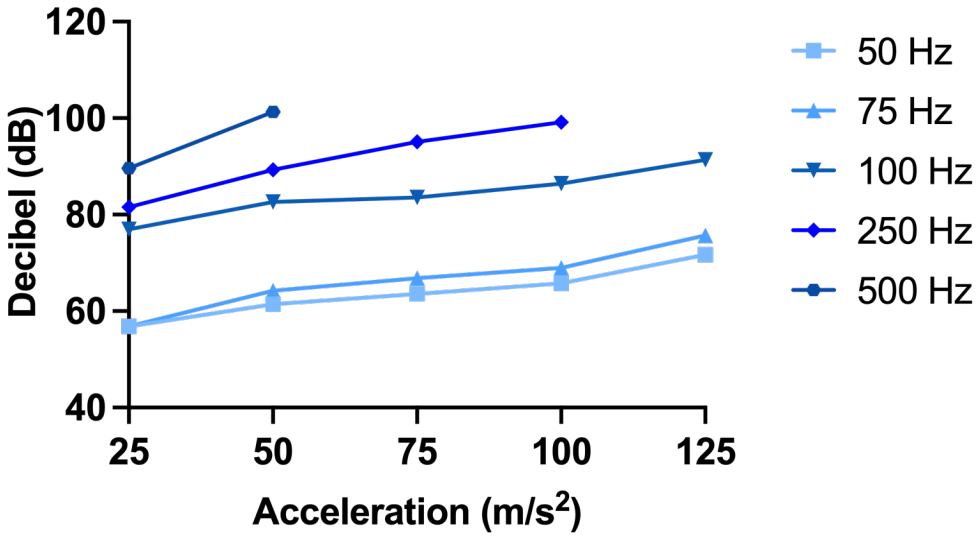

Figure S2. Correlation of sound intensity (decibel) and acceleration generated by the speaker setup in the frequency range from 25 to 500 Hz.

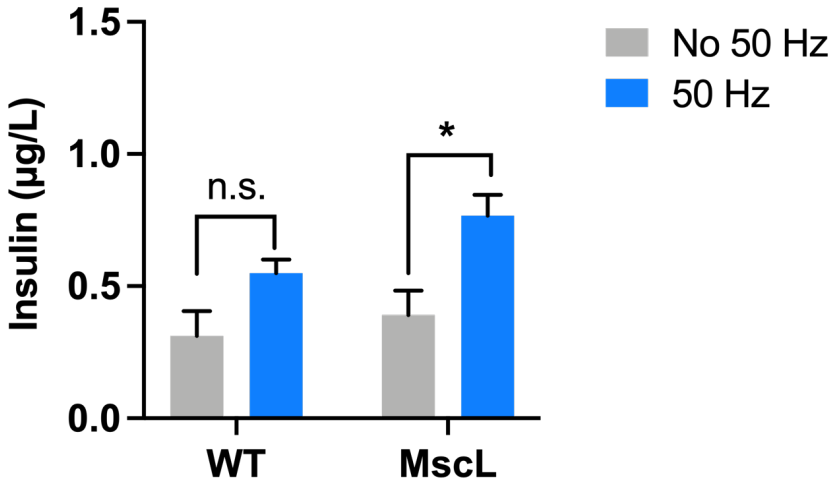

Figure S3. Stimulation of suspended β cell clusters from wild-type (WT) or MscL engineered mice. Aliquots of a suspension of β-cell clusters were transferred to a flexible-bottom 6-well plate and exposed to the speaker system (0.1 V, 50 Hz) for 15 min. Data are means ± SEM. Statistical analysis was done with a two-tailed Mann-Whitney non-parametric test (n = 6). n.s. not significant, *P < 0.05. The P value indicates the significance of differences in the mean values between the "No 50 Hz" and "50 Hz" groups.

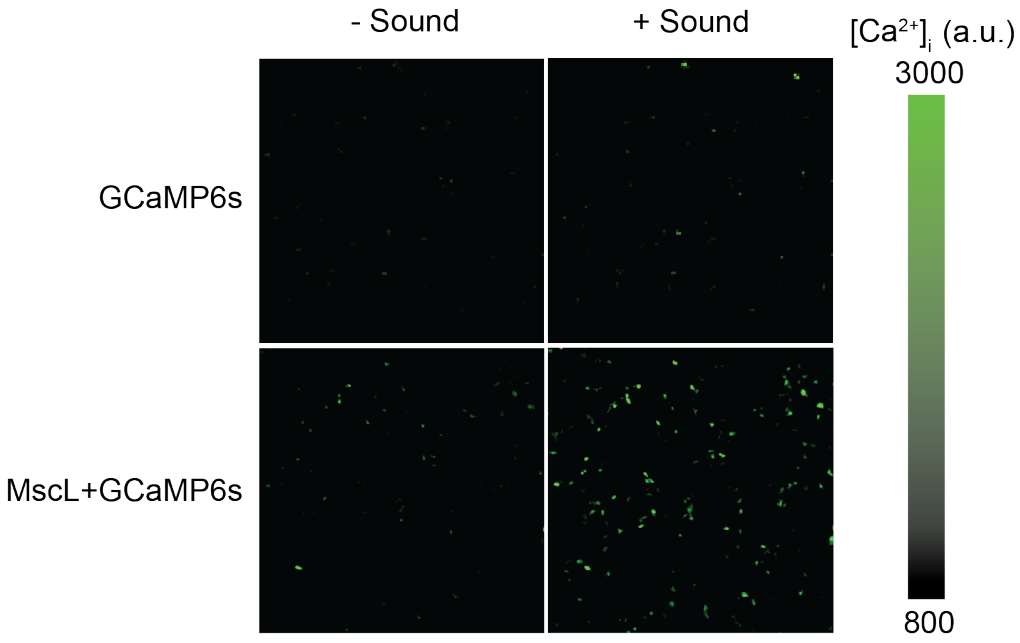

Figure S4. Intracellular calcium imaging. Representative quantitative intracellular calcium fluorescence micrographs of cells transiently transfected with MscL and/or the genetically encoded calcium sensor GCaMP6s and cultivated in the presence or absence of sound stimulation for 10 min at 70 Hz. a.u., arbitrary units.

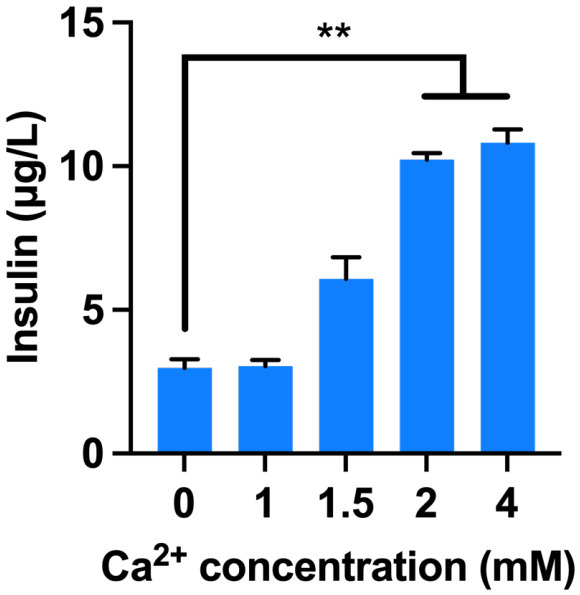

Figure S5. Insulin secretion by sound-stimulated $MUSIC_{INS}$ cells (50 Hz during 15 min) cultured in medium with different calcium chloride concentrations. Data are means ± SEM. Statistical analysis was done with a two-tailed Mann-Whitney non-parametric test (n = 6). **P < 0.01. The P value indicates the significance of differences in the mean values between the "0 mM" group and "2 mM" or "4 mM" groups.

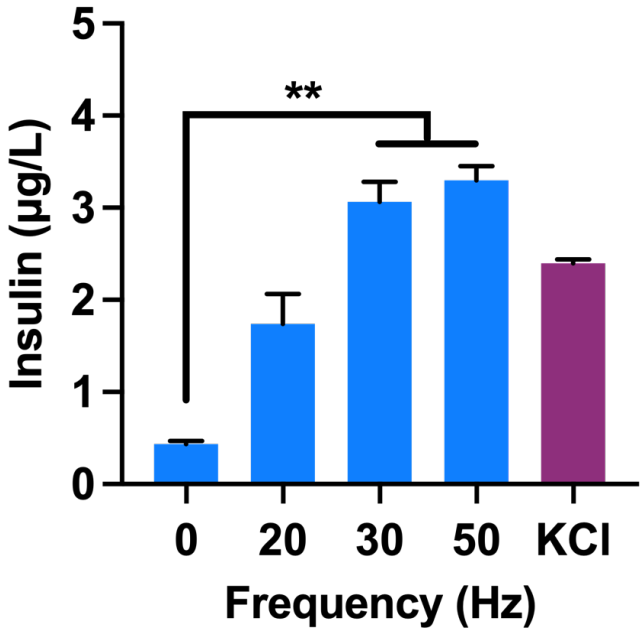

Figure S6. Insulin secretion by $MUSIC_{INS}$ cells stimulated with piston-induced shear forces at different frequencies. Data are means ± SEM. Statistical analysis was done with a two-tailed Mann-Whitney non-parametric test (n = 6). **P < 0.01. The P value indicates the significance of differences in the mean values between the "0 Hz" group and "30 Hz" or "50 Hz" groups.

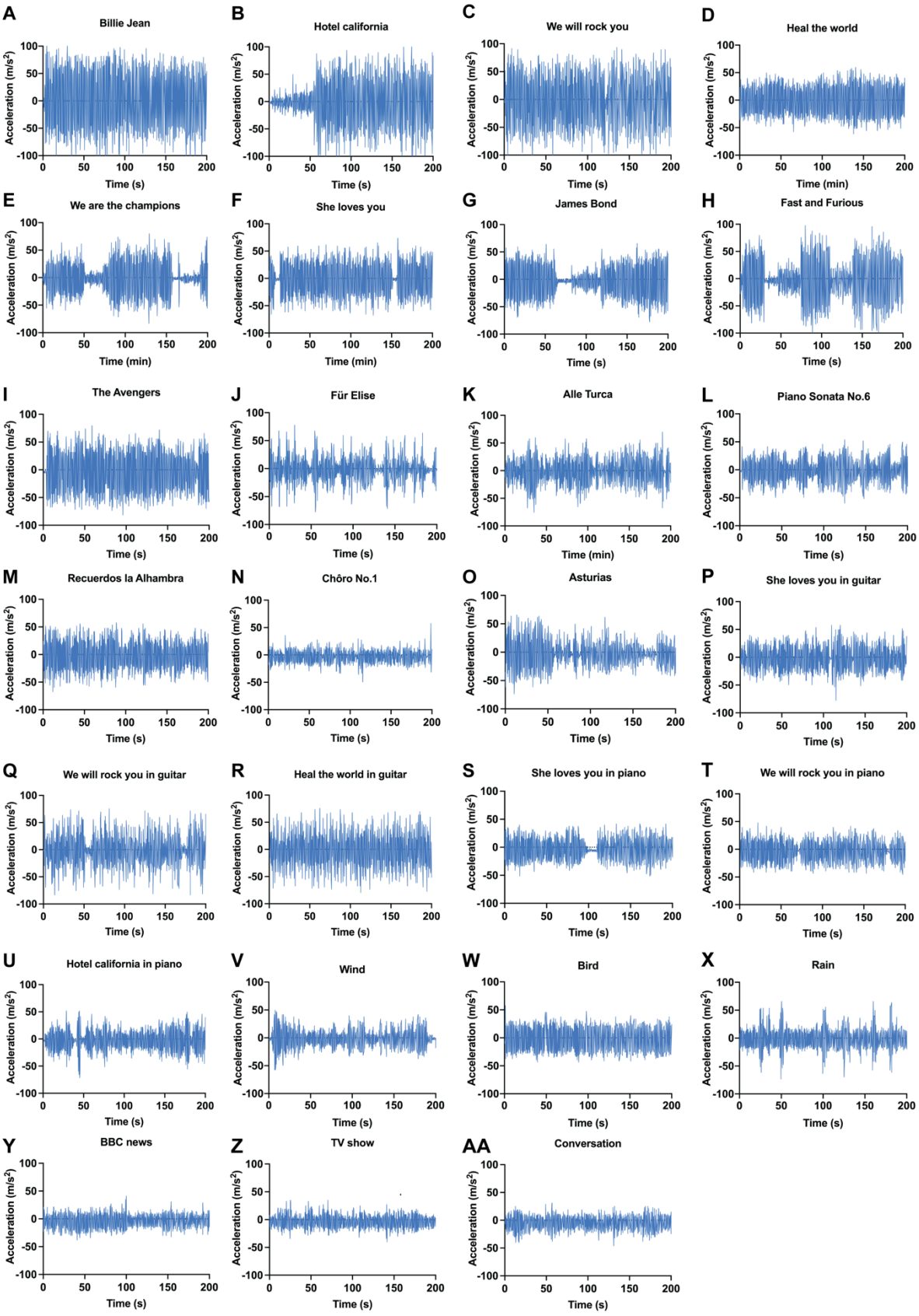

Figure S7. Recordings of acceleration pulses generated by different songs at 85 dB.

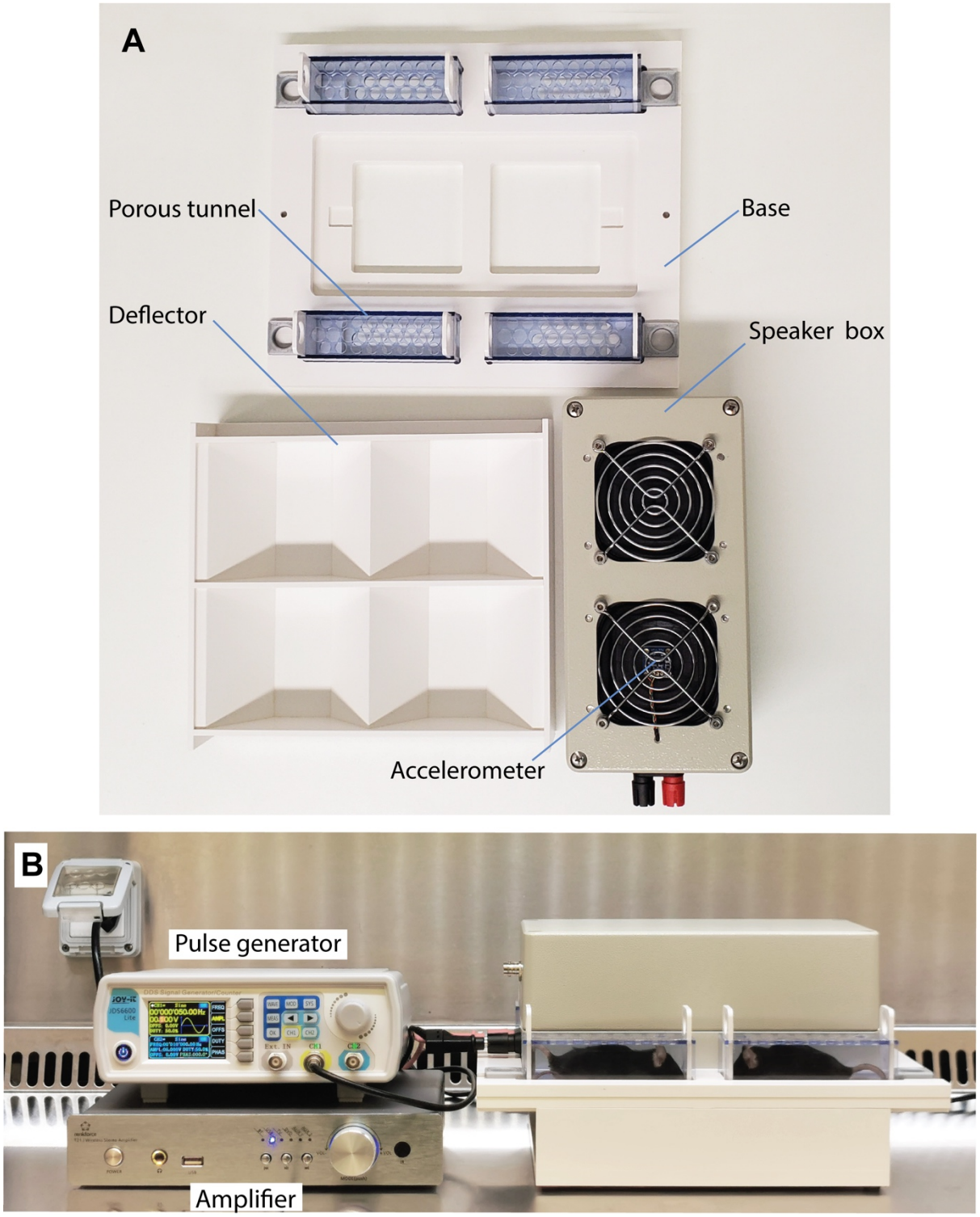

Figure S8. Photos of the speaker setup for the in vivo study. (A) The picture of the speaker setup components. (B) Speaker setup with amplifier and pulse generator.

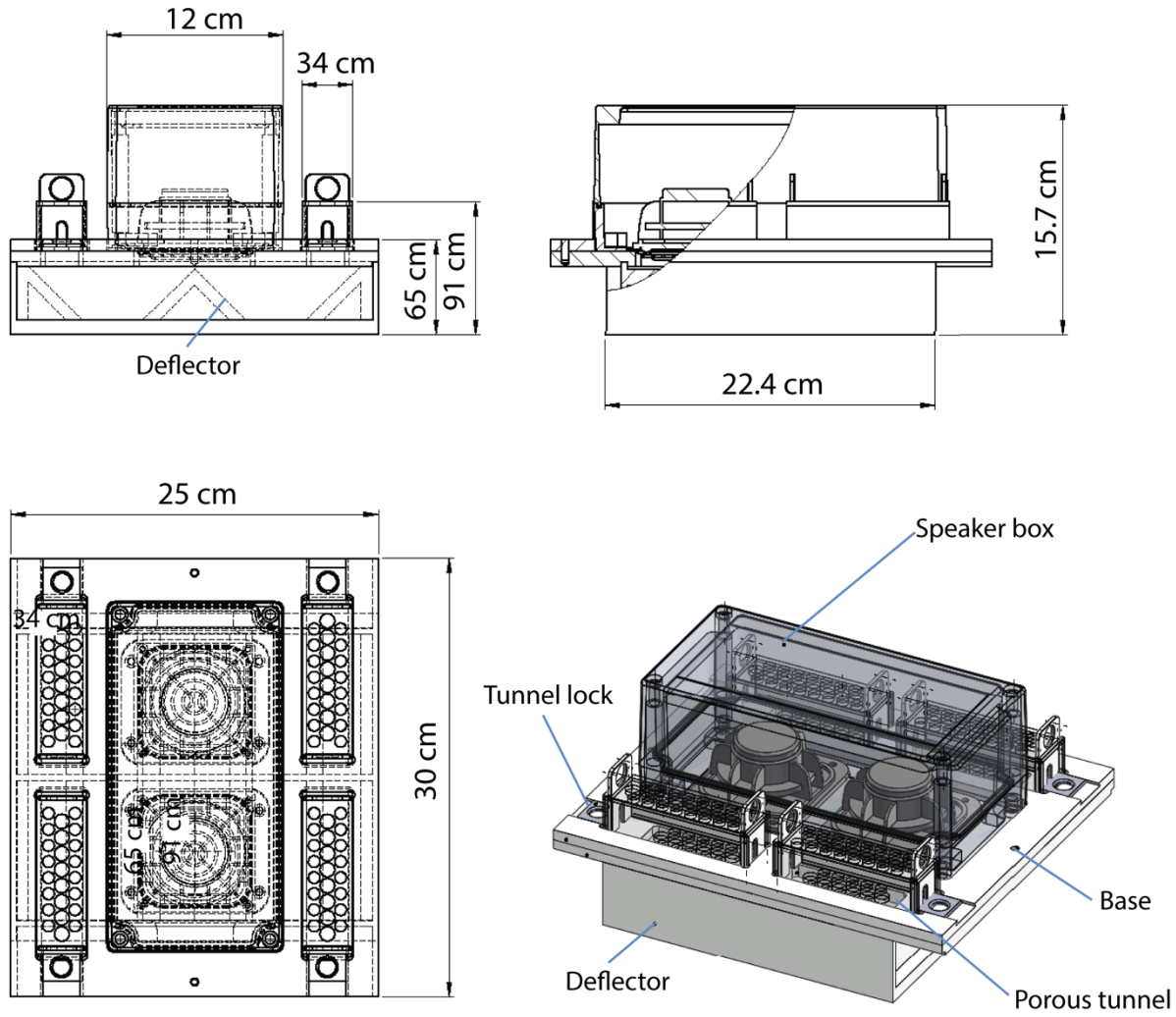

Figure S9. Three-dimensional and perspective views of the speaker setup for the in vivo study, with scale details.

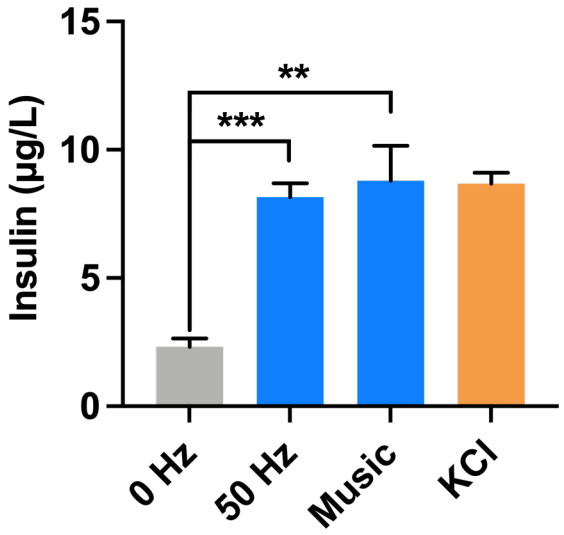

Figure S10. Alginate-encapsulated $MUSIC_{INS}$ stimulation at 50 Hz or "We Will Rock You" for 15 min. The statistical significance of the differences between the 50 Hz/music and 0 Hz groups was calculated. Data are means ± SEM. Statistical analysis was done with a two-tailed t-test (n = 4). **P < 0.01, ***P < 0.001.

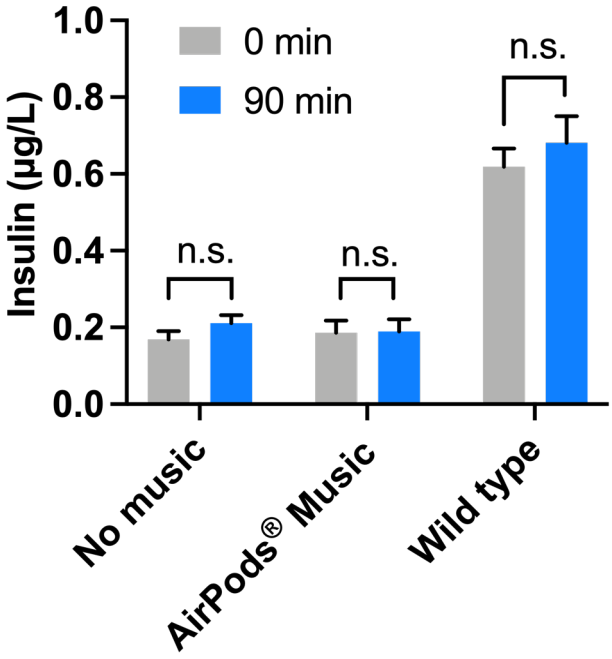

Figure S11. The $MUSIC_{INS}$ implanted type-1 diabetic mice were stimulated with "We Will Rock You" for 15 min via Apple AirPods®. Blood samples were collected at 90 min after stimulation. Type-1 diabetic mice without music stimulation were used as the negative control. Data are means ± SEM. Statistical analysis was done with a two-tailed t-test (n = 5). ns not significant.

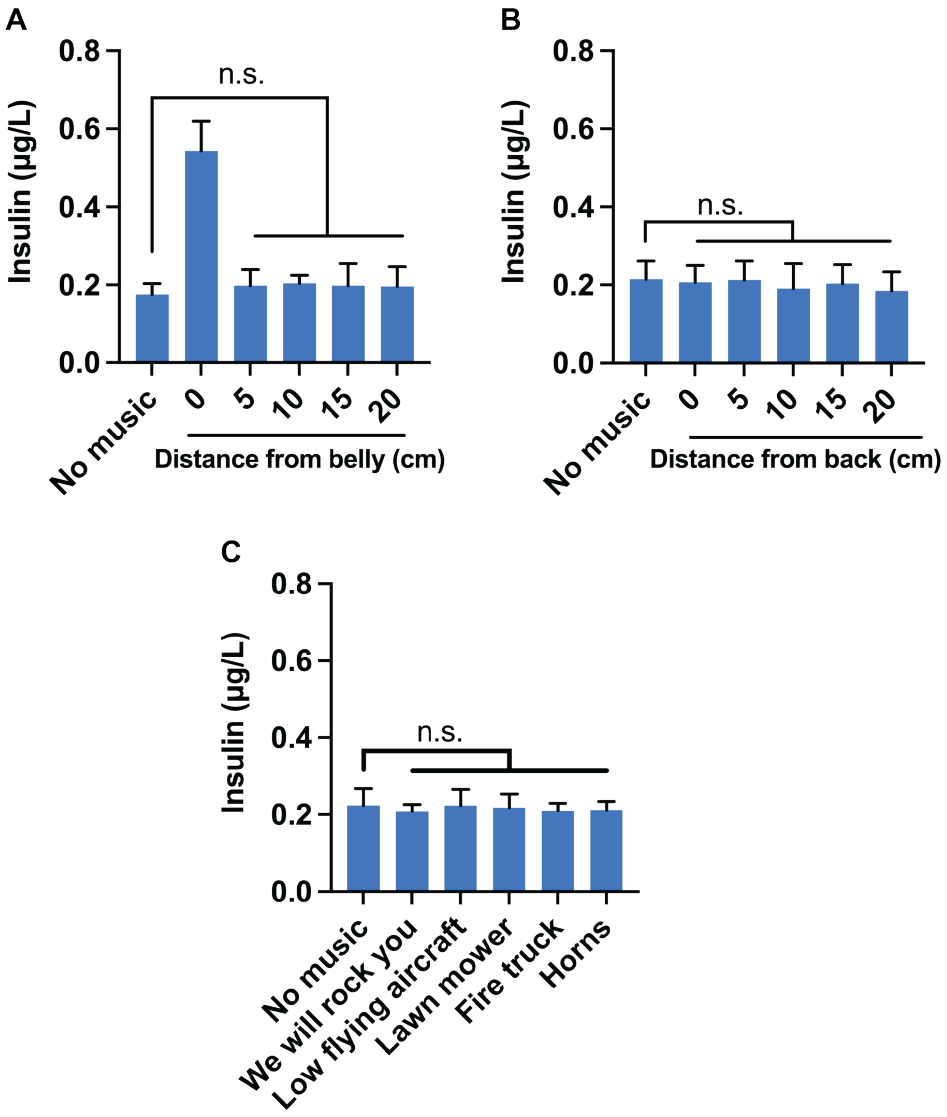

Figure S12. $MUSIC_{INS}$-implanted type-1 diabetic mice were exposed to music and various environmental noises from different distances and directions during 15 min via a portable loudspeaker. (A-B) Distance and direction dependence in the case of music exposure. Sound waves were directed from the loudspeaker to the belly (A) or the back (B) of the mice from different distances. The statistical analysis compared the "No music" group with the different distance groups. (C) The insulin secretion levels of mice exposed to loud environmental noises, delivered via the loudspeaker at the same level as the music, while walking normally in the cage. Blood samples were collected at 90 min after stimulation. The statistical analysis compared the "No music" group and the groups exposed to different types of environmental noise. Type-1 diabetic mice without music stimulation were used as the negative control. Data

are means ± SEM. Statistical analysis was done with a two-tailed Mann-Whitney non-parametric test (n = 5). n.s. not significant.

Table S1. Key plasmids used in this study.

Plasmid	Description and cloning strategy	Reference or Source
pcDNA3.1 (+)	Mammalian expression vector (P_{hCMV}-MCS-pA).	Life Technologies, CA
pCMV-MscL-PA	Vector for integration of two expression cassettes flanked by insertion and recognition sites of Sleeping Beauty transposase (SB). The first cassette contains P_{hCMV}-driven mammalian bacterial large conductance mechanosensitive ion channel (MscL). The second cassette comprises P_{RPBSA}-driven mRUBY fluorescent protein coupled to zeocin resistance marker (ZeoR) (ITR-P_{hCMV}-MscL-pA: P_{RPBSA}-mRUBY-P2A-ZeoR-pA-ITR)	Strittmatter et al. 2021
pCMV-MscS-PA	Vector for integration of two expression cassettes flanked by insertion and recognition sites of Sleeping Beauty transposase (SB). The first cassette contains P_{hCMV}-driven mammalian bacterial small conductance mechanosensitive ion channel (MscS). The second cassette comprises P_{RPBSA}-driven mRUBY fluorescent protein coupled to zeocin resistance marker (ZeoR) (ITR-P_{hCMV}-MscS-pA: P_{RPBSA} -mRUBY-P2A-ZeoR-pA-ITR)	Unpublished
pCMV-T7-SB100	Constitutive SB100X expression vector (P_{hCMV}-SB100X-pA) (Addgene no. 34879).	Mates et al. 2009
pJH49	Vector for stable integration expression cassettes flanked by insertion and recognition sites of Sleeping beauty transposase (SB). Cassette contains P_{RPBSA}-driven yellow florescent protein (YPet) couple to puromycin resistance marker (ITR-P_{RPBSA}-YPet-P2A-PuroR-pA-ITA)	Unpublished
pMD2.G	Constitutive VSV-G expression vector (P_{hCMV}-VSV-G-pA). (Addgene no. 12259).	Follenzi et al. 2002
pProinsulin-Nluc	Lentiviral vector for constitutive expression of Proinsulin-NanoLuc (LTR-P_{hCMV}-Proinsulin-NanoLuc-pA: PhPGK-BlastR-pA-LTR). (Addgene no. 62057).	Burns et al. 2015
pTS391	Vector for stable integration of two expression cassettes flanked by insertion and recognition sites of Sleeping Beauty transposase (SB). Cassette one contains P_{hCMV}-driven mammalian Piezo1 (mPiezo1). Cassette two comprises P_{RPBSA}-driven blue fluorescent protein (BFP) coupled to puromycin resistance marker (PuroR). (ITR-	Strittmatter et al. 2021

	P_{hCMV}-mPiezo1-pA:P_{RPBSA}-BFP-p2a-PuroR-pA-ITA)	
psPAX2	Lentiviral packaging vector. (Addgene no. 12260)	Aichberger et al. 2005
pHZ010	SB100X-specific transposon containing a MscL channel couple with PuroR expression unit and a constitutive marker of mRUBY and ZeoR expression unit (ITR-P_{hCMV}-MscL-P2A-PuroR-pA:P_{RPBSA}-mRUBY-P2A-ZeoR-pA-ITR). P2A-PuroR was PCR-amplified from JH49 using oligonucleotides oHZ040 (5'- cagaataaccgctctgctagcAGTGGTGGTTCTGGTGG-3'), oHZ041 (5'-ctgatcagcgagctgaagcttTCAGGCACCGGGCTTGCG-3'), restricted with NheI/HindIII and cloned into the corresponding sites (NheI/HindIII) of pTS416.	This work
pHZ030	SB100X-specific transposon containing a MscS channel couple with PuroR expression unit and a constitutive marker of mRUBY and ZeoR expression unit (ITR-P_{hCMV}-MscS-P2A-PuroR-pA:P_{RPBSA}-mRUBY-P2A-ZeoR-pA-ITR). P2A-PuroR was PCR-amplified from JH49 using oligonucleotides oHZ040 (5'-cagaataaccgctctgctagcAGTGGTGGTTCTGGTGG-3'), oHZ041 (5'-ctgatcagcgagctgaagcttTCAGGCACCGGGCTTGCG-3'), restricted with NheI/HindIII and cloned into the corresponding sites (NheI/HindIII) of pTS414.	This work
pHZ031	SB100X-specific transposon containing a PIEZO1 channel couple with PuroR expression unit and a constitutive marker of mRUBY and ZeoR expression unit (ITR-P_{hCMV}-PIEZO1-P2A-PuroR-pA:P_{RPBSA}-mRUBY-P2A-ZeoR-pA-ITR). PIEZO1 was excised from pTS391 using EcoRI /NheI and cloned into the corresponding sites of EcoRI /NheI of pHZ010.	This work

Abbreviations: BFP, blue fluorescent protein; **BlastR**, blasticidin resistance gene; **ITR**, inverted terminal repeat of SB100X; **NanoLuc**, *Oplophorus gracilirostris* luciferase; **pA**, polyadenylation signal; **mRUBY**, monomeric red fluorescent reporter; **mPIEZO1**, mammalian Piezo1 mechanosensitive ion channel; **LTR**, long terminal repeat; **MCS**, multiple cloning site; **MscL**, bacterial large conductance mechanosensitive ion channel; **MscS**, bacterial small conductance mechanosensitive ion channel; **P2A**, porcine teschovirus-1 2A self-cleaving peptide; **PCR**, polymerase chain reaction; **P_{hCMV}**, human cytomegalovirus immediate early promoter; **P_{mPGK}**, mouse phosphoglycerate promoter; **Proinsulin-NanoLuc**, modified proinsulin with its C-peptide replaced by NanoLuc; **P_{RPBSA}**, constitutive synthetic mammalian promoter; **PuroR**, puromycin resistance gene; **SB**, sleeping Beauty; **SB100X**, optimized

Sleeping Beauty transposase; **VSV-G**, vesicular stomatitis virus protein G; **YPet**, yellow fluorescent reporter; **ZeoR**, zeocin resistance gene.

References

1 Blood, A. J., Zatorre, R. J., Bermudez, P. & Evans, A. C. Emotional responses to pleasant and unpleasant music correlate with activity in paralimbic brain regions. *Nat Neurosci* **2**, 382-387, doi:10.1038/7299 (1999).

2 Koelsch, S. Brain correlates of music-evoked emotions. *Nat Rev Neurosci* **15**, 170-180, doi:10.1038/nrn3666 (2014).

3 Trehub, S. E. The developmental origins of musicality. *Nat Neurosci* **6**, 669-673, doi:10.1038/nn1084 (2003).

4 Lindlahr, S. *Forecast of Digital Music users by segment in the World 2017-2025*, <https://www.statista.com/forecasts/456558/digital-music-users-in-the-world-forecast#statisticContainer> (2021).

5 Blood, A. J. & Zatorre, R. J. Intensely pleasurable responses to music correlate with activity in brain regions implicated in reward and emotion. *Proc Natl Acad Sci U S A* **98**, 11818-11823, doi:10.1073/pnas.191355898 (2001).

6 Salimpoor, V. N., Benovoy, M., Larcher, K., Dagher, A. & Zatorre, R. J. Anatomically distinct dopamine release during anticipation and experience of peak emotion to music. *Nat Neurosci* **14**, 257-262, doi:10.1038/nn.2726 (2011).

7 Zatorre, R. J., Chen, J. L. & Penhune, V. B. When the brain plays music: auditory-motor interactions in music perception and production. *Nat Rev Neurosci* **8**, 547-558, doi:10.1038/nrn2152 (2007).

8 Fukui, H. & Toyoshima, K. Music facilitate the neurogenesis, regeneration and repair of neurons. *Med Hypotheses* **71**, 765-769, doi:10.1016/j.mehy.2008.06.019 (2008).

9 Archie, P., Bruera, E. & Cohen, L. Music-based interventions in palliative cancer care: a review of quantitative studies and neurobiological literature. *Support Care Cancer* **21**, 2609-2624, doi:10.1007/s00520-013-1841-4 (2013).

10 Panksepp, J. & Bernatzky, G. Emotional sounds and the brain: the neuro-affective foundations of musical appreciation. *Behav Processes* **60**, 133-155, doi:10.1016/s0376-6357(02)00080-3 (2002).

11 Angelucci, F., Ricci, E., Padua, L., Sabino, A. & Tonali, P. A. Music exposure differentially alters the levels of brain-derived neurotrophic factor and nerve growth factor in the mouse hypothalamus. *Neurosci Lett* **429**, 152-155, doi:10.1016/j.neulet.2007.10.005 (2007).

12 Keeler, J. R. *et al.* The neurochemistry and social flow of singing: bonding and oxytocin. *Front Hum Neurosci* **9**, 518, doi:10.3389/fnhum.2015.00518 (2015).

13 Boso, M., Politi, P., Barale, F. & Enzo, E. Neurophysiology and neurobiology of the musical experience. *Funct Neurol* **21**, 187-191 (2006).

14 Jespersen, K. V., Koenig, J., Jennum, P. & Vuust, P. Music for insomnia in adults. *Cochrane Database Syst Rev*, CD010459, doi:10.1002/14651858.CD010459.pub2 (2015).

15 Jespersen, K. V., Otto, M., Kringelbach, M., Van Someren, E. & Vuust, P. A randomized controlled trial of bedtime music for insomnia disorder. *J Sleep Res* **28**, e12817, doi:10.1111/jsr.12817 (2019).

16 Cochen De Cock, V. *et al.* Rhythmic abilities and musical training in Parkinson's disease: do they help? *NPJ Parkinsons Dis* **4**, 8, doi:10.1038/s41531-018-0043-7 (2018).

17 van Bruggen-Rufi, M., Vink, A., Achterberg, W. & Roos, R. Music therapy in Huntington's disease: a protocol for a multi-center randomized controlled trial. *BMC Psychol* **4**, 38, doi:10.1186/s40359-016-0146-z (2016).
18 Flaherty, M., Libert, K. & Monson, B. B. Extended high-frequency hearing and head orientation cues benefit children during speech-in-speech recognition. *Hear Res* **406**, 108230, doi:10.1016/j.heares.2021.108230 (2021).
19 Muller, U. & Barr-Gillespie, P. G. New treatment options for hearing loss. *Nat Rev Drug Discov* **14**, 346-365, doi:10.1038/nrd4533 (2015).
20 Handler, A. & Ginty, D. D. The mechanosensory neurons of touch and their mechanisms of activation. *Nat Rev Neurosci* **22**, 521-537, doi:10.1038/s41583-021-00489-x (2021).
21 Zeng, W. Z. *et al.* PIEZOs mediate neuronal sensing of blood pressure and the baroreceptor reflex. *Science* **362**, 464-467, doi:10.1126/science.aau6324 (2018).
22 Kohl, P. & Ravens, U. Cardiac mechano-electric feedback: past, present, and prospect. *Prog Biophys Mol Biol* **82**, 3-9, doi:10.1016/s0079-6107(03)00022-1 (2003).
23 Barritt, G. & Rychkov, G. TRPs as mechanosensitive channels. *Nat Cell Biol* **7**, 105-107, doi:10.1038/ncb0205-105 (2005).
24 Corey, D. P. *et al.* TRPA1 is a candidate for the mechanosensitive transduction channel of vertebrate hair cells. *Nature* **432**, 723-730, doi:10.1038/nature03066 (2004).
25 Coste, B. *et al.* Piezo1 and Piezo2 are essential components of distinct mechanically activated cation channels. *Science* **330**, 55-60, doi:10.1126/science.1193270 (2010).
26 Feng, J. *et al.* Piezo2 channel-Merkel cell signaling modulates the conversion of touch to itch. *Science* **360**, 530-533, doi:10.1126/science.aar5703 (2018).
27 Lin, Y. C. *et al.* Force-induced conformational changes in PIEZO1. *Nature* **573**, 230-234, doi:10.1038/s41586-019-1499-2 (2019).
28 Kim, S. E., Coste, B., Chadha, A., Cook, B. & Patapoutian, A. The role of Drosophila Piezo in mechanical nociception. *Nature* **483**, 209-212, doi:10.1038/nature10801 (2012).
29 Bass, R. B., Strop, P., Barclay, M. & Rees, D. C. Crystal structure of Escherichia coli MscS, a voltage-modulated and mechanosensitive channel. *Science* **298**, 1582-1587, doi:10.1126/science.1077945 (2002).
30 Zhang, Y. *et al.* Visualization of the mechanosensitive ion channel MscS under membrane tension. *Nature* **590**, 509-514, doi:10.1038/s41586-021-03196-w (2021).
31 Liu, Z., Gandhi, C. S. & Rees, D. C. Structure of a tetrameric MscL in an expanded intermediate state. *Nature* **461**, 120-124, doi:10.1038/nature08277 (2009).
32 Sukharev, S. I., Blount, P., Martinac, B., Blattner, F. R. & Kung, C. A large-conductance mechanosensitive channel in E. coli encoded by mscL alone. *Nature* **368**, 265-268, doi:10.1038/368265a0 (1994).
33 Nourse, J. L. & Pathak, M. M. How cells channel their stress: Interplay between Piezo1 and the cytoskeleton. *Semin Cell Dev Biol* **71**, 3-12, doi:10.1016/j.semcdb.2017.06.018 (2017).
34 Ohashi, K., Fujiwara, S. & Mizuno, K. Roles of the cytoskeleton, cell adhesion and rho signalling in mechanosensing and mechanotransduction. *J Biochem* **161**, 245-254, doi:10.1093/jb/mvw082 (2017).
35 Doerner, J. F., Febvay, S. & Clapham, D. E. Controlled delivery of bioactive molecules into live cells using the bacterial mechanosensitive channel MscL. *Nat Commun* **3**, 990, doi:10.1038/ncomms1999 (2012).
36 Konijnenberg, A. *et al.* Global structural changes of an ion channel during its gating are followed by ion mobility mass spectrometry. *Proc Natl Acad Sci U S A* **111**, 17170-17175, doi:10.1073/pnas.1413118111 (2014).

37 Auslander, S., Auslander, D., Muller, M., Wieland, M. & Fussenegger, M. Programmable single-cell mammalian biocomputers. *Nature* **487**, 123-127, doi:10.1038/nature11149 (2012).
38 Auslander, S. & Fussenegger, M. Synthetic biology: Toehold gene switches make big footprints. *Nature* **516**, 333-334, doi:10.1038/516333a (2014).
39 Auslander, S. & Fussenegger, M. Synthetic biology. Dynamic genome engineering in living cells. *Science* **346**, 813-814, doi:10.1126/science.aaa1246 (2014).
40 Auslander, D. *et al.* Programmable full-adder computations in communicating three-dimensional cell cultures. *Nat Methods* **15**, 57-60, doi:10.1038/nmeth.4505 (2018).
41 Bojar, D., Scheller, L., Hamri, G. C., Xie, M. & Fussenegger, M. Caffeine-inducible gene switches controlling experimental diabetes. *Nat Commun* **9**, 2318, doi:10.1038/s41467-018-04744-1 (2018).
42 Franko, N., Teixeira, A. P., Xue, S., Charpin-El Hamri, G. & Fussenegger, M. Design of modular autoproteolytic gene switches responsive to anti-coronavirus drug candidates. *Nat Commun* **12**, 6786, doi:10.1038/s41467-021-27072-3 (2021).
43 Liu, Y. *et al.* Immunomimetic Designer Cells Protect Mice from MRSA Infection. *Cell* **174**, 259-270 e211, doi:10.1016/j.cell.2018.05.039 (2018).
44 Tigges, M., Marquez-Lago, T. T., Stelling, J. & Fussenegger, M. A tunable synthetic mammalian oscillator. *Nature* **457**, 309-312, doi:10.1038/nature07616 (2009).
45 Xie, M. *et al.* beta-cell-mimetic designer cells provide closed-loop glycemic control. *Science* **354**, 1296-1301, doi:10.1126/science.aaf4006 (2016).
46 Bluestone, J. A. & Tang, Q. Treg cells-the next frontier of cell therapy. *Science* **362**, 154-155, doi:10.1126/science.aau2688 (2018).
47 Cubillos-Ruiz, A. *et al.* Engineering living therapeutics with synthetic biology. *Nat Rev Drug Discov* **20**, 941-960, doi:10.1038/s41573-021-00285-3 (2021).
48 Kemmer, C. *et al.* Self-sufficient control of urate homeostasis in mice by a synthetic circuit. *Nat Biotechnol* **28**, 355-360, doi:10.1038/nbt.1617 (2010).
49 Schukur, L., Geering, B., Charpin-El Hamri, G. & Fussenegger, M. Implantable synthetic cytokine converter cells with AND-gate logic treat experimental psoriasis. *Sci Transl Med* **7**, 318ra201, doi:10.1126/scitranslmed.aac4964 (2015).
50 Rossger, K., Charpin-El-Hamri, G. & Fussenegger, M. A closed-loop synthetic gene circuit for the treatment of diet-induced obesity in mice. *Nat Commun* **4**, 2825, doi:10.1038/ncomms3825 (2013).
51 Wang, H., Xie, M., Charpin-El Hamri, G., Ye, H. & Fussenegger, M. Treatment of chronic pain by designer cells controlled by spearmint aromatherapy. *Nat Biomed Eng* **2**, 114-123, doi:10.1038/s41551-018-0192-3 (2018).
52 Kojima, R., Scheller, L. & Fussenegger, M. Nonimmune cells equipped with T-cell-receptor-like signaling for cancer cell ablation. *Nat Chem Biol* **14**, 42-49, doi:10.1038/nchembio.2498 (2018).
53 Tastanova, A. *et al.* Synthetic biology-based cellular biomedical tattoo for detection of hypercalcemia associated with cancer. *Sci Transl Med* **10**, doi:10.1126/scitranslmed.aap8562 (2018).
54 Bai, P. *et al.* A fully human transgene switch to regulate therapeutic protein production by cooling sensation. *Nat Med* **25**, 1266-1273, doi:10.1038/s41591-019-0501-8 (2019).
55 Krawczyk, K. *et al.* Electrogenetic cellular insulin release for real-time glycemic control in type 1 diabetic mice. *Science* **368**, 993-1001, doi:10.1126/science.aau7187 (2020).
56 Ye, H. *et al.* Self-adjusting synthetic gene circuit for correcting insulin resistance. *Nat Biomed Eng* **1**, 0005, doi:10.1038/s41551-016-0005 (2017).

57 Folcher, M. *et al.* Mind-controlled transgene expression by a wireless-powered optogenetic designer cell implant. *Nat Commun* **5**, 5392, doi:10.1038/ncomms6392 (2014).
58 Gomelsky, M. Photoactivated cells link diagnosis and therapy. *Sci Transl Med* **9**, doi:10.1126/scitranslmed.aan3936 (2017).
59 Kim, T., Folcher, M., Doaud-El Baba, M. & Fussenegger, M. A synthetic erectile optogenetic stimulator enabling blue-light-inducible penile erection. *Angew Chem Int Ed Engl* **54**, 5933-5938, doi:10.1002/anie.201412204 (2015).
60 Mansouri, M. *et al.* Smart-watch-programmed green-light-operated percutaneous control of therapeutic transgenes. *Nat Commun* **12**, 3388, doi:10.1038/s41467-021-23572-4 (2021).
61 Mansouri, M. *et al.* Smartphone-Flashlight-Mediated Remote Control of Rapid Insulin Secretion Restores Glucose Homeostasis in Experimental Type-1 Diabetes. *Small* **17**, e2101939, doi:10.1002/smll.202101939 (2021).
62 Shao, J. *et al.* Smartphone-controlled optogenetically engineered cells enable semiautomatic glucose homeostasis in diabetic mice. *Sci Transl Med* **9**, doi:10.1126/scitranslmed.aal2298 (2017).
63 Ye, H., Daoud-El Baba, M., Peng, R. W. & Fussenegger, M. A synthetic optogenetic transcription device enhances blood-glucose homeostasis in mice. *Science* **332**, 1565-1568, doi:10.1126/science.1203535 (2011).
64 Zhou, Y. *et al.* A small and highly sensitive red/far-red optogenetic switch for applications in mammals. *Nat Biotechnol*, doi:10.1038/s41587-021-01036-w (2021).
65 Pan, Y. *et al.* Mechanogenetics for the remote and noninvasive control of cancer immunotherapy. *Proc Natl Acad Sci U S A* **115**, 992-997, doi:10.1073/pnas.1714900115 (2018).
66 Ortner, V. *et al.* Magnetic field-controlled gene expression in encapsulated cells. *J Control Release* **158**, 424-432, doi:10.1016/j.jconrel.2011.12.006 (2012).
67 Qin, S. *et al.* A magnetic protein biocompass. *Nat Mater* **15**, 217-226, doi:10.1038/nmat4484 (2016).
68 Stanley, S. A., Sauer, J., Kane, R. S., Dordick, J. S. & Friedman, J. M. Remote regulation of glucose homeostasis in mice using genetically encoded nanoparticles. *Nat Med* **21**, 92-98, doi:10.1038/nm.3730 (2015).
69 Wheeler, M. A. *et al.* Genetically targeted magnetic control of the nervous system. *Nat Neurosci* **19**, 756-761, doi:10.1038/nn.4265 (2016).
70 Huang, H., Delikanli, S., Zeng, H., Ferkey, D. M. & Pralle, A. Remote control of ion channels and neurons through magnetic-field heating of nanoparticles. *Nat Nanotechnol* **5**, 602-606, doi:10.1038/nnano.2010.125 (2010).
71 Stanley, S. A. *et al.* Radio-wave heating of iron oxide nanoparticles can regulate plasma glucose in mice. *Science* **336**, 604-608, doi:10.1126/science.1216753 (2012).
72 Stefanov, B. A. *et al.* Genetically Encoded Protein Thermometer Enables Precise Electrothermal Control of Transgene Expression. *Adv Sci (Weinh)* **8**, e2101813, doi:10.1002/advs.202101813 (2021).
73 Kushibiki, T., Okawa, S., Hirasawa, T. & Ishihara, M. Optogenetic control of insulin secretion by pancreatic beta-cells in vitro and in vivo. *Gene Ther* **22**, 553-559, doi:10.1038/gt.2015.23 (2015).
74 Weber, W. *et al.* A synthetic mammalian electro-genetic transcription circuit. *Nucleic Acids Res* **37**, e33, doi:10.1093/nar/gkp014 (2009).
75 Yin, J. *et al.* A green tea-triggered genetic control system for treating diabetes in mice and monkeys. *Sci Transl Med* **11**, doi:10.1126/scitranslmed.aav8826 (2019).

76 Stockley, J. H. *et al.* Surpassing light-induced cell damage in vitro with novel cell culture media. *Sci Rep* **7**, 849, doi:10.1038/s41598-017-00829-x (2017).
77 Auslander, D. *et al.* A designer cell-based histamine-specific human allergy profiler. *Nat Commun* **5**, 4408, doi:10.1038/ncomms5408 (2014).
78 Nguyen, P. Q. *et al.* Wearable materials with embedded synthetic biology sensors for biomolecule detection. *Nat Biotechnol* **39**, 1366-1374, doi:10.1038/s41587-021-00950-3 (2021).
79 Andersson, H. A., Kim, Y. S., O'Neill, B. E., Shi, Z. Z. & Serda, R. E. HSP70 promoter-driven activation of gene expression for immunotherapy using gold nanorods and near infrared light. *Vaccines (Basel)* **2**, 216-227, doi:10.3390/vaccines2020216 (2014).
80 Gudipaty, S. A. *et al.* Mechanical stretch triggers rapid epithelial cell division through Piezo1. *Nature* **543**, 118-121, doi:10.1038/nature21407 (2017).
81 Solis, A. G. *et al.* Mechanosensation of cyclical force by PIEZO1 is essential for innate immunity. *Nature* **573**, 69-74, doi:10.1038/s41586-019-1485-8 (2019).
82 Heureaux, J., Chen, D., Murray, V. L., Deng, C. X. & Liu, A. P. Activation of a bacterial mechanosensitive channel in mammalian cells by cytoskeletal stress. *Cell Mol Bioeng* **7**, 307-319, doi:10.1007/s12195-014-0337-8 (2014).
83 Zhao, Y. *et al.* A Novel Tension Machine Promotes Bone Marrow Mesenchymal Stem Cell Osteoblastic and Fibroblastic Differentiation by Applying Cyclic Tension. *Stem Cells Int* **2021**, 6647651, doi:10.1155/2021/6647651 (2021).
84 Daniel, E. Noise and hearing loss: a review. *J Sch Health* **77**, 225-231, doi:10.1111/j.1746-1561.2007.00197.x (2007).
85 Thelin, J. W., Joseph, D. J., Davis, W. E., Baker, D. E. & Hosokawa, M. C. High-frequency hearing loss in male farmers of Missouri. *Public Health Rep* **98**, 268-273 (1983).
86 Zaw, A. K. *et al.* Assessment of Noise Exposure and Hearing Loss Among Workers in Textile Mill (Thamine), Myanmar: A Cross-Sectional Study. *Saf Health Work* **11**, 199-206, doi:10.1016/j.shaw.2020.04.002 (2020).
87 Barlow, C. Potential hazard of hearing damage to students in undergraduate popular music courses. *Med Probl Perform Art* **25**, 175-182 (2010).
88 Nesher, R. & Cerasi, E. Modeling phasic insulin release: immediate and time-dependent effects of glucose. *Diabetes* **51 Suppl 1**, S53-59, doi:10.2337/diabetes.51.2007.s53 (2002).
89 Dashti, H. S., Scheer, F., Saxena, R. & Garaulet, M. Timing of Food Intake: Identifying Contributing Factors to Design Effective Interventions. *Adv Nutr* **10**, 606-620, doi:10.1093/advances/nmy131 (2019).
90 Jacobs-Tulleneers-Thevissen, D. *et al.* Sustained function of alginate-encapsulated human islet cell implants in the peritoneal cavity of mice leading to a pilot study in a type 1 diabetic patient. *Diabetologia* **56**, 1605-1614, doi:10.1007/s00125-013-2906-0 (2013).
91 Tan, X., Letendre, J. H., Collins, J. J. & Wong, W. W. Synthetic biology in the clinic: engineering vaccines, diagnostics, and therapeutics. *Cell* **184**, 881-898, doi:10.1016/j.cell.2021.01.017 (2021).
92 Xie, M. & Fussenegger, M. Designing cell function: assembly of synthetic gene circuits for cell biology applications. *Nat Rev Mol Cell Biol* **19**, 507-525, doi:10.1038/s41580-018-0024-z (2018).
93 Bacchus, W. *et al.* Synthetic two-way communication between mammalian cells. *Nat Biotechnol* **30**, 991-996, doi:10.1038/nbt.2351 (2012).
94 Fussenegger, M. *et al.* Streptogramin-based gene regulation systems for mammalian cells. *Nat Biotechnol* **18**, 1203-1208, doi:10.1038/81208 (2000).

95 Weber, W. *et al.* Macrolide-based transgene control in mammalian cells and mice. *Nat Biotechnol* **20**, 901-907, doi:10.1038/nbt731 (2002).
96 Vithani, K., Jannin, V., Pouton, C. W. & Boyd, B. J. Colloidal aspects of dispersion and digestion of self-dispersing lipid-based formulations for poorly water-soluble drugs. *Adv Drug Deliv Rev* **142**, 16-34, doi:10.1016/j.addr.2019.01.008 (2019).
97 Rawson, T. M. *et al.* Optimizing antimicrobial use: challenges, advances and opportunities. *Nat Rev Microbiol* **19**, 747-758, doi:10.1038/s41579-021-00578-9 (2021).
98 Wang, H., Ye, H., Xie, M., Daoud El-Baba, M. & Fussenegger, M. Cosmetics-triggered percutaneous remote control of transgene expression in mice. *Nucleic Acids Res* **43**, e91, doi:10.1093/nar/gkv326 (2015).
99 Anikeeva, P. & Jasanoff, A. Problems on the back of an envelope. *Elife* **5**, doi:10.7554/eLife.19569 (2016).
100 Meister, M. Physical limits to magnetogenetics. *Elife* **5**, doi:10.7554/eLife.17210 (2016).
101 Ibsen, S., Tong, A., Schutt, C., Esener, S. & Chalasani, S. H. Sonogenetics is a non-invasive approach to activating neurons in Caenorhabditis elegans. *Nat Commun* **6**, 8264, doi:10.1038/ncomms9264 (2015).
102 Xhima, K. *et al.* Focused ultrasound delivery of a selective TrkA agonist rescues cholinergic function in a mouse model of Alzheimer's disease. *Sci Adv* **6**, eaax6646, doi:10.1126/sciadv.aax6646 (2020).
103 Huang, Y. S. *et al.* Sonogenetic Modulation of Cellular Activities Using an Engineered Auditory-Sensing Protein. *Nano Lett* **20**, 1089-1100, doi:10.1021/acs.nanolett.9b04373 (2020).
104 Lee, W. *et al.* Synergy between Piezo1 and Piezo2 channels confers high-strain mechanosensitivity to articular cartilage. *Proc Natl Acad Sci U S A* **111**, E5114-5122, doi:10.1073/pnas.1414298111 (2014).
105 Petho, Z., Najder, K., Bulk, E. & Schwab, A. Mechanosensitive ion channels push cancer progression. *Cell Calcium* **80**, 79-90, doi:10.1016/j.ceca.2019.03.007 (2019).
106 Vandewauw, I. *et al.* A TRP channel trio mediates acute noxious heat sensing. *Nature* **555**, 662-666, doi:10.1038/nature26137 (2018).
107 Cinar, E. *et al.* Piezo1 regulates mechanotransductive release of ATP from human RBCs. *Proc Natl Acad Sci U S A* **112**, 11783-11788, doi:10.1073/pnas.1507309112 (2015).
108 Ranade, S. S. *et al.* Piezo1, a mechanically activated ion channel, is required for vascular development in mice. *Proc Natl Acad Sci U S A* **111**, 10347-10352, doi:10.1073/pnas.1409233111 (2014).
109 Burns, S. M. *et al.* High-throughput luminescent reporter of insulin secretion for discovering regulators of pancreatic Beta-cell function. *Cell Metab* **21**, 126-137, doi:10.1016/j.cmet.2014.12.010 (2015).
110 Mahameed, M., Xue, S., Stefanov, B. A., Hamri, G. C. & Fussenegger, M. Engineering a Rapid Insulin Release System Controlled By Oral Drug Administration. *Adv Sci (Weinh)*, e2105619, doi:10.1002/advs.202105619 (2022).
111 Mates, L. *et al.* Molecular evolution of a novel hyperactive Sleeping Beauty transposase enables robust stable gene transfer in vertebrates. *Nat Genet* **41**, 753-761, doi:10.1038/ng.343 (2009).
112 Whitesell, L. *et al.* HSP90 empowers evolution of resistance to hormonal therapy in human breast cancer models. *Proc Natl Acad Sci U S A* **111**, 18297-18302, doi:10.1073/pnas.1421323111 (2014).

113 Christiansen, M. *et al.* A New, Wireless-enabled Blood Glucose Monitoring System That Links to a Smart Mobile Device: Accuracy and User Performance Evaluation. *J Diabetes Sci Technol* **11**, 567-573, doi:10.1177/1932296817691301 (2017).
114 Lim, F. & Sun, A. M. Microencapsulated islets as bioartificial endocrine pancreas. *Science* **210**, 908-910, doi:10.1126/science.6776628 (1980).

Discussion

In this work, we developed a physically-actuated bioelectronic implants controlling designer therapeutic with great promise for advancing disease therapy. In chapter 2, we presented a novel approach using piezoelectric materials combined with electrogenetics to create a self-powered and voltage-based system for programming engineered cells. In Chapter 3, we explored a unique approach for tuning cellular insulin release by utilizing music as a real-time control mechanism. The following sections provide a short summary of each chapter and a discussion of the broader implications of the results.

Conductive scaffold for electrogenetics applications

The field of synthetic biology has witnessed remarkable advancements, and one such cutting-edge technique is electrogenetics. This innovative approach involves the conversion of various forms of energy, such as light, into electricity to program gene expression or trigger therapeutic peptide secretion within engineered cells. In 2020, a significant milestone was achieved when Krawczyk, K. et al. developed the first truly direct interface between electronic devices and engineered therapeutic cells, eliminating the need for additional small compound cofactors[1]. This breakthrough brought the promise implants that can function for extended periods without frequent charging, making it an attractive avenue for therapeutic interventions.

However, despite these exciting prospects, electrogenetics faced challenges when it came to the requirement of sophisticated or bulky electronic devices to assist with cell-based interventions, particularly in emergency situations. This limitation hindered the widespread translation of electrogenetics-based therapies into practical clinical applications. To overcome this challenge and realize the full potential of electrogenetics as a therapeutic implant for patients, to explore novel solutions combine different technologies are needed.

In the chapter 2, we developed a promising direction involves leveraging piezoelectric materials to generate voltage through mechanical deformation. Piezoelectric materials have been extensively utilized in health monitoring and tissue engineering applications due to their ability to convert mechanical energy into electrical signals. Among the biocompatible options, polyvinylidene difluoride (PVDF) has emerged as a suitable power source for implantable devices. The core idea is to create a finger-pushing-controlled "button" that can trigger insulin secretion through electrosensitive cells. By using a high conductive cell culture chamber in conjunction with the piezoelectric material, the generated voltage can efficiently stimulate the engineered cells, leading to insulin secretion.

The proposed "button" implant comprises a sandwich structure, consisting of a conductive cell chamber, PVDF film as the piezoelectric material, and a reinforcement ring. The conductive cell chamber layer contains a semipermeable membrane coated with platinum (Pt) layer, which enables the exchange of nutrients and therapeutic proteins while providing a high conductive surface for electro-stimulation by low voltage. The platinum wires link the chamber and PVDF film, transferring the voltage generated from the PVDF film. The reinforcement ring serves the dual purpose of protecting the semipermeable membrane from mechanical forces during finger pushing and providing more space for PVDF film deformation.

By combining the piezoelectric material and the conductive chamber, we have created a small and low voltage suitable implant powered solely by finger pushing. This eliminates the reliance on bulky external devices, providing a more practical solution for therapeutic interventions. Moreover, the implant efficiently delivers electro stimulus to the engineered cells, successfully triggering the fast insulin secretion pathway, even with low voltage.

Looking towards the future, one of the main limitations in translating the device from the bench to the bedside will be the cell capacity of the implant that produces sufficient insulin to meet the needs of patients. The integration of conductive hydrogels[2-7] control engineered tissue will represents a significant advancement in the field of bioelectronic implants. By utilizing conductive hydrogels for engineered tissue instead of a plastic chamber for monolayer cells, it could overcome the limitation associated with cell capacity within the implant, allowing for more efficient and potent therapeutic interventions. Conductive hydrogels offer a three-dimensional structure that supports the growth and function of a larger number of engineered cells, enabling enhanced control and manipulation of cellular behavior[8].

Conductive hydrogels can be engineered to possess conductivity properties similar to native tissues, allowing them to effectively interact with and modulate calcium channel activity within the engineered tissue[2]. For example, Dvir, T. et al. have developed conductive hydrogel-based platforms for the precise control of calcium channel activity in neurons[2]. These hydrogels incorporate conductive polymers or nanoparticles, which enable electrical stimulation and modulation of calcium channel dynamics.

In one study, conductive hydrogels composed of a blend of polypyrrole and Collagen (PPy/Collagen) were utilized to control calcium channel activity in neural stem cell[9]. The conductive hydrogel was patterned into microstructures, creating an electrically addressable platform. Electrical stimulation of the hydrogel resulted in the influx of calcium ions through voltage-gated calcium channels in the neurons, triggering neuronal activation and downstream signaling events[10]. This platform demonstrated the ability to precisely control calcium channel

activity and manipulate neuronal responses. In another example, conductive hydrogels based on carbon nanotubes or graphene have been employed to modulate calcium channel activity in cardiac cells[11]. These conductive hydrogels mimic the electrical conductivity of native cardiac tissue, allowing for precise electrical stimulation and modulation of calcium channel dynamics. By applying electrical signals through the conductive hydrogel, it is able to regulate calcium influx and the subsequent contraction of cardiac cells. This approach holds potential for developing bioelectronic implants for cardiac tissue engineering and therapeutic interventions for cardiac disorders.

The use of conductive hydrogels to control calcium channel activity offers several advantages. Firstly, the three-dimensional structure of hydrogels provides a more physiologically relevant environment for the engineered tissue, allowing cells to interact and communicate in a manner that closely resembles native tissue. Secondly, the electrical conductivity of the hydrogel enables precise and localized stimulation, offering precise control over calcium channel activity for localized insulin secretion. Moreover, conductive hydrogels can be designed to exhibit other desirable properties such as biocompatibility, mechanical flexibility, and tunable conductivity, making them suitable for various applications in tissue engineering, regenerative medicine and even therapeutic protein secretion dosage in our case. These hydrogels can be tailored to match the specific requirements of different tissues and cell types, further expanding their potential in controlling calcium channel activity and modulating cellular responses. The integration of conductive hydrogels in bioelectronic implants represents a promising approach for controlling calcium channel activity and manipulating cellular behavior. The three-dimensional structure and conductivity properties of these hydrogels enable precise electrical stimulation and modulation of calcium channel dynamics within engineered tissue.

In conclusion, the combination of electrogenetics, piezoelectric materials and conductive vector holds tremendous potential for the development of self-powered therapeutic implants. The "button" implant presented in this study represents a significant step towards eliminating the reliance on external devices and enabling finger-pushing-controlled therapeutic interventions. By harnessing the capabilities of conductive hydrogels, we could develop more efficient and potent therapeutic interventions for a wide range of conditions, including neurological disorders, cardiac diseases, and endocrine dysfunctions. Further research and development in this area hold the potential to revolutionize the field of bioelectronic implants and pave the way for innovative treatment strategies.

The application of MUSICs inducible system in the future

In the chapter 3, by mimicking the hearing process, we developed a customized speaker capable of transmitting sound waves as mechanical force to induce membrane deformation which leads to the activation of insulin secretion process in $MUSIC_{INS}$ cells. The sound wave controlled genetic tool was successfully developed and included into the toolbox of synthetic biology.

On the one hand, the project's primary objective was to create a system that could activate insulin secretion in response to music, offering a new way to regulate glucose levels in diabetic individuals. In the case of MUSIC-transgenic cells, the simplicity of stimulation through portable battery-powered commercial loudspeakers enables easy and convenient dosing of biopharmaceuticals multiple times a day, even in settings without medical infrastructure. The foundation of this technology lies in mechanosensitive channels, which respond to mechanical forces and convert them into electrical signals and chemical signals within cells. These channels play crucial roles in various cellular functions, including the sensation of touch[12], proprioception[13], and hearing[14]. By rewiring the insulin secretion pathway in pancreatic β cells to respond to mechanical deformation, the MUSICs system can induce insulin vesicle release upon exposure to specific sound frequencies.

We focused on the MscL ion channel, which demonstrated high efficiency in transducing sound energy and initiating calcium influx, leading to insulin vesicle release. This channel's large conductance and high mechanosensitivity made it an ideal candidate for this application. By fine-tuning the stimulation frequency and employing different types of music, the insulin secretion level of the MUSICs system can be precisely controlled, potentially offering an on-demand insulin release system. The development of this system opens up exciting possibilities for diabetes treatment. Unlike conventional methods that rely on systematic administration or invasive procedures, the MUSICs system can be easily activated using a regular speaker, making it a non-invasive and user-friendly option for real-time glucose regulation. This could improve the quality of life for diabetic patients, providing an easy access and more convenient way to manage their condition.

On the other hand, for the investigation of hearing related diseases, the constructed music-inducible cellular control device (MUSIC) provides an effective platform to mimic hearing process in terms of cochlea membrane deformation and hair cell activation. Compared to other mechanical force stimulation methods, such as blunt probes or ultrasound, the utilization of sound waves within the human hearing range offers several advantages in terms of sensitivity and safety. The auditory system is inherently designed to detect and process sound

waves, making it an ideal platform for sound wave sensing and manipulation. By using the natural pathway of inner hair cells, which sense audible sounds through cell membrane deformation, there is potential to develop strategies for programming hair cell behavior to treat hearing disorders.

Blunt probes and ultrasound are commonly used mechanical force stimulation methods in various biological and biomedical applications. However, they often involve more direct and forceful interactions with cells or tissues, which may introduce unintended consequences or potential damage. In contrast, sound waves within the human hearing range provide a gentler and weaker stimulus, making them a more sensitive and suitable option for studying cellular responses to mechanical forces.

The intricate structure of the inner ear and its components, including the cochlea and the hair cells, enable the perception of sound[15]. Hair cells, particularly the inner hair cells, play a vital role in converting mechanical vibrations into electrical signals that can be processed and interpreted by the brain. These hair cells possess mechanosensitive channels on their cell membranes, which respond to mechanical deformation and trigger a cascade of cellular events leading to the generation of electrical signals[16,17]. The understanding of how inner hair cells sense and respond to mechanical deformation has profound implications for the field of auditory research. By unraveling the mechanisms through which these cells transduce mechanical forces into electrical signals, it becomes possible to engineer and program their behavior to address hearing-related conditions.

Hearing loss and other hearing-related conditions can result from a variety of factors, including genetic mutations, age-related degeneration, exposure to loud noise, or damage to the inner ear. The concept of utilizing mechanosensitive (MS) channel engineering techniques to modulate hair cell behavior could be a promising strategy for treating hearing disorders. By rewiring the pathways involved in mechanotransduction, it may be possible to manipulate the responses of hair cells to mechanical forces, leading to potential therapeutic interventions for various hearing disorders. These mechanosensitive channels, such as MscL, could be designed to respond to specific mechanical cues or exhibit enhanced sensitivity to mechanical forces, enabling more efficient transduction of sound waves into electrical signals. By introducing these modified channels into hair cells, it may be possible to restore their ability to detect and process sound, even in cases where native channels are dysfunctional or damaged.

The utilization of sound waves within the human hearing range as a gentle and sensitive stimulus holds great potential in the field of auditory research. By focusing on the natural pathway of inner hair cells and the mechanosensitive channels involved in sound perception, it

becomes possible to develop strategies for programming hair cell behavior to address hearing-related conditions. The application of MS channel engineering techniques in this context opens up exciting possibilities for advancing our understanding of hearing disorders and developing novel therapeutic approaches for their treatment.

The application of synthetic biology in developmental systems

The application of synthetic biology tools in developmental models is still in its early stages, primarily demonstrated through proof of concept in simple cellular systems. However, the potential of synthetic biology in the field of development is vast and largely unexplored. By precisely manipulating the genetic and molecular pathways that govern cell fate and differentiation, we can guide the formation of tissue structures with improved characteristics. Additionally, we can explore the possibility of constructing non-natural tissue structures specifically designed to fulfill particular functions, pushing the boundaries of what is achievable in tissue engineering and regenerative medicine.

To modify tissue structure, one approach involves directly engineering and refining the intrinsic developmental programs within progenitor cells. By fine-tuning the intricate genetic and molecular networks that control cell behavior, we can shape the development of tissues with greater precision and efficiency[18-20]. Another strategy involves engineering synthetic "niche" or "organizer" cells that can exert influence over native progenitor cells through instructive signals[21]. These synthetic cells have the potential to orchestrate the behavior and developmental trajectories of surrounding cells, leading to the desired tissue architecture. Even subtle modifications in our current approaches to in vitro development hold the potential to overcome existing limitations in organoid models, allowing for more accurate representations of native tissue architecture and function.

Refining the structure and function of organoid systems is another promising avenue in which synthetic biology tools can play a pivotal role. By harnessing the power of synthetic circuits and genetic switches, we can precisely engineer cellular interactions, manipulate cell types, and control spatial organization within organoids. This heightened level of control enables us to create organoids that more faithfully mimic the intricate architecture and functional properties of native tissues. By fine-tuning cellular behaviors and responses, we can improve functionality and enhance the modeling capabilities of organoid systems, allowing for more accurate and reliable research outcomes.

Furthermore, synthetic biology offers the potential for achieving spatiotemporally defined delivery of signals to the developing tissue[22-24]. Through the design of synthetic

signaling systems, we can exert precise control over the timing, location, and duration of molecular cues that influence tissue development. This capability opens up a realm of opportunities for studying the dynamic processes underlying tissue development and investigating the impact of specific signals on tissue patterning and morphogenesis. Traditionally, the study of tissue development has been hindered by the inability to precisely manipulate and control the spatiotemporal aspects of signaling events. However, with synthetic biology tools at our disposal, we can overcome these limitations and delve into the intricate details of tissue formation. By engineering synthetic signaling pathways that replicate the natural signaling dynamics occurring during embryonic development, we can create artificial gradients, pulses, or oscillations of signaling molecules. This innovative approach allows us to investigate how the precise timing and dosage of signaling molecules influence the differentiation and spatial organization of cells within developing tissues. By delivering signals in a controlled manner, we can uncover the underlying mechanisms governing tissue patterning and gain insights into how different signaling profiles influence the intricate process of morphogenesis.

Moreover, synthetic biology empowers us to introduce spatial constraints to the delivery of signals. By designing synthetic microenvironments or scaffold structures, we could guide the distribution of signaling molecules within organoids or tissue constructs. This spatial control enables us to study the formation of complex tissue architectures and explore the interplay between different cell types in a more controlled and predictable manner. It allows us to investigate how spatial organization influences cellular behavior and tissue development, providing valuable insights into the intricate processes that shape native tissue structures.

In summary, the integration of modular synthetic biology tools holds great promise for advancing the field of developmental biology. By combining these tools, we can create more complex developmental systems, ranging from refining native tissue structures to constructing novel tissue architectures. Synthetic biology can refine organoid structure and function, and enable precise spatiotemporal control over molecular signals, leading to significant advancements in developmental research and tissue engineering. These advancements would have the potential to revolutionize our understanding of developmental processes, drive progress in regenerative medicine, and pave the way for the creation of functional tissues and organs in the future.

Conclusion

In this discussion, we have explored two innovative approaches that have great potential for advancing disease therapy: physically-actuated bioelectronic implants and the utilization of sound waves for cellular control.

In Chapter 2, we introduced a novel method that combines piezoelectric materials with electrogenetics to create a self-powered and voltage-based system for programming engineered cells. This approach eliminates the need for bulky external devices and offers a more practical solution for therapeutic interventions. By harnessing the capabilities of conductive hydrogels, we could overcome limitations associated with cell capacity within the implant and enhance the efficiency and potency of therapeutic interventions. Conductive hydrogels provide a three-dimensional structure that supports the growth and function of engineered cells, allowing for enhanced control and manipulation of cellular behavior. They offer biocompatibility, mechanical flexibility, and tunable conductivity, making them suitable for various applications in tissue engineering and regenerative medicine. The integration of conductive hydrogels in bioelectronic implants represents a promising avenue for controlling calcium channel activity and modulating cellular responses.

In Chapter 3, we focused on the application of music-inducible cellular control (MUSIC) for regulating insulin secretion and studying hearing-related conditions. By mimicking the hearing process, we developed a customized speaker capable of transmitting sound waves as mechanical force to induce membrane deformation and activate insulin secretion in MUSIC-transgenic cells. This approach provides a non-invasive and user-friendly option for real-time glucose regulation, potentially improving the quality of life for diabetic patients. Furthermore, the utilization of sound waves within the human hearing range offers several advantages in terms of sensitivity and safety compared to other mechanical force stimulation methods. By understanding the mechanisms through which inner hair cells transduce mechanical forces into electrical signals, we can explore strategies for programming hair cell behavior to address hearing-related conditions. Modulating mechanosensitive channels in hair cells could restore their ability to detect and process sound, offering potential therapeutic interventions for various hearing disorders.

In conclusion, the combination of physically-actuated bioelectronic implants and sound wave sensing and manipulation holds tremendous promise for advancing disease therapy. The presented approaches offer practical and accessible solutions for delivering therapeutics, regulating cellular behavior, and addressing hearing-related conditions. Further research and

development in these areas will undoubtedly contribute to the development of novel treatment modalities and improve the lives of patients worldwide.

Reference

1 Krawczyk, K. *et al.* Electrogenetic cellular insulin release for real-time glycemic control in type 1 diabetic mice. *Science* **368**, 993-1001, doi:10.1126/science.aau7187 (2020).

2 Dvir, T. *et al.* Nanowired three-dimensional cardiac patches. *Nat Nanotechnol* **6**, 720-725, doi:10.1038/nnano.2011.160 (2011).

3 Shevach, M., Fleischer, S., Shapira, A. & Dvir, T. Gold nanoparticle-decellularized matrix hybrids for cardiac tissue engineering. *Nano Lett* **14**, 5792-5796, doi:10.1021/nl502673m (2014).

4 Ramon-Azcon, J. *et al.* Dielectrophoretically aligned carbon nanotubes to control electrical and mechanical properties of hydrogels to fabricate contractile muscle myofibers. *Adv Mater* **25**, 4028-4034, doi:10.1002/adma.201301300 (2013).

5 Schipper, M. L. *et al.* A pilot toxicology study of single-walled carbon nanotubes in a small sample of mice. *Nat Nanotechnol* **3**, 216-221, doi:10.1038/nnano.2008.68 (2008).

6 Liang, S. *et al.* Paintable and Rapidly Bondable Conductive Hydrogels as Therapeutic Cardiac Patches. *Adv Mater* **30**, e1704235, doi:10.1002/adma.201704235 (2018).

7 Qian, Y. *et al.* An integrated multi-layer 3D-fabrication of PDA/RGD coated graphene loaded PCL nanoscaffold for peripheral nerve restoration. *Nat Commun* **9**, 323, doi:10.1038/s41467-017-02598-7 (2018).

8 Shin, S. R. *et al.* Carbon nanotube reinforced hybrid microgels as scaffold materials for cell encapsulation. *ACS Nano* **6**, 362-372, doi:10.1021/nn203711s (2012).

9 Xu, X. *et al.* Conductive Collagen-Based Hydrogel Combined With Electrical Stimulation to Promote Neural Stem Cell Proliferation and Differentiation. *Front Bioeng Biotechnol* **10**, 912497, doi:10.3389/fbioe.2022.912497 (2022).

10 Wang, S. *et al.* Electrical stimulation enhances the neuronal differentiation of neural stem cells in three-dimensional conductive scaffolds through the voltage-gated calcium ion channel. *Brain Res* **1798**, 148163, doi:10.1016/j.brainres.2022.148163 (2023).

11 Ashtari, K. *et al.* Electrically conductive nanomaterials for cardiac tissue engineering. *Adv Drug Deliv Rev* **144**, 162-179, doi:10.1016/j.addr.2019.06.001 (2019).

12 Handler, A. & Ginty, D. D. The mechanosensory neurons of touch and their mechanisms of activation. *Nat Rev Neurosci* **22**, 521-537, doi:10.1038/s41583-021-00489-x (2021).

13 Bornstein, B. *et al.* The mechanosensitive ion channel ASIC2 mediates both proprioceptive sensing and spinal alignment. *Exp Physiol*, doi:10.1113/EP090776 (2023).

14 Jia, Y. *et al.* TMC1 and TMC2 Proteins Are Pore-Forming Subunits of Mechanosensitive Ion Channels. *Neuron* **105**, 310-321 e313, doi:10.1016/j.neuron.2019.10.017 (2020).

15 Goutman, J. D., Elgoyhen, A. B. & Gomez-Casati, M. E. Cochlear hair cells: The sound-sensing machines. *FEBS Lett* **589**, 3354-3361, doi:10.1016/j.febslet.2015.08.030 (2015).

16 Glowatzki, E. & Fuchs, P. A. Transmitter release at the hair cell ribbon synapse. *Nat Neurosci* **5**, 147-154, doi:10.1038/nn796 (2002).

17 Goutman, J. D. & Glowatzki, E. Time course and calcium dependence of transmitter release at a single ribbon synapse. *Proc Natl Acad Sci U S A* **104**, 16341-16346, doi:10.1073/pnas.0705756104 (2007).

18 Saxena, P., Bojar, D., Zulewski, H. & Fussenegger, M. Generation of glucose-sensitive insulin-secreting beta-like cells from human embryonic stem cells by incorporating a synthetic lineage-control network. *J Biotechnol* **259**, 39-45, doi:10.1016/j.jbiotec.2017.07.018 (2017).
19 Glykofrydis, F., Cachat, E., Berzanskyte, I., Dzierzak, E. & Davies, J. A. Bioengineering Self-Organizing Signaling Centers to Control Embryoid Body Pattern Elaboration. *ACS Synth Biol* **10**, 1465-1480, doi:10.1021/acssynbio.1c00060 (2021).
20 Daringer, N. M., Dudek, R. M., Schwarz, K. A. & Leonard, J. N. Modular extracellular sensor architecture for engineering mammalian cell-based devices. *ACS Synth Biol* **3**, 892-902, doi:10.1021/sb400128g (2014).
21 Shimotohno, A., Heidstra, R., Blilou, I. & Scheres, B. Root stem cell niche organizer specification by molecular convergence of PLETHORA and SCARECROW transcription factor modules. *Genes Dev* **32**, 1085-1100, doi:10.1101/gad.314096.118 (2018).
22 Cederquist, G. Y. *et al.* Specification of positional identity in forebrain organoids. *Nat Biotechnol* **37**, 436-444, doi:10.1038/s41587-019-0085-3 (2019).
23 Xu, P. F. *et al.* Construction of a mammalian embryo model from stem cells organized by a morphogen signalling centre. *Nat Commun* **12**, 3277, doi:10.1038/s41467-021-23653-4 (2021).
24 Toda, S. *et al.* Engineering synthetic morphogen systems that can program multicellular patterning. *Science* **370**, 327-331, doi:10.1126/science.abc0033 (2020).

ACKNOWLEDGEMENTS

I would like to thank Prof. Dr. Martin Fussenegger for the opportunity to conduct my research in your group, for your patience, care and support.

I express my sincere gratitude to Prof. Dr. Michael Nash, Prof. Dr. Nicola Aceto, and Prof. Dr. Barbara Treutlein for their participation as members of my thesis committee. I am deeply appreciative of the time and effort to read my thesis and evaluate my doctoral work.

I am grateful to Dr. Shuai Xue, Dr. Ana Palma Teixeira and Dr. Andreas Hieholzer for your great help and support for my PhD study.

I would like to thank Nik Franko for your help and suggestions, and for provide a great atmosphere in 5.10 for our scientific work.

I would like to thank Marie-Didiée Hussherr and Peter Buchmann for supporting my projects.

I express my gratitude to both current and former members of the Fussenegger Lab for creating an enjoyable atmosphere through their meaningful discussions, cheerful moments, and the presence of refreshments such as beer and cakes. They are Silvia, Jinbo, Gokberk, Mohamed, Bozhidar-Adrian, Adrian Bertschi, Mirta, Dmytro, Zhihua, Jingjing, Ping, Guipeng, Haojie, Yuqing, Wenhui, Clélia, Preetam, Debasis, Daniel, Clemens, Samson, Mingqi, Hui, Ying, Peng, Pascal Tobias, Leo, Fabian, Krzysztof, David, Elsa, Viktor, Maysam, Pengli.

A notable mention of my great friends, Jiaji, Qinmei, Kai Zheng, Juan, Ruize, Renxuan, Qiao, Xin, Meng, Weiwei, Xiaohan, Jingxiang, Kaili, Gabi, Hinrik, Wolfgang, Vivek, Kai, Mark and Robert.

Finally, I would like to acknowledge the immense support and encouragement that I received from my parents, sisters, and most importantly, my wife Ya Peng during the entirety of my doctoral studies.

CURRICULUM VITAE